EVALUATION OF AMPEROMETRIC SENSORS CONTAINING ENZYMES IMMOBILIZED IN HYDROGELS THAT INCORPORATE THE REDOX MEDIATOR $[Os(bpy)_2(py)Cl]^{+/2+}$

by

Joseph Jerrold Mitala Jr.

B.S. Chemistry, Delaware Valley College, 2000

Submitted to the Graduate Faculty of

Arts and Sciences in partial fulfillment

of the requirements for the degree of

Doctor of Philosophy

University of Pittsburgh

2008

UNIVERSITY OF PITTSBURGH

ARTS AND SCIENCES

This dissertation was presented

by

Joseph J. Mitala Jr.

It was defended on

May 29, 2008

and approved by

Xinyan Tracy Cui, Assistant Professor, Bioengineering

Shigeru Amemiya, Assistant Professor, Chemistry

Stephen G. Weber, Professor, Chemistry

Dissertation Advisor: Adrian C. Michael, Associate Professor, Chemistry

EVALUATION OF AMPEROMETRIC SENSORS CONTAINING ENZYMES IMMOBILIZED IN HYDROGELS THAT INCORPORATE THE REDOX MEDIATOR $[Os(bpy)_2(py)Cl]^{+/2+}$

Joseph J. Mitala Jr., PhD

Quantification of extracellular levels of neurotransmitters in the brain with a high degree of quality and reliability has been a fundamental challenge for analytical chemists for years. With the ability to characterize how neurotransmitter levels change in response to the administration of different pharmacological agents, it is possible to learn about the mechanisms by which drugs elicit their effect. Characterizing neurotransmitter levels in diseased states enables mapping of a disease or treatment, and may guide the development of novel therapies.

In the early 1990's, redox hydrogels composed of a poly(4-vinylpyridine) backbone with pendent osmium-centered redox complexes ($[Os(bpy)_2(py)Cl]^{+/2+}$, where bpy = 2,2'-bipyridine and py = a pyridine ring of the polymer backbone) were found to be successful at mediating electron transfer between horseradish peroxidase and an electrode. Since that time, a number of amperometric sensors utilizing this mediator have been developed to detect analytes such as hydrogen peroxide, glucose, glutamate, choline, lactate, etc. The performance of these sensors has been characterized *in vitro* and evaluated *in vivo;* however, an overall lack of reproducibility has limited the usefulness of these sensors. My findings demonstrate several factors that contribute to the poor reproducibility of these sensors include: 1) precipitation of the redox polymer and enzymes, 2) reactions of exposed enzyme metal centers with hydroquinones (e.g., dopamine and DOPAC), 3) reaction of oxidized $[Os(bpy)_2(py)Cl]^{+/2+}$ with hydroquinones, 4) the ability of hydroquinone/quinone to mediate electron transfer between horseradish peroxidase and

the electrode, and 5) the accumulation of an insulative hydroquinone oxidation product in the hydrogel which disconnects horseradish peroxidase from the $[Os(bpy)_2(py)Cl]^{+/2+}$ mediator, and neighboring $[Os(bpy)_2(py)Cl]^{+/2+}$ sites from one another. To prepare sensors that resist interference from hydroquinones, it is necessary to minimize the flux of hydroquinones into the hydrogel/enzyme layer, and maintain the integrity of enzymes entrapped in the redox hydrogel. Herein, I describe the use of thick Nafion films and SDS to produce sensors for monitoring cationic and neutral analytes in vivo.

TABLE OF CONTENTS

LIST OF TABLES

LIST OF FIGURES

LIST OF SCHEMES

LIST OF REACTIONS

PREFACE

First of all, I would like to thank my parents, Joe and Marlene, for their continuous support and encouragement during my long and enduring time as a student. I would also like to thank my beautiful wife Christina, for her patience, love, wisdom, and understanding, especially on those days when nothing ever seemed to work the way you would expect it to, and my son, Joseph Michael, for all of the happiness he has brought into my life. I would also like to thank the members of the Michael lab, both past and present for lending an open ear, and making the lab an exciting place to come and work every day.

Most of all, I would like to thank Dr. Michael for his guidance and constructive criticism that he offered as my advisor. I am especially grateful that Dr. Michael talked me into finishing up the Ph.D. program, when I had my mind set on leaving with a Masters. That is one conversation that has changed my life.

1.0 BRIEF OVERVIEW OF AMPEROMETRIC ENZYME SENSORS AND OTHER DEVICES FOR ANALYSIS OF MOLECULES IN INTACT BRAIN TISSUE

Quantitative analysis of the components in the living brain has been an ongoing objective for several decades. With an understanding of the resting levels of biologically important molecules (e.g. neurotransmitters, glucose, reactive oxygen species, etc.) in healthy, diseased, and damaged brain tissue, and how these levels fluctuate under various conditions, much can be learned about how the brain functions. In this chapter, the challenges of measuring molecules in intact brain tissue are discussed. The term intact brain tissue refers to tissue samples in which the spatial arrangement of structural components (e.g., neurons and glia) are similar to that found in the living brain. Thus, the entire brain as a whole, or isolated, but intact brain regions such as brain slices are considered intact brain tissue [3]. Monitoring molecules in brain homogenate, cultured neurons, freshly dissociated neurons, etc., although important, are not discussed here.

1.1 DETECTION OF MOLECULES: TWO APPROACHES

Molecules can be detected at devices placed in intact brain tissue (*in situ*), or molecules can be withdrawn from the brain and detected elsewhere (*ex situ*). Each has their advantages and disadvantages, and depending on the objective of the experiment at hand, one may be more suitable than the other.

1.1.1 In Situ Detection

When molecules are detected in situ, they remain in their native environment, which is a critical factor for understanding proper function. The need for sample handling is eliminated, which minimizes potential determinate errors. In addition, because the sample is not diluted, many analytes are present at concentrations above the detection limits of the methods used to detect them. Provided the means of detection is rapid, fluctuations in the concentration of analyte can be monitored in real time, which is essential should kinetic parameters such as uptake and release rates be determined. One of the drawbacks of monitoring samples in situ, however, is that there are relatively few means of detection that allow for quantification: electrochemical and optical methods appear to be most common.

1.1.1.1 Electrochemical Methods

Numerous electrochemical methods exist, and can be distinguished by the manner in which a potential is applied to the working electrode [4]. Of the electrochemical methods, chronoamperometry [5, 6], cyclic voltammetry [7], and amperometry are a few of the more commonly used techniques in monitoring molecules in neuroscience. Briefly, in chronoamperometry, an initial potential is applied to an electrode that does not cause oxidation or reduction of molecules in the surrounding solution. The potential is then stepped to a new potential, slightly beyond the potential where oxidation or reduction of the molecule takes place. The concentration of substrate at the electrode decreases, and a concentration gradient between the solution and the electrode surface arises. The current, which is measured over time, is initially due to a combination of capacitive (i.e. charging current) and faradaic current, and later followed by faradaic current. Faradaic current arises from the oxidation or reduction of analyte.

Chronoamperometry is a popular electrochemical method because the capacitive current associated with stepping the potential is small and consistent, which improves the signal-to-background ratio.

In cyclic voltammetry, the potential is typically swept from an initial potential to a final potential, and back to the initial potential. The current is continuously recorded as the potential is swept, and multiple voltammograms (i.e., a plot of current vs. applied potential) are generated. This is typically done at a specific rate, known as the sweep rate (υ). As the capacitive current increases with the sweep rate, it is necessary to subtract out the capacitive current from voltammograms when the potential is swept rapidly (e.g., as in fast scan cyclic voltammetry, FSCV). To do this, a voltammogram taken in the absence of analyte is subtracted from a voltammogram taken in the presence of analyte. Not only do voltammograms, or background-subtracted voltammograms (in the case of FSCV) contain quantitative information, but the shape of the voltammogram, and the potentials at which the oxidation and reduction peaks are observed are typically unique for each molecule. Caution must still be exercised when using voltammograms to identify species, however, because many structurally similar molecules found in the brain (e.g., hydroquinones) produce similar voltammograms.

In amperometry, an electrode is held at a constant potential. The current produced at the electrode is monitored over time, and is the result of oxidation or reduction reactions. Because many species in the brain are both electroactive, and amenable to oxidation or reduction directly on the electrode surface, great care must be exercised when assigning an identity to the species believed to be generating the amperometric response *in situ*. The difficulty associated with using amperometry is providing evidence that the response observed is the result of a selective oxidation or reduction reaction [8]. For this reason, amperometric methods are commonly used to

monitor: 1) a single species in vivo, in areas where that single species predominates, or 2) a class of molecules (e.g., hydroquinones) in vivo, in areas where multiple species of the same class co-exist, and possess similar electroactive properties [8]. Many amperometric enzyme sensors have also been prepared which provide selective responses, because they are operated in conjunction with control sensors. Control sensors identify when the current generated at a sensor arises from 'unintentional' oxidation or reduction reactions. That is, oxidation or reduction of species other than the analyte of interest, or species which are attributable to the analyte of interest (in the case a redox mediator is employed).

Since electrochemical sensitivity is largely influenced by the electrode surface area, and sensors for *in situ* use must be small to minimize damage to brain tissue, preparing sensors with a great enough sensitivity to identify small fluctuations in analyte becomes increasingly difficult as the size of the sensors decrease. Also, many electrochemical methods lack the selectivity to positively identify the molecule responsible for producing the change in amperometric current.

1.1.1.2 Optical Methods

Optical methods are a more recent technology being used to probe neurochemical events. In the mid to late 1990's, the development of green (GFP) and red (DsRed) fluorescent proteins, from the jellyfish *Aequorea victoria*, and the sea anemone *Discosoma striata*, respectively, have revolutionized the ability to visualize proteins in living cells, neurons, and tissue [9]. These proteins, and their variants can be fused to virtually any protein [10], and imaged with techniques including one-photon [11], two-photon [11], or multiphoton excitation fluorescence microscopy [12]. Since the discovery of GFP and DsRed, more than 25 additional fluorescent proteins have been isolated from different marine organisms [13]. With the development of new vital (i.e., living) fluorophores, the creation of viral vectors, and transgenic methods for expressing fluorescent

proteins in select classes of cells, fluorescence imaging techniques have been increasingly useful for visualizing protein location, dynamics, and interactions, as well as quantifying proteins in living cells [14]. In regards to visualization of neuronal dynamics, genetically encoded fluorescent probes have been used to indicate membrane voltage [15], ion concentrations [16, 17], and synaptic transmission [18, 19].

Water-soluble fluorescent semiconductor nanocrystals, (quantum dots or qdots) have also been used in conjunction with multiphoton fluorescence imagining in vivo [20, 21]. These are bright, photostable fluorophores that have a broad excitation spectrum, and a narrow, size-dependent, tunable emission [21, 22]. One of the challenges of imaging quantum dots in vivo arises from exciting the quantum dot in vivo. External illumination is one method by which quantum dots can be excited, but this produces strong background autofluorescence from ubiquitous endogenous chromophores such as collagens, porphyrins, and flavins [23]. Also, because tissue can absorb or scatter optical photons, little light is available to excite quantum dots in some tissue locations [24]. More recently, quantum dot conjugates that luminesce by bioluminescence resonance energy transfer, and do not require external excitation have been developed [22]. These offer several advantages over existing quantum dots, including being able to emit in deep tissue, and a greatly enhanced sensitivity in small animal imaging [22]. Yet, like fluorescent proteins, quantum dots are still in their early stages of development for in vivo applications, in regards to quantification of molecules. With continued progress in quantum dots and fluorescent proteins research, it is likely they will gain a larger role in molecular quantification in the near future.

1.1.2 Ex Situ Detection

Removing the sample from the brain, as is done in microdialysis and push-pull perfusion techniques [25, 26], allows the sample to be analyzed by other detection methods. The sample can be separated from interferants using separation methods such as chromatography or capillary electrophoresis [27, 28], and concentrated, should the concentration of analyte below the detection limit of a given method. Separation allows multiple analytes within the sample to be detected simultaneously, and can, when hyphenated with detection systems such as mass spectrometry, provide positive confirmation of the molecular identity.

Removing the sample from the brain removes the sample from its native environment. In the case of microdialysis and push-pull perfusion techniques, this also requires that the volume extracellular fluid removed be replaced. Artificial cerebral spinal fluid (aCSF), which has an ionic composition and pH similar to the extracellular fluid, is frequently used for this purpose; however, it is unknown how this affects the amounts of neurochemical in the extracellular space of the brain.

1.2 EXPECTATIONS OF AMPEROMETRIC ENZYME SENSORS

Many enzymes are capable of selectively interacting with their substrate in a complex matrix. However, despite the nearly 50 years of research on amperometric enzyme sensors, relatively few investigators have measured the concentration of molecules directly in the extracellular space of the brain with these analytical tools. As accounts of new sensors appear in journals regularly, the challenge of monitoring molecules in the extracellular space does not

appear to be preparing sensors that work in a beaker, in the presence a physiological buffer (e.g., artificial cerebral spinal fluid or phosphate buffered saline). Rather, the challenge appears to be preparing sensors that exhibit good temporal (ms) and spatial resolution (100 nm-10 μm), which respond selectively, and with a great enough sensitivity, in the presence of interferants. These appear to be the criteria that some consider 'essential' for sensors to possess to be considered 'useful' for extracellular measurements[29]. Certainly, these are all desirable characteristics for a sensor to possess; however, the reality is that it is difficult to prepare sensors that possess all of these attributes, simultaneously. Much can be learned from sensors that respond selectively and with a great enough sensitivity, in the presence of interferants. Indeed, good temporal and spatial resolution are desirable characteristics that are necessary to monitor the kinetics of uptake and release in discrete regions of the brain; however, useful information can still be gathered from devices which lack these attributes (e.g., microdialysis).

1.3 THREE STYLES OF AMPEROMETRIC ENZYME SENSORS

Three different styles of amperometric enzyme sensors have been developed over the last 50 years. They are often referred to as first-, second-, and third-generation amperometric enzyme sensors (Figure 1). They all require the enzymes be in close proximity to the electrode surface, but differ in the mechanism by which signal transduction occurs.

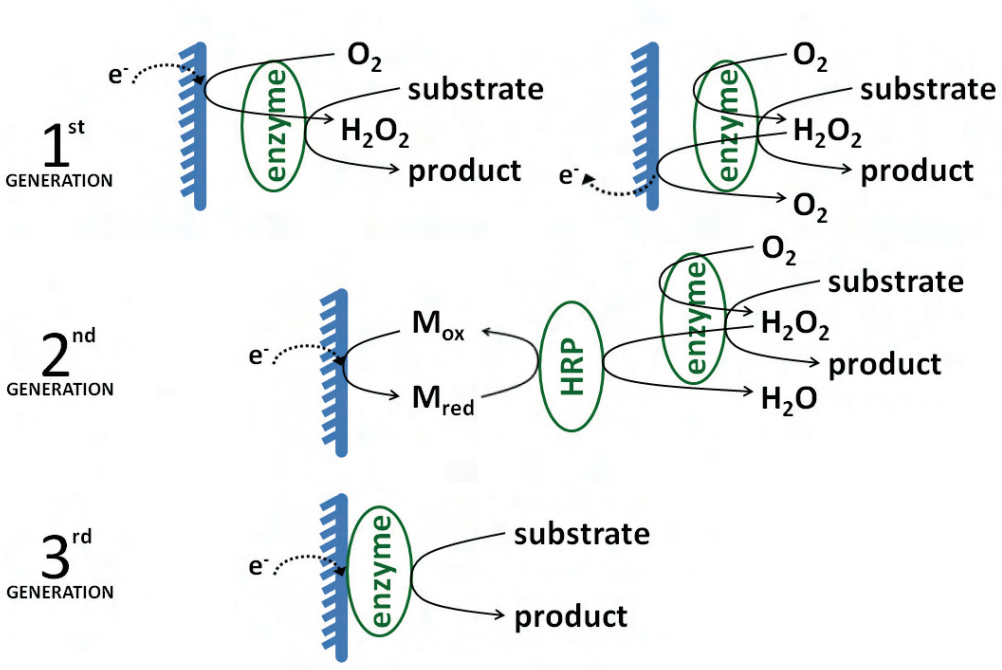

Figure 1-1. Schematic of first, second, and third generation amperometric enzyme sensors.

1.3.1 First Generation Amperometric Enzyme Sensors

First generation amperometric enzyme sensors were first proposed by Clark and Lyons in 1962, and later implemented by Updike and Hicks in 1967 [30, 31]. Updike and Hicks coined the term *enzyme sensors* [30]. These sensors possess oxidase enzymes in close proximity to the electrode surface, which, upon interacting with substrate, consume oxygen (O_2) and produce hydrogen peroxide (H_2O_2) (Figure 1). Because O_2 and H_2O_2 are electroactive and diffusible, the amount of O_2 consumed or H_2O_2 produced by the reaction of the oxidase enzyme with substrate is used as a measure of substrate present [30, 32, 31].

1.3.2 Second Generation Amperometric Enzyme Sensors

Second generation sensors also rely on a mediated electron-transfer mechanism for signal transduction to occur. These sensors typically incorporate horseradish peroxidase (HRP) and an oxidase enzyme to oxidize the substrate. These sensors operate on the principle that H_2O_2 is produced from the reaction of the oxidase enzyme with substrate, and HRP, an oxidoreductase, can both reduce H_2O_2 , and oxidize a mediator to initiate the electron transfer process (Figure 1). The amount of oxidized mediator detected amperometrically at the electrode is used as a measure of the amount of substrate present. Redox mediators may be diffusible or non-diffusible[33-36] . In the case that mediators are diffusible, some redox equivalents may be lost to diffusion, (i.e., diffuse out of the sensor and never be detected at the electrode). Because a loss of redox equivalents corresponds to 'lost signal', polymeric hydrogels that incorporate non-diffusible redox components have been prepared. The non-diffusible redox mediators utilize an electron hopping mechanism to facilitate electron transfer between redox sites. This prevents a loss of redox equivalents because electrons will hop from one redox site to another until they are detected at the electrode surface.

1.3.3 Third Generation Amperometric Enzyme Sensors

Third generation enzyme sensors rely on a direct, rather than mediated, electron transfer mechanism. The amperometric current measured is the result of oxidation or reduction of the enzyme's prosthetic group, which serves as temporary trap of electrons or electron vacancies (Figure 1). Third generation enzyme sensors frequently use self assembled monolayers (SAMs) to align the enzymes in a proper orientation, and connect the enzymes' prosthetic groups to the

electrode. As explained by Marcus theory, electron transfer decays exponentially with distance; hence, minimizing the distance between the enzymes' prosthetic groups and the electrode is essential for the success of these sensors. In the event that an oxidase enzyme is attached to the self-assembled monolayer, electron transfer is not affected by the amount of O_2 present. O_2 must be present to withdraw electrons from oxidase enzymes in first and second generation amperometric enzyme sensors. However, in the case of third generation enzyme sensors, this can be accomplished by controlling the voltage applied to the electrode.

1.3.4 Choosing a Sensor for use in Intact Brain Tissue: A Few Considerations

Choosing an amperometric enzyme sensor to use in intact brain tissue can be difficult. Indeed, many questions need to be considered before a decision is made. What is the substrate? What is the charge on the substrate? Are there enzymes that can oxidize or reduce this substrate? How long are the experiments to be carried out for? Are the experiments going to be carried out in brain slices, or in the whole brain? What region of the brain are the experiments to be carried out in? What type of temporal resolution is needed? What type of spatial resolution is needed? How much sensitivity is needed? These are a few questions that need to be considered before choosing an appropriate style of sensor. A clear understanding of the objectives of the experiment at hand and the limitations of the different styles of amperometric enzyme sensors are essential to make a sound decision.

I have found that amperometric enzyme sensors containing the $[Os(bpy)_2(py)Cl]^{+/2+}$ redox mediator interact with hydroquinones in several ways. As hydroquinones are present in the extracellular space of the brain where we intend to use these sensors, I have documented these interactions and discussed the significance of these interactions in the following chapters.

2.0 IMPROVING THE SELECTIVITY AND SENSITIVITY OF AMPEROMETRIC ENZYME SENSORS BY MAINTAINING THE INTEGRITY OF ENZYMES ENTRAPPED IN A REDOX HYDROGEL

2.1 ABSTRACT

Microsensors based on carbon fiber microelectrodes coated with enzyme-entrapping redox hydrogels facilitate the in vivo detection of substances of interest within the central nervous system, including hydrogen peroxide, glucose, choline, and glutamate. The hydrogel, formed by cross-linking a redox polymer, entraps the enzymes and mediates electron transfer between the enzymes and the electrode. It is important that the enzymes are entrapped in their enzymatically active state. Should entrapment cause enzyme denaturation, the sensitivity and the selectivity of the sensor may be compromised. Synthesis of the redox polymer according to published procedures may yield a product that precipitates when added to aqueous enzyme solutions. Casting hydrogels from solutions that contain the precipitate produces microsensors with low sensitivity and selectivity, suggesting that the precipitation disrupts the structure of the enzymes. The low selectivity is the result of exposure of the enzymes' metal centers, which display a high degree of reactivity toward hydroquinones. Herein we show that a surfactant, sodium dodecyl sulfate (SDS), can prevent the precipitation, eliminate the reactivity of the sensors to hydroquinones, and hence, improve the sensitivity and selectivity of the sensors.

2.2 INTRODUCTION

Enzyme-modified electrodes facilitate the electrochemical detection of substances that are electroinactive, and substances that are electroactive, but which are oxidized or reduced at greater potentials. Detection may be accomplished by monitoring the consumption of an electroactive enzyme cosubstrate, such as oxygen [37, 38], or the formation of an electroactive product, such as hydrogen peroxide [39, 38, 40]. Alternatively, electron transport between enzymes and electrodes can be achieved with redox mediators [35, 36, 41]. The term 'wired enzyme' has been applied to the case where the redox mediator is incorporated into the structure of a cross linkable polymer that both entraps the enzymes and mediates electron transfer between the enzymes and the electrode [41]. It is important that the entrapped enzymes remain in their enzymatically active state, otherwise the sensitivity and selectivity of the microsensor could be compromised [41].

We have coated carbon fiber microelectrodes with enzyme-entrapping polymeric redox hydrogels to prepare microsensors for several substances of interest in brain tissue [42-49]. The redox hydrogel consists of a poly(4-vinylpyridine) backbone with pendent osmium-centered redox complexes ($[Os(bpy)_2(py)Cl]^{+/2+}$, where bpy = 2,2'-bipyridine and py = a pyridine ring of the polymer backbone). Some of the pyridine units of the polymer are quaternized with ethylamine groups, which serve as sites for reaction with a diepoxide crosslinker, poly(ethylene glycol) diglycidyl ether (PEGDE)[36].

The osmium-centered redox complex enables electron transport by a hopping mechanism that involves electron self-exchange between neighboring complexes [35, 36]. The complexes also exchanges electrons with horseradish peroxidase [50], allowing for the detection of hydrogen peroxide via the following reactions:

Reaction 1

$$2\ [Os(bpy)_2(py)Cl]^{+} + H_2O_2 + 2\ H^{+} \xrightarrow{HRP} 2\ [Os(bpy)_2(py)Cl]^{2+} + 2\ H_2O$$

Reaction 2

$$[Os(bpy)_2(py)Cl]^{+} + [Os(bpy)_2(py)Cl]^{2+} \longrightarrow [Os(bpy)_2(py)Cl]^{2+} + [Os(bpy)_2(py)Cl]^{+}$$

Reaction 3

$$[Os(bpy)_2(py)Cl]^{2+} + e^{-} \longrightarrow [Os(bpy)_2(py)Cl]^{+}$$

where Rxn. 1 is the HRP-catalyzed peroxidation of the mediator, Rxn. 2 represents electron hopping, and Rxn. 3 occurs at the electrode surface at potentials negative with respect to the half-wave potential (ca. 325 mV wrt. Ag/AgCl) of the mediator.

During experiments in brain tissue, we operate the microsensors at an applied potential of -100 mV wrt. Ag/AgCl. This 'low applied potential' is convenient because it prevents the oxidation of several substances present in brain tissue (ascorbate, urate, hydroquinones and their metabolites, etc.) directly on the electrode surface. The brain environment contains a high concentration of ascorbate, which can reduce the $[Os(bpy)_2(py)Cl]^{2+}$ form of the mediator and thereby interfere with the detection of hydrogen peroxide. To minimize the ascorbate interference, ascorbate oxidase, which produces water rather than hydrogen peroxide upon oxidation of ascorbate [51], is co-immobilized in the hydrogel. The hydrogel is coated with Nafion to further limit the permeability of ascorbate and to improve the biocompatibility of the microsensors.

Hydrogen peroxide is produced by several oxidase enzymes as they oxidize their substrates, some of which are compounds with significant functions in brain function, including

glucose, choline, and glutamate. Hence, microsensors for these substances can be prepared by co-immobilization of the relevant oxidase (glucose oxidase, choline oxidase, glutamate oxidase) in the hydrogel with HRP and ascorbate oxidase [52, 42-46, 48, 53-59].

For in vivo experiments with any of these microsensors, it is necessary to use a sentinel (see Experimental section, Films without SDS) sensor to assess the electrochemical background signal. The sentinel sensor is one constructed in similar fashion to the relevant microsensor except that a key enzyme is omitted from the hydrogel. For in vivo hydrogen peroxide measurements, HRP is omitted from the hydrogel. The sentinel electrode is placed in the tissue side-by-side with the microsensor. When a manipulation of the tissue produces a response at the microsensor without affecting the amperometric current at the sentinel electrode, the response can be attributed to the substance targeted by the microsensor.

The successful preparation of these microsensors requires redox polymer suitable for enzyme immobilization. However, we find that synthesis of the redox polymer may lead to a product that precipitates when added to aqueous enzyme solutions [45, 46, 49]. Casting hydrogels from the heterogeneous polymer-enzyme mixtures containing the precipitate may lead to discontinuous layers of uneven thickness [45] and microsensors with inadequate sensitivity and selectivity for in vivo experiments (vide infra).

To date, our strategy has been to repeat the polymer synthesis until a batch is obtained that provides adequate sensor performance. This strategy is practical because each sensor consumes microgram quantities of the polymer whereas the polymer can be synthesized in 100-mg quantities. So, a single batch of polymer provides a large number of sensors. However, the polymer synthesis is both labor-intensive and expensive, so we are interested in ways to improve the likelihood that individual batches of polymer will provide adequate sensor performance.

The present report describes the use of a surfactant, sodium dodecyl sulfate, as a reagent for preventing precipitation when the polymer is mixed with enzymes. The use of SDS for this purpose enables the successful preparation of sensors with a batch of polymer that is otherwise unsuitable for this purpose.

2.3 EXPERIMENTAL

2.3.1 Reagents

All reagents were used as received from their respective supplier. Horseradish peroxidase (EC 1.11.1.7, type II, HRP), ascorbate oxidase (EC 1.10.3.3; from *Cucurbita sp*., AAOx), L-ascorbate, dopamine, dihydroxyphenyl acetic acid (DOPAC), sodium hydrosulfite, and 2-bromoethylamine were from Sigma (St. Louis, MO). Nafion (5 % wt. solution in a mixture of lower aliphatic alcohols and water, 1100 equiv. wt. diluted to 0.5% with 2-propanol before use), ammonium hexafluorophosphate, 4-(2-hydroxyethyl)-1-piperazineethanesulfonic acid (HEPES), and HEPES sodium salt were from Aldrich (Milwaukee, WI). Poly(ethylene glycol 400 diglycidyl ether) (PEGDE) and poly(4-vinylpyridine) (MW 150-200K) were from Polysciences, Inc. (Warrington, PA). Sodium dodecyl sulfate (BioChemika Ultra for molecular biology) was from Fluka (St. Louis, MO). Potassium hexachloroosmate was from Alpha Aesar (Ward Hill, MA). 2,2´-Bipyridine was from Acros (Morris Plains, NJ). Anion exchange beads (AG1-X4) were from Bio Rad (Hercules, CA).

The batch of redox polymer used for this study was synthesized according to a published procedure [36] with the following two modifications: first, the amount of osmium complex (*cis*-

bis(2,2´-bipyridine-N,N´)di-chloroosmium(II) [60]) relative to the amount of poly (vinyl pyridine) was decreased by 75%. Generally, we have noticed that decreasing the amount of osmium complex improves the success of sensor preparation although polymer batches synthesized according to the modified procedure, including the batch described in this study, may still precipitate upon addition to enzyme-containing solution. Second, a higher molecular weight PVP was used.

2.3.2 Carbon Fiber Microelectrodes

Microelectrodes were prepared by sealing individual carbon fibers, (10-μm diameter, Thornell P-55 fibers, Union Carbide, Greenville, SC), in pulled borosilicate glass capillary tubes (1.0 mm O.D, 0.58 mm I.D.) (Sutter Instrument Co., Novato, CA) with a low viscosity epoxy (Spurr low viscosity embedding kit, Polysciences, Inc., Warrington, PA). The epoxy was cured at 80 ^{O}C, after which the fibers were cut to a length of 400 μm with a scalpel blade.

2.3.3 Hydrogel Films

The redox polymer (1 mg·mL^{-1}) and crosslinker (PEGDE, 3 mg·mL^{-1}) were dissolved in nano-pure DI water (Nanopure, Barnstead, Dubuque, IA). Enzymes were dissolved in HEPES buffer (pH 8.0) prepared by the addition of the HEPES sodium salt to a 10 mM solution of the acid. Redox polymer, HEPES buffer, and crosslinker were prepared fresh every three to four days, while enzymes were prepared fresh daily. The redox polymer, crosslinker, and enzymes were all prepared in borosilicate glass vials.

2.3.4 Films without SDS

Peroxide sensors were prepared by combining and thoroughly mixing aliquots of the redox polymer (20 μL, 1 mg·mL^{-1}), PEGDE (4 μL, 3 mg·mL^{-1}), AAOx (10 μL, 1400 U·mL^{-1}), and HRP (10 μL, 660 U·mL^{-1}) in a borosilicate glass vial. A precipitate formed rapidly after mixing. A 4-μL aliquot of the mixture was suspended on the end of a pipette tip and painted onto carbon fiber electrodes for 5 min. The sensors were dried at 37 ^{O}C for 1 hr, soaked in nanopure water for 15 min, dried in ambient air for 1 hour, and finally dipped in a 0.5% Nafion solution 7 times (3 seconds per dip) at 60-s intervals. The sensors were used immediately or were stored overnight in a desiccator at 4-6 ^{O}C.

During in vivo measurements, the peroxide sensor is used alongside a so-called sentinel microsensor, which is designed to provide a measure of the electrochemical background during in vivo measurements [8-15]. In previous work, sentinel microsensors have been referred to as background or control sensors. Sentinel microsensors were prepared in the same way as the peroxide microsensors except that the aliquot of HRP solution was replaced with 10 μL of HEPES buffer.

Two of the experiments reported herein involved an enzyme-free hydrogel containing Cu^{2+} ion. The hydrogel was cast from a solution containing the redox polymer (20 μL, 1 mg·mL^{-1}), PEGDE (4 μL, 3 mg·mL^{-1}), $CuSO_4$ (20 μL, 10 mM in nanopure water) and HEPES buffer (10 μL, 10 mM). The casting solution did not precipitate prior to casting, and a 4-μL aliquot of the mixture was painted onto carbon fiber electrodes for either 5 or 10-20 min. These hydrogels were not coated with Nafion.

2.3.5 Films with SDS

The redox polymer (10 μL, 1 mg·mL^{-1}) and SDS (20 μL, 1 mM) were combined and mixed thoroughly. This produced a turbid, colloidal-like suspension containing particles too small to be seen under 40x magnification. Several transmission electron microscopy (TEM) images of the turbid, colloidal-like suspension upon drying are depicted in Appendix A. The redox polymer/SDS mixture was then combined and mixed with PEGDE (4 μL, 3 mg·mL^{-1}), AAOx (10 μL, 1400 U·mL^{-1}), HRP (10 μL 660 U·mL^{-1}), and HEPES buffer (10 μL, 10 mM). No precipitation was observed upon addition of the enzymes and crosslinker to the mixture of polymer/SDS mixture; however, the mixture remained turbid. A 4-μL aliquot of the mixture was suspended on the end of a pipette and painted onto carbon fiber electrodes for 10 min. A longer deposition time was used because deposition from the SDS-containing solutions was slower. In the absence of SDS, the precipitate, which is insoluble in water, built up rapidly on the carbon fibers. This did not occur when the SDS was used to prevent the precipitation, so the deposition time was increased. The hydrogels were cured, soaked, dried, and coated with Nafion by the same procedure described for hydrogels prepared without SDS.

2.3.6 Electrochemical Techniques

Amperometry was performed with the microsensors immersed in a 50-mL cell containing 40 mL of well stirred artificial cerebrospinal fluid (aCSF: 145 mM Na^+, 1.2 mM Ca^{2+}, 2.7 mM K^+, 1.0 mM Mg^{2+}, 152 mM Cl^-, 2.0 mM phosphate, pH adjusted to 7.4 with NaOH). Most experiments were performed at room temperature (ca. 22 ^{O}C). However, sensor calibration (see Figure 8) was performed at body temperature, 37 ^{O}C. The amperometry was carried out in 2-

electrode mode, i.e., without an auxiliary electrode. The second electrode was a Ag/AgCl reference electrode. The potential applied to the sensors was amplified with a potentiostat made in-house. The current signal was amplified with a current amplifier (Keithley, model 428, Cleveland, OH). The gain and filter rise time settings on the current amplifier were typically set to 10^8 to 10^9 $V \cdot A^{-1}$ and 100 to 300 ms, respectively. The amplifier output was digitized at a 20 kHz sampling rate with a 12-bit digital-to-analog converter (Labmaster PGH-DMA, Scientific Solutions, Solon, OH). Standard solutions were prepared in aCSF and were added manually to the cell with a pipette.

2.3.7 Animal and Surgical Procedures

In vivo experiments were carried out on male Sprague-Dawley rats (Hilltop Lab Animals Inc., Scottdale, PA, USA), with the approval of the Institutional Animal Care and Use Committee of the University of Pittsburgh. The rats weighed between 250 and 375 g, and were anesthetized with an initial dose of chloral hydrate (400 mg/kg i.p.) and given atropine (0.1 $mg \cdot kg^{-1}$ i.p.). Subsequent chloral hydrate was delivered when gentle pressure to the hind paw resulted in any detectable motor response. The anesthetized rats were placed in a stereotaxic surgical frame with the incisor bar positioned 5 mm above the interaural line[61], and were wrapped in a homeothermic blanket that maintained body temperature at 37 ^{O}C. A midline incision made through the scalp allowed the scalp to be retracted and the skull exposed. Holes drilled in appropriate positions through the skull with a Dremel™ tool permitted the placement of the electrodes and microinfusion pipette. A peroxide sensor was positioned in the striatum, at a point 4.5 mm below dura, 2.5 mm anterior to bregma, and 2.5 mm lateral to the midline. A sentinel sensor was placed in the same coronal plane, approximately 150 μm away, at an 8^{O}

angle to the peroxide sensor. A salt bridge, created by placing a Kimwipe® in the tapered end of a 1-mL disposable pipette tip filled with aCSF, functioned as the electrical contact between the brain and a Ag/AgCl reference electrode. This was typically placed in a small hole drilled in the anterior-most region of the exposed skull, away from the sensors.

Microinfusion pipettes were prepared from fused silica capillary tubing (25±1 μm I.D.; 360 μm O.D.) (Polymicro Technologies Inc., Phoenix, AZ, USA). The outlet end was etched to 35-40 μm O.D. with hydrofluoric acid, while the inlet end was attached to a 50-μL Gastight ™ syringe (Hamilton, Reno, Nevada, USA) mounted on a microprocessor-controlled driver (NA-1, Sutter Instruments, Novato, CA, USA).

2.4 RESULTS AND DISCUSSION

2.4.1 Microsensors Based on Enzymes Entrapped in a Polymeric Redox-Hydrogel

Figures 1-3 are photographs taken through a microscope that show the casting of an enzyme-containing hydrogel onto carbon fiber microelectrodes. The casting solution is an aqueous mixture containing the redox polymer, crosslinking agent, HRP, and AAOx. The polymer-enzyme mixture in Figure 1 contains a precipitate that formed when the polymer was mixed with the enzymes in a borosilicate glass vial. The precipitate particles are of a similar dimension to the carbon fiber. Figure 2 illustrates that the precipitate adheres to the electrode, and to itself (i.e., flocculation), as the polymer-enzyme mixture is passed over the electrodes. Before the sensors are dried, as long as they remain in contact with the aqueous casting mixture, the precipitate remains swollen. After drying for as little as 30 s however, the hydrogel shrivels around the electrode (Figure 3). In the case of the latter, the resultant hydrogel film was uneven and discontinuous.

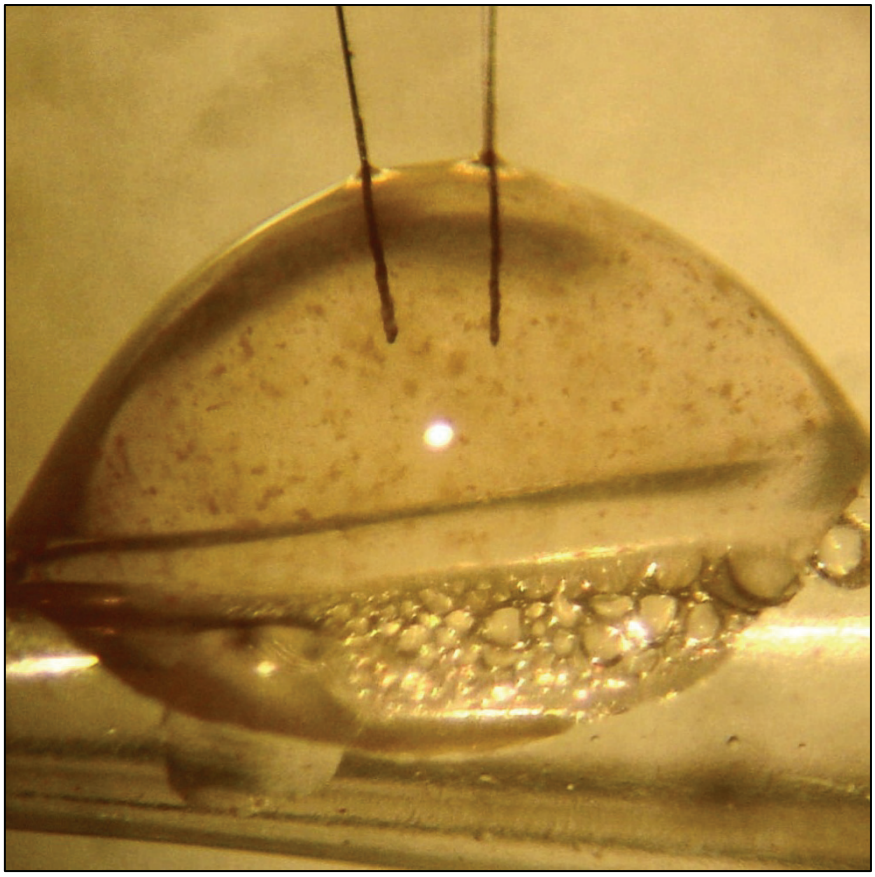

Figure 2-1. Photograph of two carbon fiber microelectrodes in a droplet of the casting mixture containing the redox polymer, crosslinker, horseradish peroxidase, and ascorbate oxidase. Note the presence of precipitate.

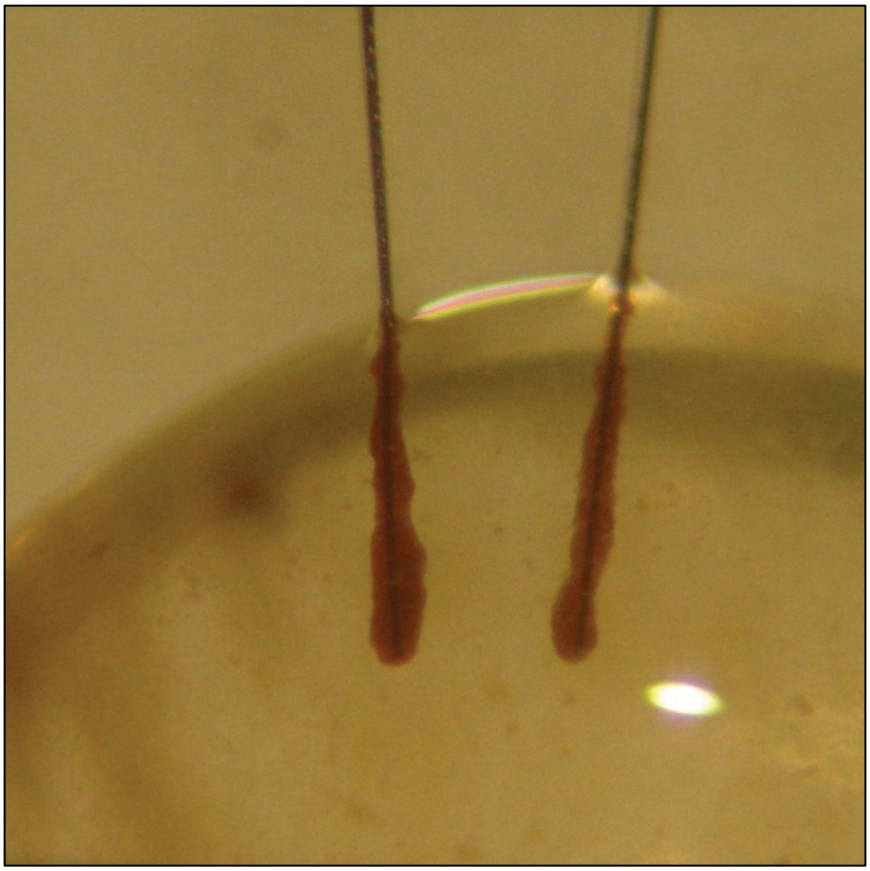

Figure 2-2. The precipitate depicted in Figure 1 adheres to the microelectrodes and to itself as the drop containing the casting solution is passed over the electrodes.

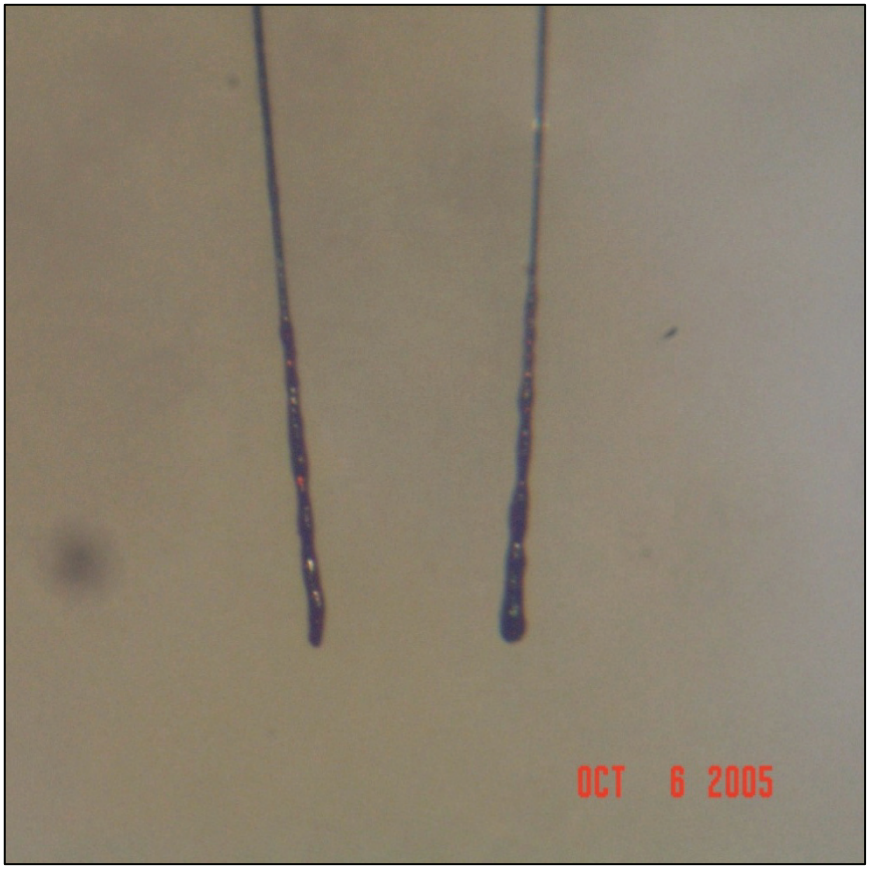

Figure 2-3. The precipitate that adhered to the electrode in Figure 2 shrivels, forming an uneven and discontinuous layer upon drying.

Brain tissue contains several biogenic amine neurotransmitters and their acidic metabolites, many of which can be classified as hydroquinones (e.g., dopamine and DOPAC). These substances are electroactive and are themselves the frequent targets of electrochemical measurements in brain tissue [7]. Thus, it is important that the microsensors do not exhibit a response to these substances. However, the microsensors prepared as in Figures 1-3 do respond to hydroquinones (Figure 4). Amperometric responses were recorded with peroxide and sentinel microsensors. Both microsensors initially exhibited a cathodic amperometric response upon addition of an aliquot of 2.5 μM dopamine to the electrochemical cell (Figure 4). This concentration of dopamine is in the physiologically interesting range [7]. Responses obtained at the peroxide microsensors are larger than that obtained at the sentinel electrodes (Figure 4). Similar responses were obtained upon addition of other hydroquinones to the cell, including pyrocatechol, 4-methylcatechol, DOPAC, L-Dopa, 1,4-dihydroxybenzene, and norepinephrine to the cell (data not included). Note: In the case of L-dopa, sensors produced a cathodic amperometric response typically only after in vivo use. These results show that the deposition of enzyme-entrapping hydrogel in the presence of the precipitate (Figures 1 to 3) compromises the selectivity of the microsensors.

The fact that the sensors used to generate Figures 1 to 3 respond to hydroquinones prevents their use for peroxide measurements in the brain. In a previous report, we have described sensors that did not respond to hydroquinones [48]. However, the sensors in our previous report were prepared with a different batch of the redox polymer. Thus, we attribute the change in the selectivity of the sensors to the fact that a different batch of polymer was used in each case. Rather than discarding the current batch, we are interested in knowing if it is possible to prepare selective sensors with it.

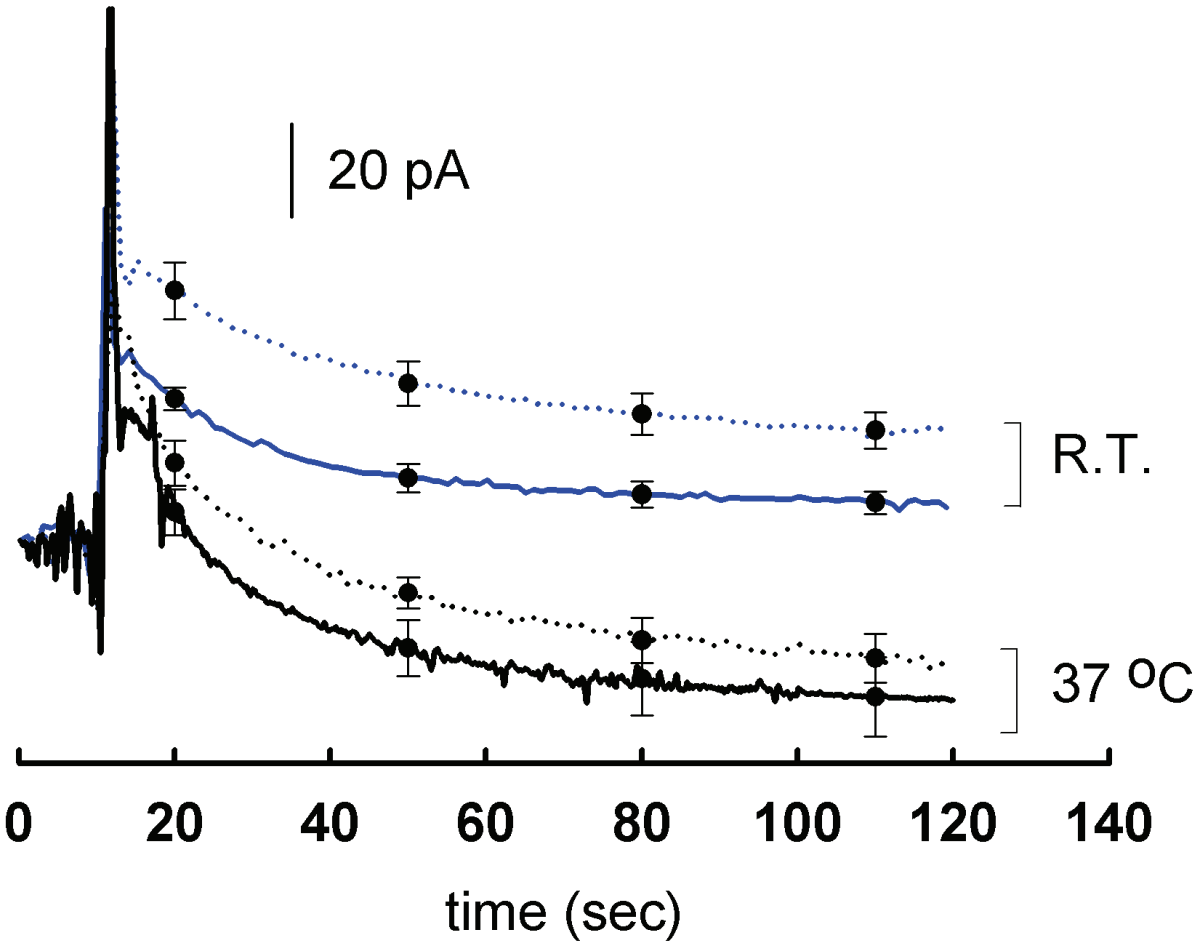

Figure 2-4. Responses of peroxide (dotted line; n=8) and sentinel (solid line; n=8) sensors upon addition of 2.5 μM dopamine at t=10 s to the electrochemical cell ($E_{applied}$= -100 mV). The current at t=0 is zero. Experiments were carried out in a well-stirred beaker of aCSF maintained at room temperature or 37 ^{O}C. Peroxide sensors contain HRP and AAOx, while sentinel sensors contain only AAOx. The standard error is depicted at several time points following the addition of dopamine.

Since the initial response to hydroquinones was cathodic, it is most likely due to the reduction of quinones produced by chemical oxidation of the hydroquinones. This raises the question of why the hydroquinones are oxidized by a component of the hydrogel/enzyme film during these experiments. No amperometric response was observed when plain carbon fiber microelectrodes were used, i.e., microelectrodes without a hydrogel layer (data not shown). Furthermore, no amperometric responses were observed at microelectrodes coated with enzyme-free hydrogels (data not shown). Together, these observations suggest that the entrapped enzymes are causing the oxidation of hydroquinones to quinones within the hydrogel.

2.4.2 Amperometric Holding Potential

To further characterize the amperometric response to dopamine, amperometric responses were recorded at several applied potentials (Figure 5). Similar cathodic responses were observed

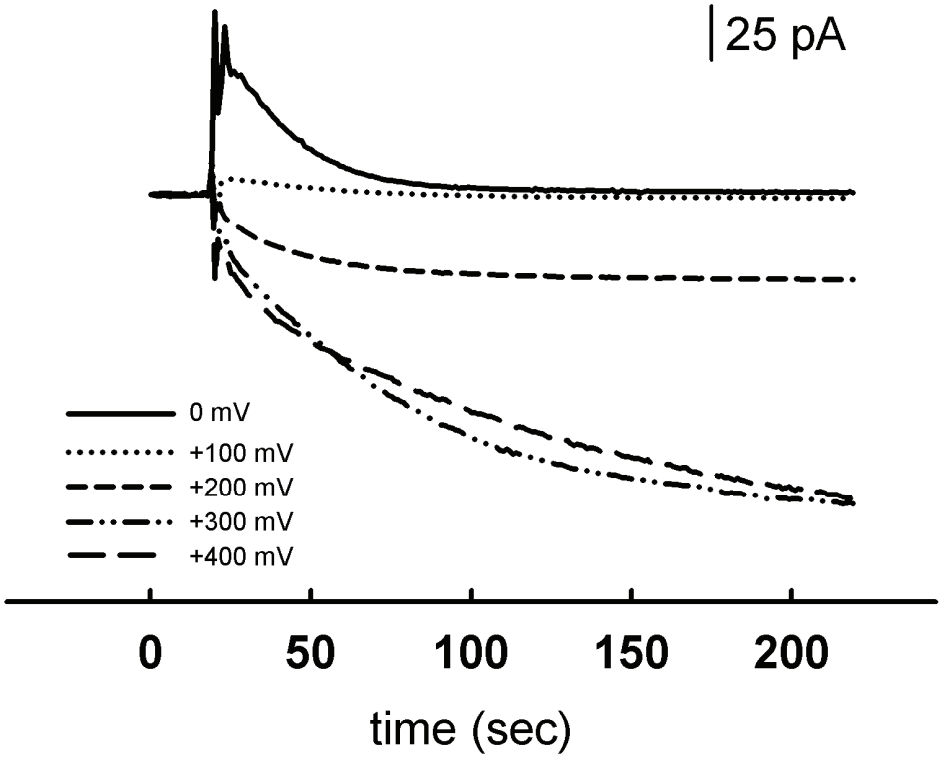

Figure 2-5. Responses of a sentinel sensor upon addition of dopamine (2.5 μM at t=20 s) to the electrochemical cell containing well-stirred aCSF at 25 ^{O}C. Responses were observed at applied potentials between 0 and 400 mV wrt. Ag/AgCl. The hydrogel was deposited from a mixture that contained precipitate. Cathodic responses at potentials below 100 mV are due to the reduction of dopamine-o-quinone. Anodic responses at potentials above 100 mV are due to the oxidation of dopamine.

at applied potentials of -100 and 0 mV Ag/AgCl. Only a small response was observed at an applied potential of +100 mV. Anodic responses were obtained at potentials more positive than +100 mV, which is attributable to the oxidation of dopamine at the surface of the carbon fiber microelectrode, as expected. The anodic responses confirm that hydroquinones penetrate the hydrogel and reach the underlying carbon surface. An interesting contrast exists between the cathodic responses observed at applied potentials less than +100 mV, which are transient in nature, and the anodic responses observed at applied potentials greater than +100 mV, which are steady state in nature (Figure 5): this is discussed further below.

We hypothesize that the oxidation of hydroquinones occurs due to the presence of denatured enzymes within the hydrogel. Denaturation of HRP and AAOx leads to the exposure of their reactive metal centers, iron and copper ions, respectively. This enables those metal centers to serve as non-selective redox catalysts. Metal ions are well known to catalyze hydroquinone oxidation [62-67] (Scheme I). This hypothesis explains that peroxide microsensors exhibited a larger cathodic response than the sentinel microsensors (Figure 4) because the hydrogels in the former entrap more enzymes. It should also be noted that metal-catalyzed hydroquinone oxidation produces hydrogen peroxide (Scheme I[1]), which might also contribute to the response.

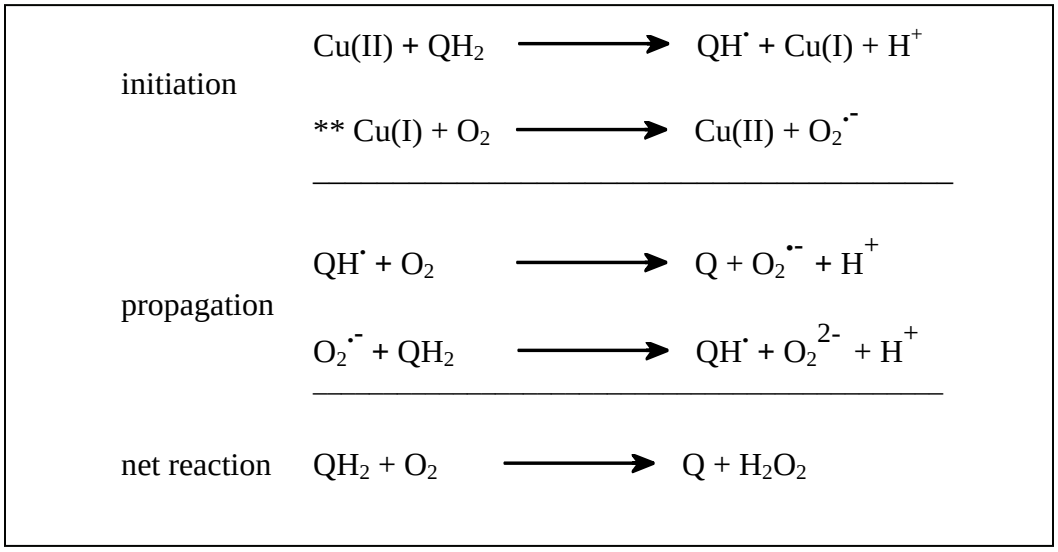

Scheme 1. A proposed mechanism for the metal-catalyzed oxidation of hydroquinones[1]. **This 'initiation' reaction is not necessary for propagation to occur, but may result in the presence of oxygen.

2.4.3 Oxidation of Dopamine by Incorporation of $CuSO_4$ in the Redox Hydrogel

To test the hypothesis that metal ions within the hydrogel could catalytically oxidize dopamine, copper (II) sulfate was added to enzyme-free hydrogel. Sensors coated for 5 or 10-20 minutes with this Cu^{2+} containing hydrogel were prepared (see Experimental section). Sensors coated for 5 min produced a cathodic response upon addition of dopamine (2.5 μM) to the cell (Figure 6B), confirming that metal ions in the hydrogel catalyze hydroquinone oxidation. Similar to the responses observed at peroxide and sentinel sensors, the responses were transient (i.e., the current reached a maximum within seconds, and immediately afterwards began to return

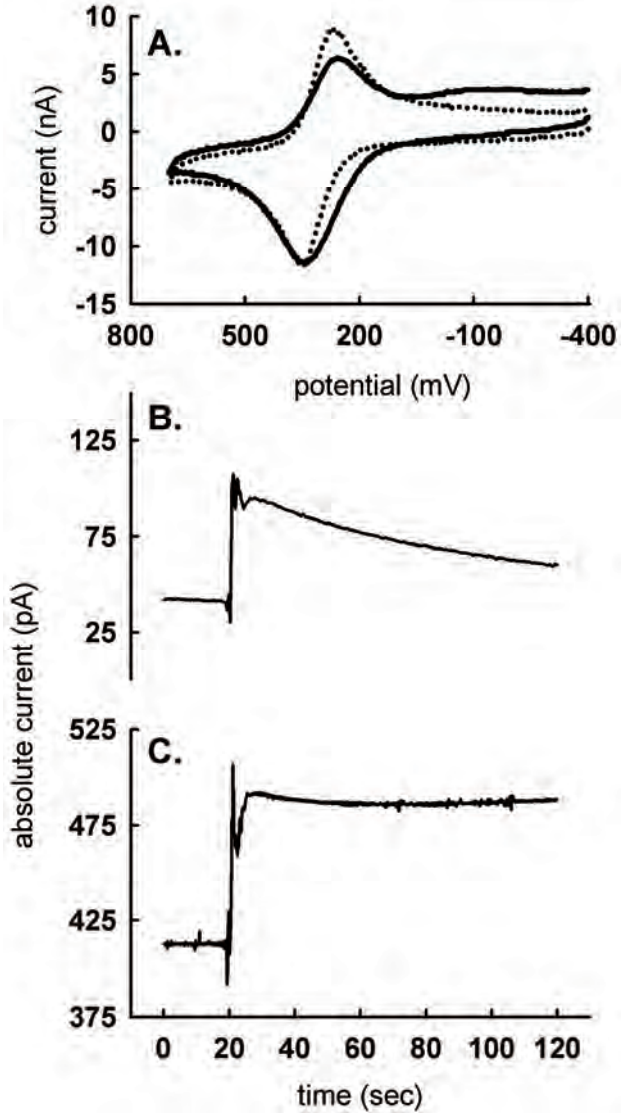

Figure 2-6. A) Cyclic voltammogram (υ = 100 mV·s^{-1}) of an electrode containing a hydrogel with (solid line) and without (dotted line) Cu^{2+} ions. B) Response of carbon fiber microelectrodes (n=6) coated with a hydrogel film containing Cu^{2+} for 5 min, to the addition of dopamine (2.5 μM at t=20 s). C) Response of carbon fiber microelectrodes (n=6) coated with a hydrogel film containing Cu^{2+} for 10-20 min, to the addition of dopamine (2.5 μM at t=20 s). All experiments were performed in well-stirred aCSF at 25 ^{O}C; $E_{applied}$ = -100 mV for amperometric experiments. Sensors were not coated with Nafion.

towards the baseline). We also noticed that these Cu^{2+} containing sensors had a larger background current than peroxide and sentinel sensors (Figure 6B). An example of the background current at sentinel sensors is shown in Figure 7. In the case of sensors coated for 5 min, the background current averaged ca. 40 pA (Figure 6B). A cyclic voltammogram (Figure 6A) shows that this is due to the reduction of the Cu(II) ion within the hydrogel.

Sensors coated for 10-20 min likewise produced a cathodic response upon addition of dopamine (2.5 μM) to the cell (Figure 6C). However, the background current of these sensors was much greater, and the response following the addition of dopamine (2.5 μM) reached a steady state, as opposed to falling back towards the baseline.

The responses at peroxide sensors (Figure 4), sentinel sensors (Figure 4), and sensors coated for only 5 minutes with the Cu^{2+} containing hydrogel (Figure 6B), appear to indicate that the involvement of oxygen in the metal-catalyzed oxidation of hydroquinones within the film provides an explanation for the transient nature of the cathodic amperometric responses. Although metal ions initiate the oxidation of hydroquinones, oxygen is consumed by the propagation reactions. Hence, the rate of oxidation could be limited by the availability of oxygen, which is depleted during these reactions. This mechanism is also supported by amperometric responses following two sequential additions of DOPAC, recorded at sentinel microsensors. The microsensors exhibited a transient cathodic response upon addition of DOPAC (20 μM) to the cell (Figure 7). Five minutes later, a second addition of DOPAC (to bring the final concentration up to 40 μM) produced a substantially smaller response (Figure 7). This result confirms that the transient nature of the cathodic response is not due to a limited supply of the hydroquinone. Thus, the transient responses in Figure 4 and Figure 6B appear to be the result of propagation reactions depleting oxygen within the hydrogel.

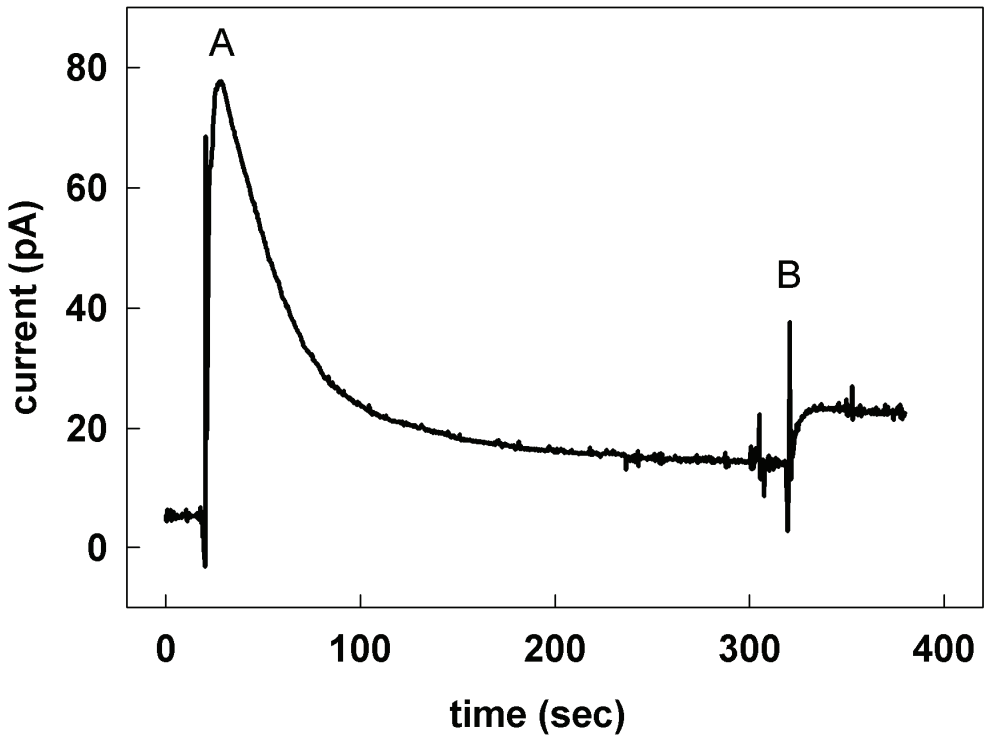

Figure 2-7. Average response of sentinel sensors (n=7) to the addition of DOPAC (A: 20 μM at t= 20 s.); $E_{applied}$ = -100 mV. A second addition of DOPAC (B: at t=320 s) increased the DOPAC concentration from 20 to 40 μM. Measurements were conducted in well-stirred aCSF (pH 7.40) at 25 ^{O}C.

Based on the above mechanism, we would expect the response at the sensors in Figure 6C to fall towards the baseline following exposure to dopamine. This however, does not occur. Instead, dopamine produces a steady state response, suggesting oxygen is not being depleted as rapidly from the hydrogel as sensors coated for only 5 min . The response observed in Figure 4C appears to indicate the involvement of H_2O_2 in the metal-catalyzed oxidation of hydroquinones within the film (Scheme II). The greater Cu^{2+} loading of the sensor in Figure 6C appears to have oxidized a greater amount of hydroquinone, and resulted in the formation of a larger amount of H_2O_2 within the hydrogel, hence explaining why this response was observed at this sensor, but not at sensors coated for shorter durations. Since H_2O_2 could not be produced without oxygen,

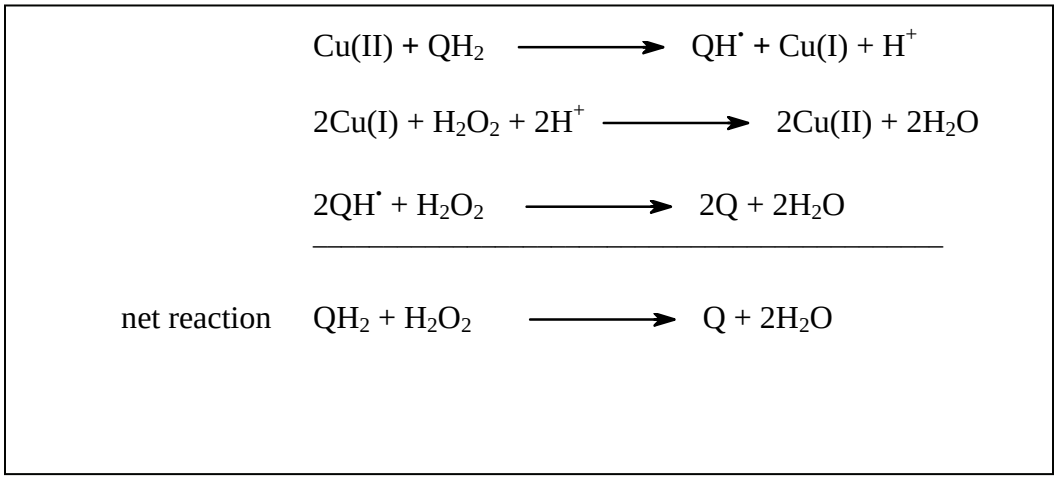

Scheme 2. Proposed role of hydrogen peroxide, in the metal-center catalyzed oxidation of hydroquinones.

yet a steady state response is seen at this sensor, the rate at which oxygen is depleted from the hydrogel in the presence of hydroquinone appears to be a function of concentration of H_2O_2 present. Specifically, the greater concentration of H_2O_2 present, the less rapidly oxygen is depleted from the hydrogel. In Figure 8, peroxide (50 μM) was added to a sentinel sensor equilibrated in the presence of a large concentration of DOPAC (1.5 mM). This figure additionally supports our hypothesis that in the presence of peroxide, in this case—an external source, oxygen levels are not depleted from the hydrogel as rapidly. Figure 8 also demonstrates that steady state responses can be achieved at sensors that do not contain added Cu^{2+} ions.

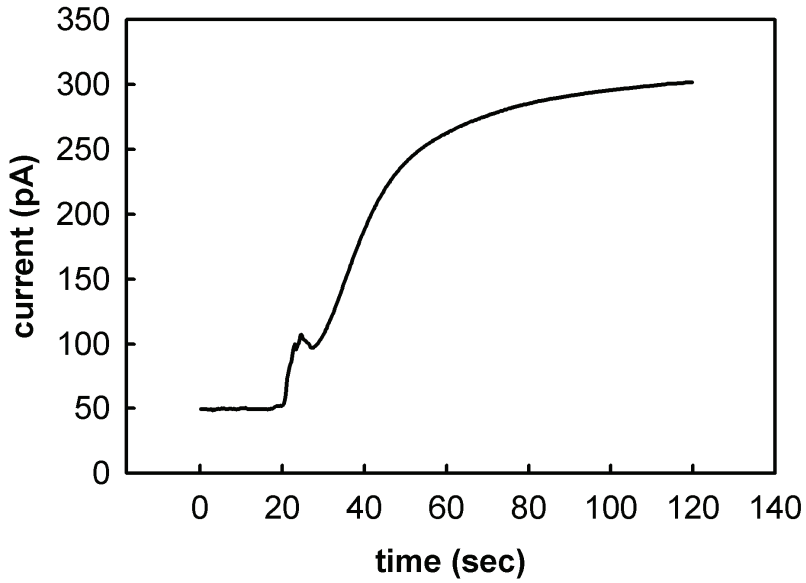

Figure 2-8. A sentinel sensor (n=1), held at -100 mV wrt. Ag/AgCl, equilibrated in 50 μM H_2O_2, and exposed to 1.5 mM DOPAC at t=20 s. Experiments were carried out at room temperature, in a well stirred beaker of aCSF.

2.4.4 Correlation between Hydroquinone Concentration and Amperometric Response

To further characterize the amperometric response to dopamine, sentinel sensors were exposed to 0.25, 0.50, 1.0, and 2.0 μM dopamine (Figure 9A) at t=20 s. The sensors were held amperometrically at -100 mV wrt. Ag/AgCl, in a well-stirred beaker of 37 ^{O}C aCSF. The greater the concentrations of dopamine sensors were exposed to, the larger the transient increase in reductive current that followed. This point is illustrated more clearly in Figure 9B. In fact, there appears to be a linear correlation between the maximum amplitude of the transient increase in reductive current and the concentration of dopamine (r^2= 0.981).

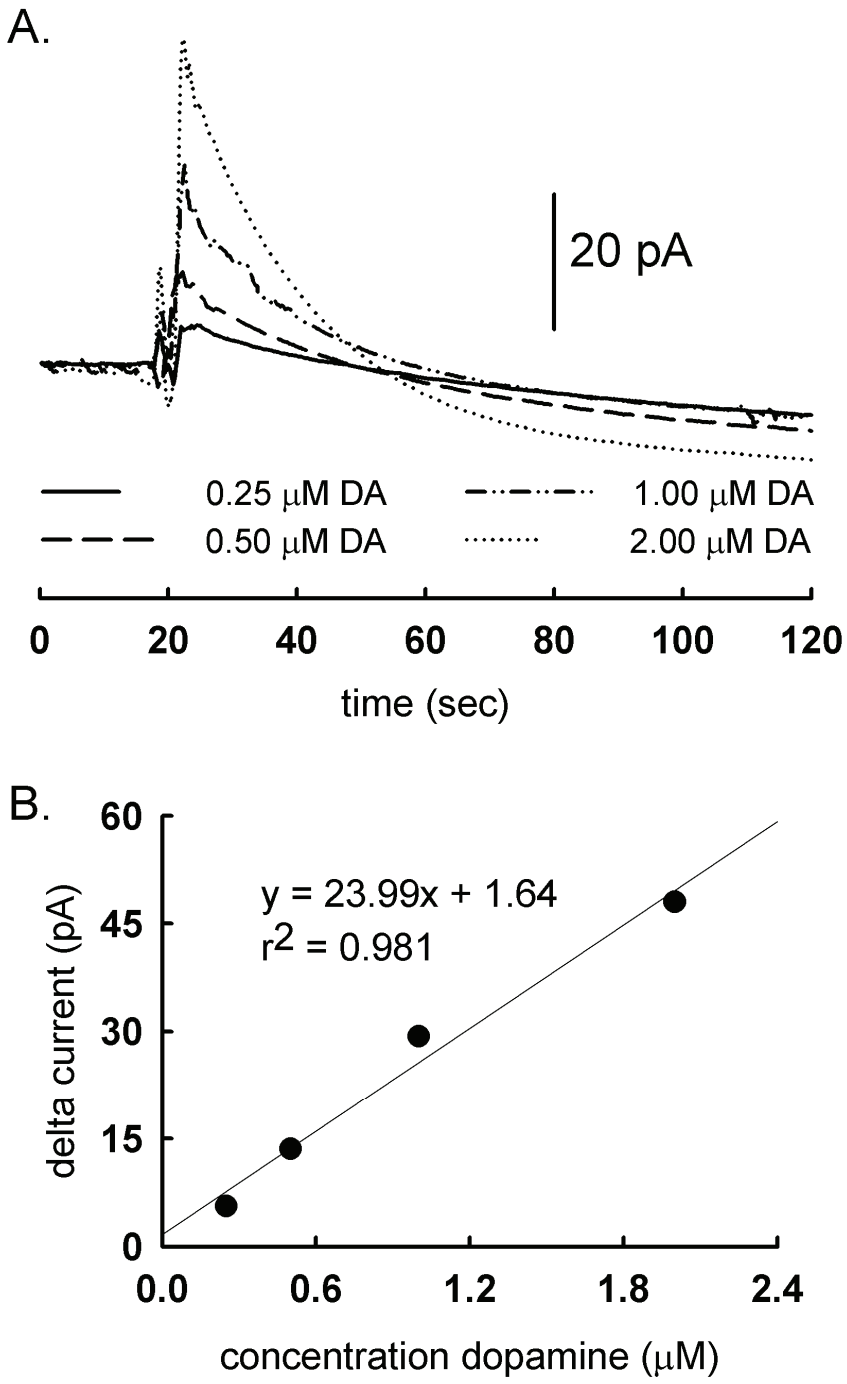

Figure 2-9. A) Responses of a sentinel sensor held amperometrically (-100 mV wrt. Ag/AgCl) upon exposure to 0.25, 0.50, 1.00, and 2.00 μM DA at t=20 s. Responses were gathered in a stirred beaker of aCSF at 37 ^{O}C. B) Linear relationship between the amplitude of the transient amperometric response and dopamine concentration.

2.4.5 Correlation between Rate of Exposure to Hydroquinones and Amperometric Response

In the Methods and Materials section, we mentioned that solutions were prepared by adding a known amount of standard to the cell using a pipette. This is important to note because the amplitude of the transient rise in reductive current is dependent on the rate at which the sensors are exposed to dopamine. The more rapidly the concentration of dopamine in the beaker is elevated, the greater the flux of dopamine into the hydrogel, and the greater the amount of dopamine oxidized by the exposed metal centers. When dopamine is pipetted into a stirred beaker, the concentration of dopamine in the beaker is elevated rapidly. As a result, a relatively large amount of ortho-quinone is generated within the hydrogel and reduced at the electrode surface. This produces a large transient increase in reductive current. When the concentration of dopamine is elevated over a longer period of time, the increase in reductive current is much smaller, and no longer transient (Figure 10). In Figure 10, a sentinel sensor operated amperometrically (-100 mV wrt. Ag/Ag/Cl) was placed in a well-stirred solution of aCSF (25 ^{O}C) and ramped from 0 to 2.5 μM dopamine over a 15 min period. The resulting increase in reductive current was about 1 pA. Compared to a similar experiment carried on sentinel sensors in which the dopamine concentration was increased from 0 to 2.5 μM in a matter of seconds with a pipette (Figure 4), the increase in reductive current observed is small in comparison (ca. 1/10 to 1/20th of the amplitude). This observation is consistent with the idea that quinones are short-lived species[68], and without the formation of a large amounts of quinone in a short period of time, there will not be a large increase in reductive current.

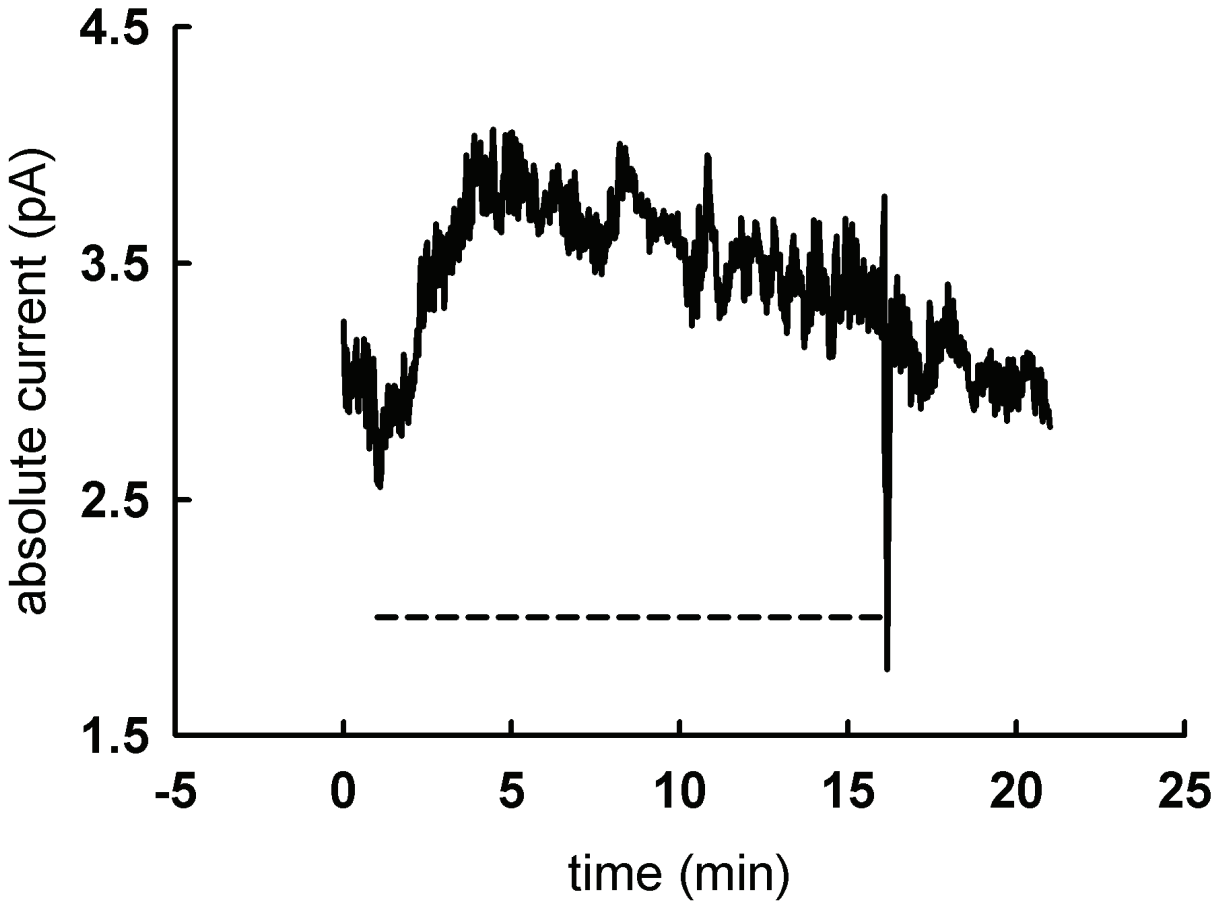

Figure 2-10. Response of a single sentinel sensor held amperometrically at -100 mV wrt. Ag/AgCl as the concentration of dopamine is ramped from 0 to 2.5 μM over a 15 minute period. The dashed line is the time over which the infusion occurred. The experiment was conducted in room temperature aCSF, in a stirred beaker.

2.4.6 Amperometric Response to Hydroquinones in the Presence of Ascorbic Acid

Reaction 4

$$AA + Q \longrightarrow H_2Q + DHA$$

Ascorbic (AA) acid reacts with quinones (Q) to generate dehydroascorbic acid (DHA) and the corresponding hydroquinone (Rxn.4). Sensors that contain exposed metal centers which are not coated with Nafion, or which contain a thin Nafion film, do not produce a transient increase in reductive current when exposed to hydroquinones in the presence of ascorbic acid (Figure 11).

Although ascorbic acid effectively eliminates the transient increase in reductive current that arises from the generation of quinones, the $[Os(bpy)_2(py)Cl]^{2+}$ form of the mediator reacts with ascorbic acid. Ascorbic acid must be kept out of the hydrogel for the Os-mediator to function properly, and hence cannot be relied upon to eliminate the response from hydroquinones.

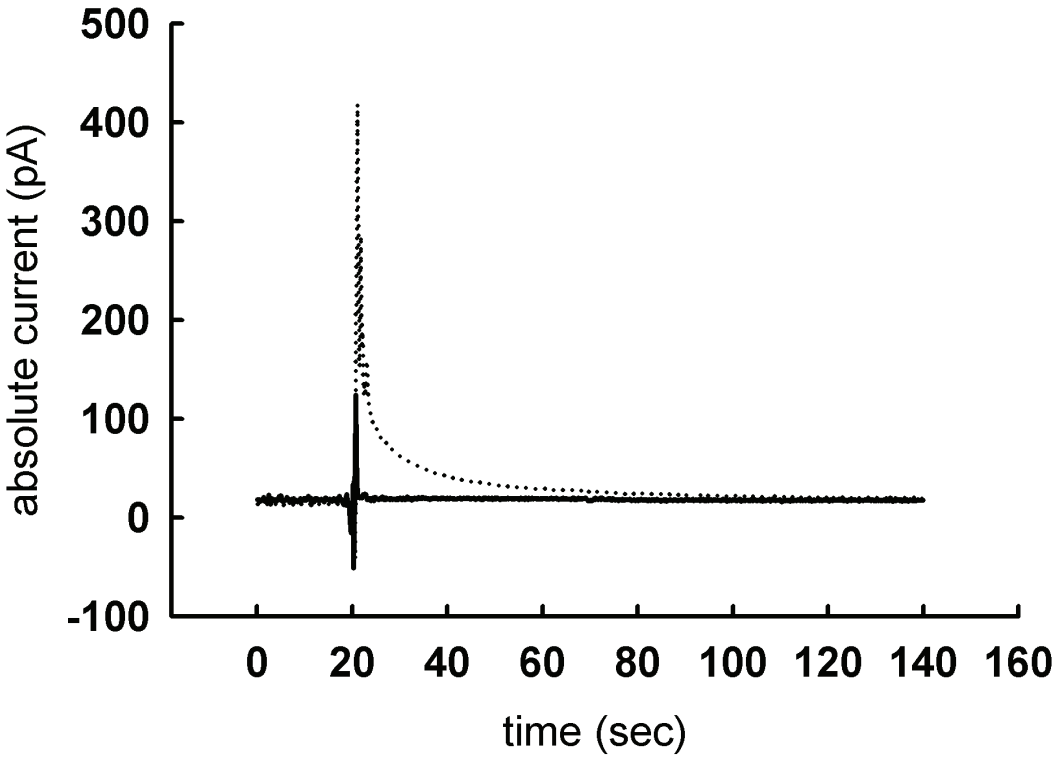

Figure 2-11. Response of a sentinel sensor upon the addition of dopamine (2.5 μM) to the electrochemical cell (t=20 s), in the presence (solid line) and absence (dotted line) of 400 μM ascorbate. When the sensor was evaluated in the presence of ascorbate, it was equilibrated in 400 μM ascorbate until the background current remained constant: at this point dopamine was added. Experiments were conducted in room temperature aCSF, in a stirred beaker.

2.4.7 Treating Sensors with EDTA to Remove Metal Centers

Since we are concerned with exposed metal centers reacting with hydroquinones, we hypothesized that treating the sensors with a chelating agent such as ethylenediaminetetraacetic acid (EDTA) would remove the exposed metal centers from the sensors. To test this hypothesis, we soaked hydrogen peroxide sensors, sentinel sensors, and sensors in which $CuSO_4$ was added to an enzyme free redox hydrogel in a stirred solution of 2 mM EDTA (pH= 7.40) for several minutes. The sensors were then removed from the EDTA solution, placed in a fresh beaker of aCSF, and exposed to 2.5 μM dopamine. Similar to the response obtained before soaking in EDTA, all sensors produced a transient increase in reductive current similar to those in (Figure 4). This treatment was unsuccessful at removing the metal centers. The above experiment was repeated, however, 2.5 μM dopamine was added to the sensors that were soaking in the EDTA solution. Using this approach, EDTA appeared to remove nearly all of the Cu (II) from sensors in which Cu (II) was added to the redox hydrogel (Figure 12). This is evident from the lower amperometric current that results when the sensor is operated amperometrically (-100 mV wrt. Ag/AgCl) in the presence of aCSF, and the absence of a response following exposure of the sensor to dopamine. This approach, however, remained ineffective for the removal of exposed metal centers from hydrogen peroxide and sentinel sensors (data not shown).

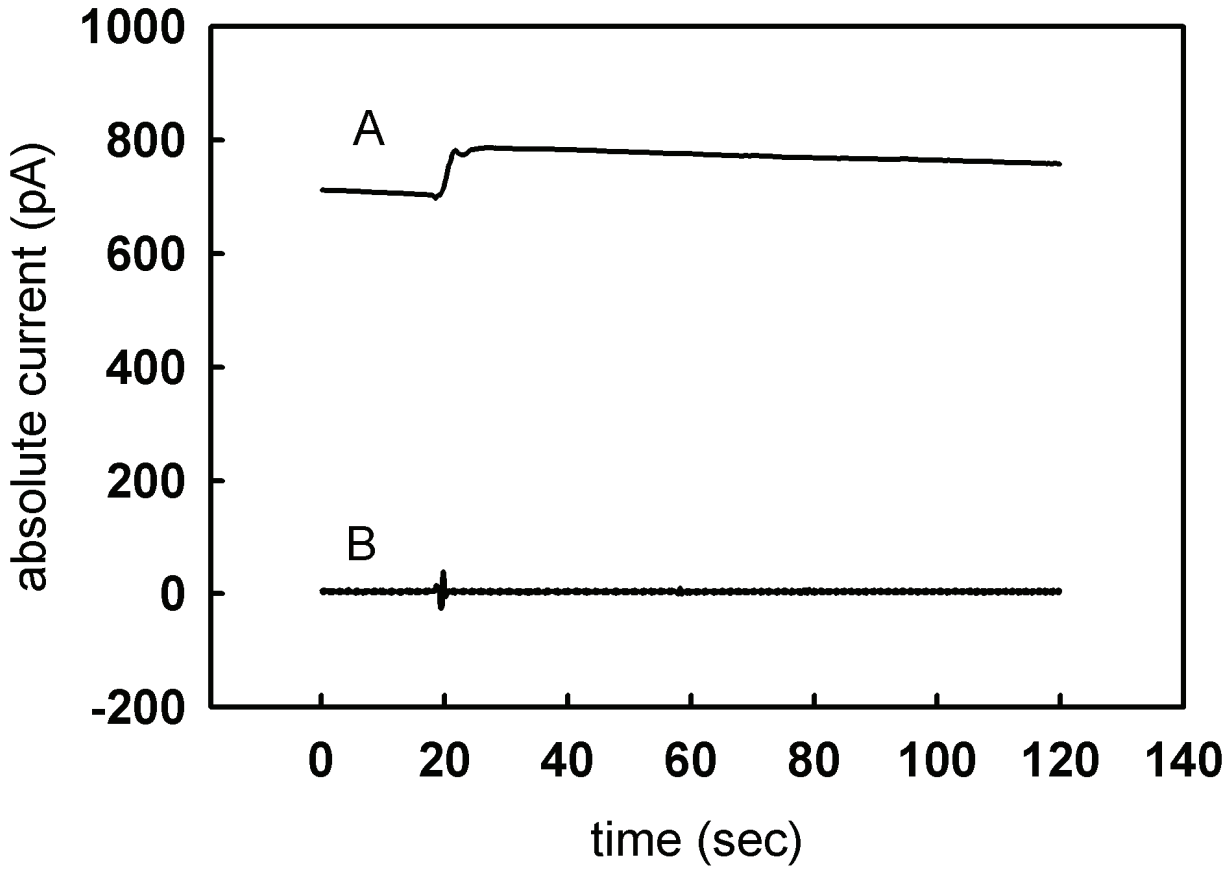

Figure 2-12. Responses following the addition of 2.5 μM dopamine (t=20 s), of a sensor coated for 10-20 min with a mixture of Cu^{2+}, redox polymer, and crosslinker, before (A) and after (B) co-treatment with dopamine and EDTA . The experiment was conducted in aCSF (pH= 7.40), in a stirred beaker, at 25 ^{O}C.

2.4.8 In Vivo Use of Sensors Prepared Without SDS

Peroxide and sentinel sensors were evaluated in vivo. Experiments were performed in the striatum of chloral hydrate anesthetized rats. In one set of experiments, responses at peroxide and sentinel sensors were evaluated in rats administered S-(-)-carbidopa (100 $mg \cdot kg^{-1}$ i.p.), followed by L-dopa (200 $mg \cdot kg^{-1}$ i.p.). This is the same drug combination that, in a previous investigation with these style of sensors, induced an increase at peroxide sensors in vivo, but not at peroxide control sensors[47].

Carbidopa is administered 30 min before L-dopa to selectively inhibit peripheral decarboxylase enzymes from oxidizing L-dopa before it reaches the brain. The peripheral nervous system is part of the vertebrate nervous system and constitutes the nerves outside of the central nervous system, including the cranial nerves, spinal nerves, and sympathetic and parasympathetic nervous systems. Administration of L-dopa following inhibition of peripheral decarboxylase enzymes is believed to increase blood levels of L-dopa, and consequentially lead to increased penetration in the brain [69]. Brain decarboxylase enzymes (e.g., Dopa decarboxylase) are not much affected by carbidopa [69]. As a result, there is a marked accumulation of catecholamines in brain tissue, particularly dopamine.

Repeating the in vivo carbidopa/L-dopa experiment described above using sensors prepared without SDS produced results that displayed a large degree of variability. Thus, each experiment was evaluated on an individual basis. The results of four of these experiments are depicted in Figure 13, where peroxide and sentinel sensors are identified as “p” or “s”, respectively. The sensors used in Figure 13D were prepared from a different batch of polymer than the sensors used in the remainder of Figure 13 to demonstrate that the responses following the administration of carbidopa/L-dopa are not just isolated to sensors prepared from a single

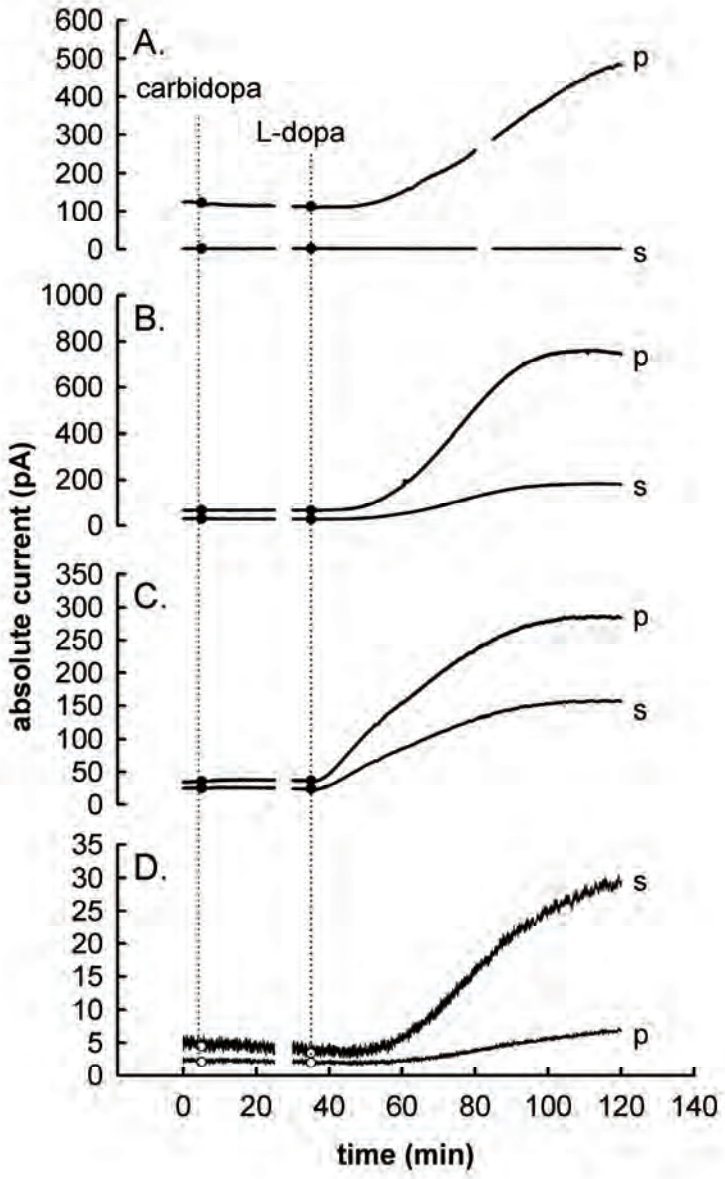

Figure 2-13. Responses at peroxide (p) and sentinel (s) sensors prepared without SDS in the striatum of anesthetized rats upon administration of carbidopa (100 mg·kg^{-1} i.p.) and L-dopa (200 mg·kg^{-1} i.p.). Sensors are operated amperometrically (-100 mV wrt. Ag/AgCl).

batch of polymer, and, although the responses differed quantitatively, they remained similar qualitatively. In some instances, the results obtained were consistent with those reported by Kulagina and Michael (e.g., Figure 13A) [47]. Other times, however, responses obtained at peroxide control sensors were also quite large (Figure 13B and Figure 13C). Although atypical, sentinel sensors occasionally produced responses greater than peroxide sensors (Figure 13D). Pre- and post-calibration sensitivities of the sensors used in Figure 13 are depicted in Appendix D. The large amperometric response at sentinel sensors appears to be the result of a non-selective reaction, perhaps similar to that depicted in Figure 8. Thus, it is likely the response at the peroxide sensors may also be due to a non-selective reaction.

As evident from Figure 4, sensors that possess a greater enzyme load contain more exposed metal centers, and are more reactive toward hydroquinones. Thus, it is foreseeable that if the in vivo responses of the sensors following the administration of carbidopa/L-dopa is non-selective and arises from exposed metal centers, coating the peroxide and sentinel sensors for the same, yet 'right amount of time', may result in responses similar to that observed in Figure 13A.

In Schemes 1 and 2, we indicated the involvement of both oxygen and peroxide in the metal-catalyzed oxidation of hydroquinones. We also provided evidence suggesting that in the presence of peroxide, oxygen was not as depleted as rapidly from the hydrogel, and as a result, steady state responses could be observed at sensors exposed to hydroquinones (Figure 6 and Figure 8). Hydrogen peroxide is also likely to be produced following the carbidopa/L-dopa experiment, because with an increase in dopamine production, there is also an increase in dopamine metabolism. Considering the irreproducibility of the data in Figure 13, the likelihood that extracellular H_2O_2 levels increase following administration of carbidopa/L-dopa, and evidence that exposure of sensors containing exposed metal centers to H_2O_2 + hydroquinones

may result in a large generation of quinones, it appears that the increase in current at peroxide sensors prepared without SDS does not arise from the HRP-catalyzed, enzymatic reduction of H_2O_2. Indeed, H_2O_2 may be contributing to the response observed at peroxide sensors, however by functioning as an oxidant in the metal-center catalyzed oxidation of hydroquinones (Scheme 2).

2.4.9 Using SDS as a Reagent to Prevent Precipitation

The results in Figures 1-13 suggest that deposition of hydrogels from mixtures containing the polymer-enzyme precipitate results in the entrapment of denatured enzymes. The denatured enzymes act as nonselective redox catalysts that compromise the selectivity of the microsensors and prevent their use for in vivo measurements. Hence, it is necessary to entrap the enzymes in their enzymatically active state. We hypothesize that preventing precipitation would be a route to accomplishing this. Because the redox polymer is highly cationic, it is possible that the precipitation is caused by electrostatic interactions. Thus, we investigated the effect of adding sodium dodecyl sulfate (SDS) to the polymer solution. SDS was effective at preventing precipitation when the polymer and enzymes were combined (Figure 14). Furthermore, microsensors prepared by deposition of hydrogels from SDS-containing, precipitate-free polymer-enzyme mixtures did not produce a cathodic response to dopamine (2.5 μM) (Figure 15). The absence of a cathodic hydroquinone response is consistent with the idea that SDS prevents precipitation and enables entrapment of the enzymes without a loss in selectivity. The decrease in cathodic current following the addition of dopamine at sensors operated at 37 ^{O}C appears to stem from an interaction between the oxidized form of the Os redox component and

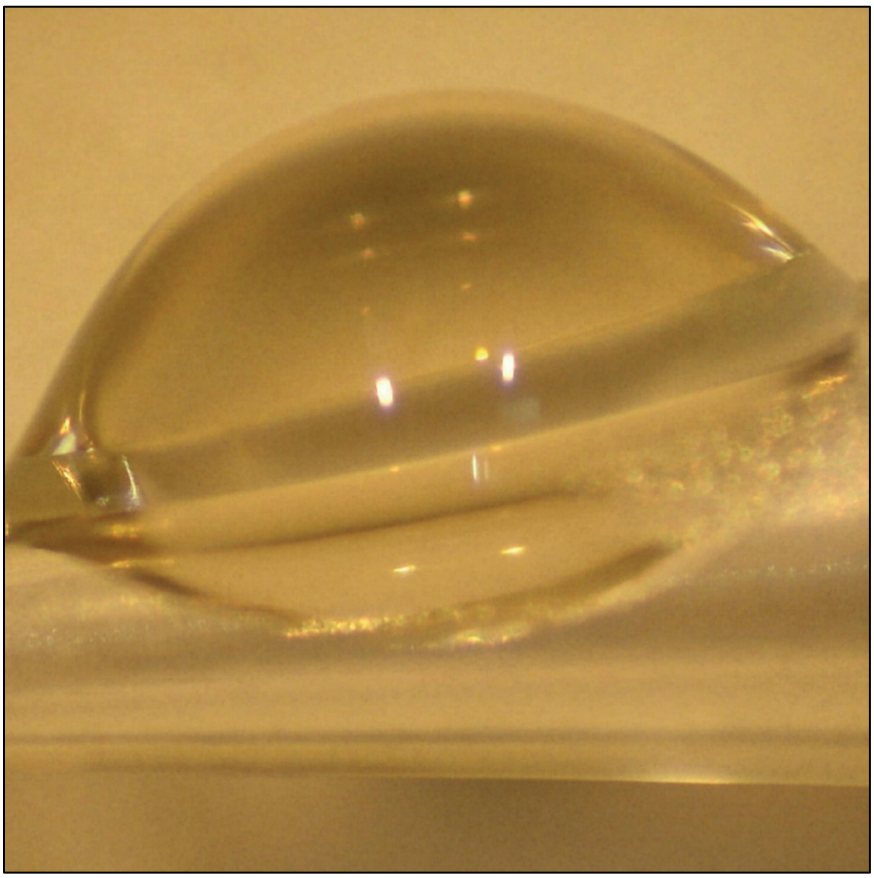

Figure 2-14. Photograph of a hydrogel deposition solution containing the redox polymer, SDS, crosslinker, horseradish peroxidase, and ascorbate oxidase. Note the absence of a precipitate in the droplet.

Reaction 5

$$H_2Q + 2[Os(bpy)_2(py)Cl]^{2+} \rightarrow Q + 2H^+ + 2[Os(bpy)_2(py)Cl]^+$$

dopamine[36, 70-72] (Rxn. 5). At greater temperatures, there appears to be an increased reactivity between the oxidized form of the mediator and dopamine. Since sensors are operated at a potential where the majority of the mediator is held in the $[Os(bpy)_2(py)Cl]^+$ state, it appears that reduction of any of the few $[Os(bpy)_2(py)Cl]^{2+}$ sites in the film by dopamine is responsible for this decrease the cathodic current.

If the use of SDS leads to the entrapment of enzymes without denaturation, improved microsensor performance is expected as a result. So, we compared the calibration performance of microsensors prepared with and without the use of SDS (Figure 16). Peroxide microsensors prepared without SDS exhibited marked interference by ascorbate (Figure 16A). The presence of ascorbate (200 μM) in the electrochemical cell decreased the slope of the peroxide calibration curve from $61.3 \pm 19.6\ pA \cdot \mu M^{-1}$ to $41.0 \pm 11.9\ pA \cdot \mu M^{-1}$ (mean ± S.D., n=4 sensors). This ascorbate interference is a sign that the entrapped ascorbate oxidase is not effectively oxidizing ascorbate, in which case the ascorbate is available to reduce the $[Os(bpy)_2(py)Cl]^{2+}$ form of the mediator and decrease the peroxide signal. However, ascorbate did not interfere with the peroxide sensitivity of microsensors prepared with use of SDS (Figure 16B). The sensitivity for peroxide obtained with and without ascorbate (200 μM) was, respectively, $119.8 \pm 44.0\ pA \cdot \mu M^{-1}$ and $111.0 \pm 44.9\ pA \cdot \mu M^{-1}$ (mean ± S.D, n = 7 sensors, no significant difference). The absence of ascorbate interference is consistent with the idea that AAOx is entrapped in its enzymatically active state and is functioning to prevent ascorbate from reducing the mediator.

We also found that sensors prepared with SDS exhibited greater peroxide sensitivity than those prepared without SDS (Figure 16). However, SDS did not affect the linearity of the peroxide calibration curves over the range of concentrations examined here, which is considered to be the physiologically interesting range. All the calibration curves for the individual sensors had r^2 values of at least 0.997.

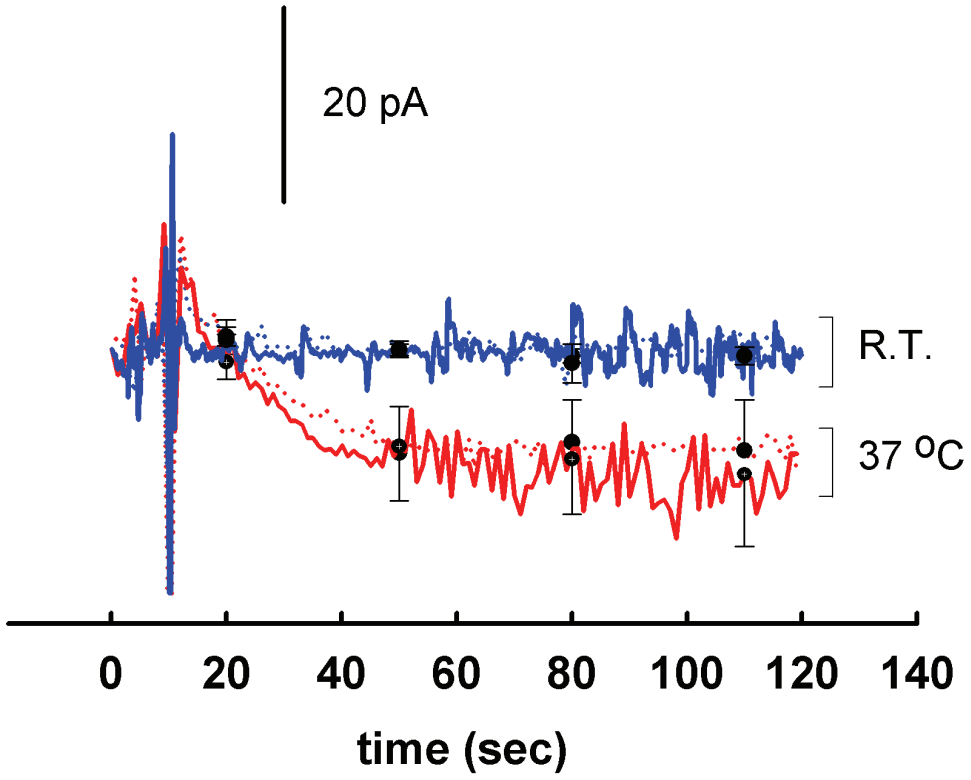

Figure 2-15. Responses of peroxide (dotted line; n=8), and sentinel (solid line; n=8) microsensors following the addition of dopamine (2.5 μM, t=10 s) to well-stirred, room temperature and 37 ^{O}C aCSF (pH 7.40) ($E_{applied}$ = -100 mV). The hydrogel in this case was deposited from precipitate-free solutions containing SDS. The standard error at several time points following the addition of dopamine is shown.

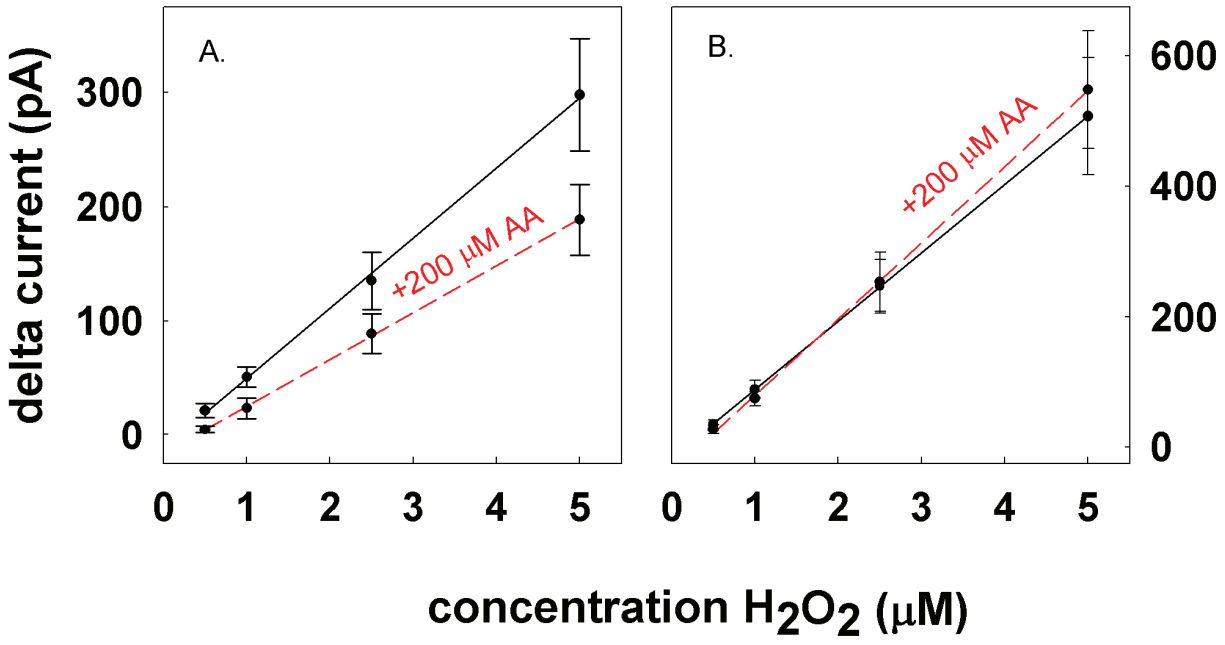

Figure 2-16. Calibration curves of peroxide sensors made (A) without SDS (n=4) and (B) with SDS (n=7) in the presence and absence of 200 μM ascorbate; $E_{applied}$ = -100 mV. Error bars show the standard error. All calibrations were performed in well-stirred 37 ^{O}C aCSF (pH 7.40). The current was quantified 50 s after the addition of peroxide or peroxide/ascorbate solutions to the aCSF.

2.4.10 In Vivo Use of Sensors Prepared With SDS

Peroxide (p) and sentinel (s) sensors prepared with SDS were evaluated in rats administered carbidopa followed by L-dopa, as described earlier (Figure 17). Responses at sensors containing SDS were more reproducible, and are strikingly different than responses gathered at sensors prepared without SDS. For example, peroxide and sentinel sensors consistently displayed resting background currents between 2 and 4 pA, and were both relatively unresponsive following the administration of carbidopa and L-dopa (Figure 17). In Figure 17C, HRP (3 mg·mL^{-1}, 1 μL) prepared in aCSF (pH 7.40) was infused adjacent to the sensors at t=80 min via a micropipette at a flow rate of 0.50 μL·min^{-1} to verify the selectivity of the sensors. Since the response of the peroxide and the sentinel sensors overlap, the response obtained at each

sensor was re-plotted on separate y-axes (Figure 18). Following the infusion of HRP, the responses at the peroxide and sentinel sensors decreased and increased, respectively. The response at the sentinel sensor following HRP appears to be an artifact of the infusion, but the decrease in current at the peroxide sensor is an indication the peroxide sensor selectively identifies fluctuations in peroxide. Thus, although the responses at peroxide and sentinel sensors prepared with and without SDS produce different results following administration of carbidopa and L-dopa, peroxide sensors containing SDS appear to be selective in vivo.

Pre- and post-calibration sensitivities of the peroxide sensors depicted in Figure 17 are reported in Appendix D. Comparison of the pre- and post-calibration sensitivities of peroxide sensors used in Figures 13 and 17 reveal two important findings. First, large increases in amperometric current following the administration carbidopa/L-dopa only occur at sensors that have lost nearly all their sensitivity in vivo. Second, sensors that contain SDS experience an increase in sensitivity over time. This is why in two of the experiments depicted in Figure 17 the post-calibration sensitivities exceed the pre-calibration sensitivities.

In a previous section, we showed that electrodes coated with a Cu^{2+} containing redox hydrogel have elevated background currents, and respond to hydroquinones. The fact that background currents at peroxide and sentinel sensors prepared with SDS are both on the order of a few pA in vivo, and sensors prepared with SDS do not respond to hydroquinones suggest that elevated in vivo background currents at sensors prepared without SDS (Figure 13) are attributable to exposed metal centers. This is also consistent with the observation that in every in vivo experiment carried out in Figure 13, sensors with greater background currents produced a larger response following the administration of L-dopa. These data demonstrate the importance

of preparing sensors that do not contain exposed metal centers. For now, incorporation of SDS into the hydrogel appears to be a means of accomplishing this.

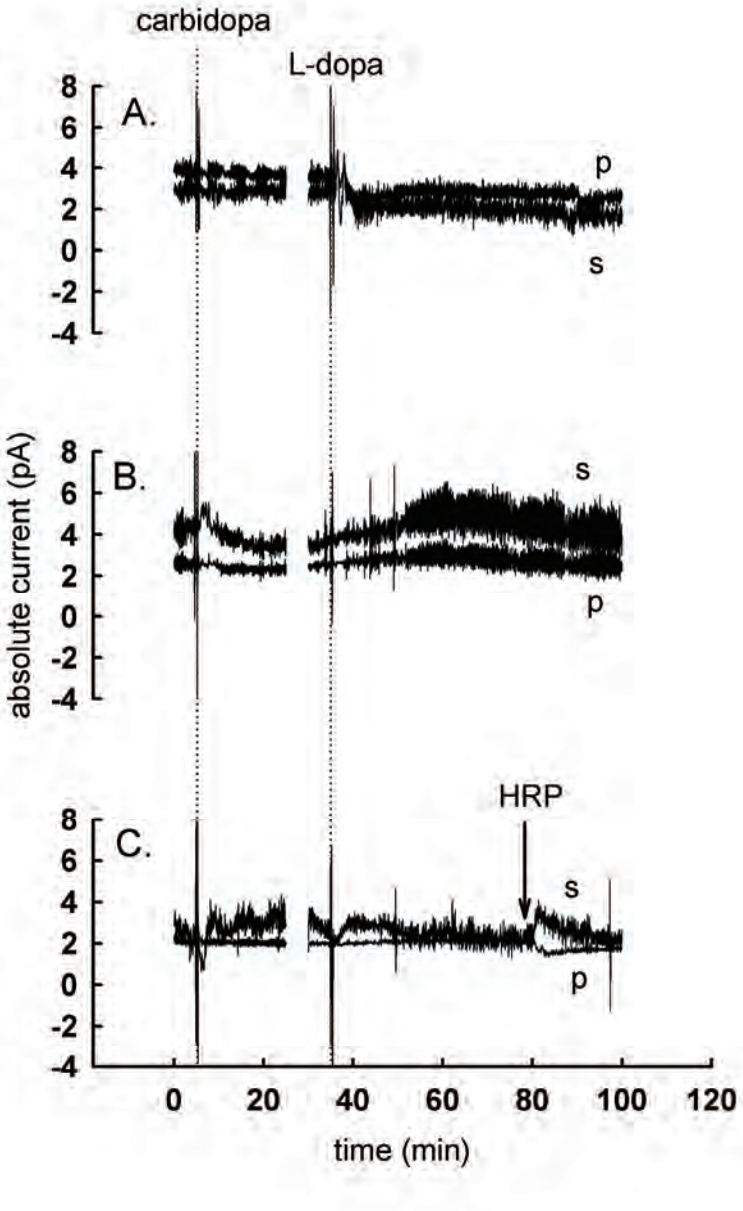

Figure 2-17. Responses of peroxide and sentinel sensors prepared with SDS, operated amperometrically (-100 mV wrt. Ag/AgCl) in the striatum following administration of carbidopa and L-dopa.

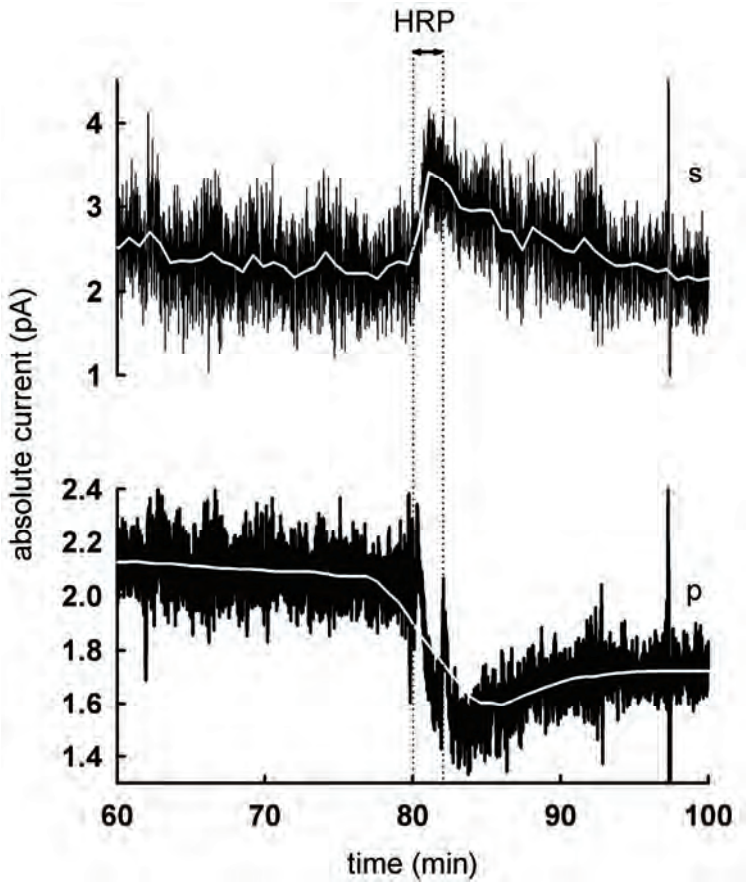

Figure 2-18. Responses of the peroxide (p) and sentinel (s) sensors depicted in Figure 17C upon infusion of HRP adjacent to the sensors.

2.5 CONCLUSION

The use of SDS appears to be an effective reagent for preventing precipitation when the redox polymer is mixed with enzymes in aqueous solution. Avoiding the precipitation appears to enable the entrapment of enzymes in their catalytically active state and enhances both the sensitivity and selectivity of the resultant microsensors. With the batch of polymer used for this study, hydrogel deposition without the use of SDS produced sensors that gave a cathodic amperometric response to hydroquinones, suffered ascorbate interference with the peroxide response, and exhibited low sensitivity towards peroxide, i.e., sensors unsuitable for their intended in vivo application. However, SDS eliminated precipitate formation, eliminated the response to hydroquinones, eliminated ascorbate interference with the peroxide response, and increased the sensitivity towards peroxide. Hence, the use of SDS appears to make the sensors more suitable for in vivo applications.

2.6 ACKNOWLEDGMENTS

This work was supported by NIH grant DA 13661. We would also like to thank Mr. Kyle Kimble for his generous help in obtaining the TEM images.

3.0 THE ORIGIN OF PRECIPITATE AND EXPOSED ENZYME METAL CENTERS IN CASTING MIXTURES USED FOR THE PREPARATION OF AMPEROMETRIC ENZYME SENSORS

3.1 ABSTRACT

Amperometric hydrogen peroxide sensors were prepared by immobilizing horseradish peroxidase in a poly(vinylpyridine)-based hydrogel, derivitized with quaternary ethyl amine groups and the $[Os(bpy)_2(py)Cl]^{+/2+}$ redox couple, on carbon fiber microelectrodes. Ascorbate oxidase was also immobilized in the hydrogel to minimize interactions between ascorbate and the oxidized state of the mediator. To immobilize the enzymes, a casting mixture composed of the hydrogel, enzymes, and crosslinker was prepared in a small borosilicate vial, and manually applied to the electrodes. An interaction between the hydrogel and enzymes resulted in the formation of a precipitate and caused the enzymes' metal centers to become exposed. The precipitate makes the film heterogeneous, and the exposed metal centers catalyze the oxidation of hydroquinones (e.g., dopamine and DOPAC). Interactions between the $[Os(bpy)_2(py)Cl]^{+/2+}$ redox couple and the enzymes appear to be responsible for exposing the enzymes' metal centers. Electrostatic interactions between deprotonated surface silanols and protonated functionalities of the polymer appear to restrict the ability of the polymer to reorient itself to an energetically favorable conformation following exposure to the enzymes. Hence, interactions between the

hydrogel and enzymes, in the presence of borosilicate, appear to be responsible for the precipitate product.

3.2 INTRODUCTION

Preparation of enzymatic sensors with a hydrogel containing the $[Os(bpy)_2(py)Cl]^{+/2+}$ redox mediator (hereafter referred to as the Os redox couple, or Os redox mediator) often produces a precipitation product following the addition of horseradish peroxidase or ascorbate oxidase to the hydrogel in a borosilicate vial (Chapter 2, Figures 2-1 to 2-3)[73]. When casting mixtures containing this precipitate are deposited on electrodes, the resulting sensors are frequently found to catalyze the oxidation of hydroquinones, and produce quinones. Exposed enzyme metal centers within the precipitate appear to be responsible for catalyzing the oxidation of the hydroquinones. Quinones can diffuse within the hydrogel and undergo reduction at the electrode surface when potentials $\leq$ +100 mV (wrt. Ag/AgCl) are applied to the sensors [73]. This poses a problem, because these sensors are typically operated at a potential of -100 mV to avoid oxidation of hydroquinones and ascorbic acid directly on the electrode surface.

Mixing sodium dodecyl sulfate (SDS) with the redox hydrogel before adding enzymes prevents formation of the precipitation product: instead, it produces a turbid, colloidal-like suspension[73]. Deposition of casting mixtures that contain this turbid, colloidal-like suspension on electrodes, produces sensors that do not respond to hydroquinones when operated amperometrically at -100 mV[73]. We have experienced difficulty preparing sensors that are specific for anionic substrates when incorporating SDS into the casting mixture. For example, glutamate sensors prepared with SDS displayed a very poor sensitivity (unpublished results).

Because we would like to reproducibly prepare glutamate sensors that do not respond to hydroquinones, and are aware that this cannot be accomplished by incorporating SDS into the hydrogel, we became interested in determining if the absence of precipitate in the casting mixture is the reason the peroxide sensors mentioned above did not respond to hydroquinones. This would allow us to determine whether the precipitation reaction is responsible for exposing the enzymes' metal centers. To answer these questions, we found a way to combine redox hydrogel and enzymes without the use of SDS that did not produce a precipitate. We then evaluated the amperometric responses of sensors prepared with and without precipitate following the addition of hydroquinones.

3.3 EXPERIMENTAL

3.3.1 Reagents

All reagents were used as received from their respective supplier. Horseradish peroxidase (EC 1.11.1.7, type II, HRP), ascorbate oxidase (EC 1.10.3.3; from *Cucurbita sp*., AAOx), 3,4-dihydroxyphenethylamine (dopamine), sodium hydrosulfite, and 2-bromoethylamine were from Sigma (St. Louis, MO). Ammonium hexafluorophosphate, 4-(2-hydroxyethyl)-1-piperazineethanesulfonic (HEPES) acid, and HEPES sodium salt were from Aldrich (Milwaukee, WI). Poly(ethylene glycol 400 diglycidyl ether) (PEGDE) and poly(4-vinylpyridine) (PVP: MW 50K) were from Polysciences, Inc. (Warrington, PA). Potassium hexachloroosmate was from Alpha Aesar (Ward Hill, MA). 2,2´-bipyridine was from Acros (Morris Plains, NJ). Anion exchange beads (AG1-X4) were from Bio Rad (Hercules, CA).

3.3.2 Redox Polymer

Four batches of redox polymer hydrogel (POs-EA) were synthesized according to the procedure of Gregg and Heller [36] with one modification. The amount of *cis*-bis(2,2´-bipyridine-N,N´)di-chloroosmium(II) [60] combined with 0.430 g PVP (50K MW) was 0, 8, 15, or 25% of the amount used by Gregg and Heller [36] (where 100% equals 0.494 g). For simplicity, we will refer to these as the 0 Os, 8 Os, 15 Os, and 25 Os polymers.

3.3.3 Carbon Fiber Microelectrodes

Microelectrodes were prepared by sealing individual carbon fibers, (10-μm diameter, Thornell P-55 fibers, Union Carbide, Greenville, SC), in pulled borosilicate glass capillary tubes (1.0 mm O.D, 0.58 mm I.D.) (Sutter Instrument Co., Novato, CA) with a low viscosity epoxy (Spurr low viscosity embedding kit, Polysciences, Inc., Warrington, PA). The epoxy was cured at 80 ^{O}C, after which the fibers were cut to a length of 400 μm with a scalpel blade.

3.3.4 Hydrogel films

Redox polymer (1 mg·mL^{-1}) and crosslinker (PEGDE, 3 mg·mL^{-1}) were dissolved in 18 Mohm-cm purified water (Nanopure, Barnstead), and were prepared fresh daily. Enzymes were dissolved in HEPES buffer (pH 8.00, freshly prepared every 2 to 3 days in a borosilicate vial by the addition of the HEPES sodium salt to a 10 mM solution of the acid). Solutions of ascorbate oxidase were prepared in the borosilicate vials in which the enzyme was received. Redox polymer solutions and horseradish peroxidase were prepared in borosilicate or polypropylene

vials (Nalgene, Rochester, NY, USA), as noted. Crosslinker and enzyme solutions were prepared fresh daily. Reagents used for more than one day were stored at 2 to 8 ^{O}C.

Peroxide sensors were prepared by combining aliquots of the redox polymer (20 μL; 1 mg·mL^{-1}), PEGDE (4 μL, 3 mg·mL^{-1}), HRP (10 μL, 660 U·mL^{-1}), AAOx (10 μL, 1400 U·mL^{-1}), and HEPES (10 μL, 10 mM) in 0.25 mL polypropylene microcentrifuge tubes (Fisher Scientific, Pittsburgh, PA) and sonicating for 15 s. A 4–μL aliquot of the polymer/crosslinker/enzyme mixture was suspended on the end of a polypropylene pipette tip and painted onto two carbon fiber electrodes for 10 min. The drop was passed over the carbon fiber tip about twice per second.

All sensors were dried at 37 ^{O}C for 1 hr, soaked in Nanopure water for 15 min, and dried in ambient air for 1 hour. In these experiments, sensors were not coated with Nafion. Sensors were used immediately or stored for up to 2 days in a desiccator at 4-6 ^{O}C.

3.3.5 Electrochemical and Calibration Techniques

Amperometry was performed with the microsensors immersed in a 50-mL cell containing 40 mL of well stirred artificial cerebrospinal fluid (aCSF: 145 mM Na^{+}, 1.2 mM Ca^{2+}, 2.7 mM K^{+}, 1.0 mM Mg^{2+}, 152 mM Cl^{-}, 2.0 mM phosphate, pH adjusted to 7.4 with NaOH). Amperometry was carried out in 2-electrode mode, i.e., without an auxiliary electrode. The second electrode was a Ag/AgCl reference electrode. The potential applied to the sensors was amplified with a potentiostat made in-house. The current signal was amplified with a current amplifier (Keithley, model 428, Cleveland, OH). The gain and filter rise time settings on the current amplifier were typically set to 10^{8} to 10^{9} V·A^{-1} and 100 to 300 ms, respectively. The

amplifier output was digitized at a 20 kHz sampling rate with a 12-bit digital-to-analog converter (Labmaster PGH-DMA, Scientific Solutions, Solon, OH). Experiments were performed in 37± 0.3 ^{O}C or room temperature (ca. 22 ^{O}C) aCSF, as noted. To maintain a constant 37± 0.3 ^{O}C environment for the duration of an experiment, beakers and submersible parts of the FIA system, including the injection loop (0.50 mL), all other fluid lines, and the flow cell were placed in a water bath (Precision Scientific, Chicago, IL, USA). Standard solutions were prepared in aCSF, and were delivered manually to beakers with a pipette.

3.3.6 Statistics

Significance was determined using one-way ANOVAs. If an ANOVA indicated a significant difference existed, then a power analysis of the ANOVA and a Duncan's Multiple Range post-hoc comparison of means were conducted.

3.4 RESULTS AND DISCUSSION

3.4.1 Behavior of Redox Polymer in Borosilicate vs. Polypropylene Vessels

The composition of the vials in which components of the casting mixture are combined appear to influence whether or not a precipitate will form. When components of the casting mixture (i.e., redox polymer, crosslinker, enzymes, etc.) are combined in borosilicate glass vials, a mixture that contains a brownish precipitate is produced[45, 46, 73]. The precipitate forms immediately after mixing the redox polymer and enzymes, or within a few minutes of doing so.

The precipitate has also been observed to form in the 4-μL aliquot suspended on the edge of a polypropylene pipette tip, even though it is no longer in contact with the borosilicate. This precipitate is described in our earlier work[73, 45]. [Note: Polymer solutions prepared in borosilicate that are six or more hours old typically form a precipitation product more rapidly than polymer solutions less than 6 hours old, when combined with enzymes in borosilicate. This is important to note because we have occasionally observed that freshly prepared polymer solutions (i.e., less than six hours old), prepared in borosilicate, do not form a precipitate when mixed with enzymes in borosilicate. In the case of the latter, there appears to be a *transformation period* over which the polymer becomes more reactive with the enzymes.]

Combination of the casting mixture components in polypropylene vials does not produce a precipitate. Rather, a turbid, colloidal-like casting mixture, similar in appearance to that observed when SDS was incorporated into the casting solution (Chapter 2, Figure 2-14), is produced. However, unlike the turbid, colloidal-like casting mixture containing SDS, the turbid, colloidal-like casting mixture prepared in polypropylene vials without SDS produces sensors that respond to hydroquinones when operated amperometrically at -100 mV. Thus, it appears the formation of precipitate is not responsible for exposing the enzymes' metal centers.

At the time we prepared our previous report, we were unaware that the borosilicate vials used to prepare the polymer solutions and combine the components of the casting mixture influenced whether the casting mixture formed a precipitate or a turbid, colloidal-like mixture [73]. Hence, we never mentioned that the reagents used to construct the casting solutions were prepared and combined in borosilicate. The findings in this work indicate that the composition of all vessels, vials, and objects that come in contact with any of the reagents of the casting mixture could influence whether a precipitate forms. Thus, in this and all future reports, the

composition of all materials that come in contact with any components of the casting mixture should be reported.

By preparing the redox polymer, and combining the redox polymer with enzymes in polypropylene vials, we have been able to reproducibly prepare turbid, colloidal-like casting mixtures. Unlike some methods which appear to prevent the precipitate only when a given batch of polymer is used (e.g., incorporation of SDS in to the casting solution[73], or preparation of enzyme solutions with HEPES[44]), this appears to be a permanent fix to the precipitation problem. We have evaluated multiple batches of redox polymer, and each one, when prepared in, and combined with enzymes in a polypropylene vial, forms a turbid, colloidal-like casting mixture. Sensors prepared with casting mixtures containing colloidal-like suspensions have more homogenous films than mixtures containing precipitate. Hence, we anticipate that by being able to reproducibly prepare thin layer films with turbid, colloidal-like casting mixtures, we will also be able to increase the reproducibility of the electrochemical responses at these sensors.

3.4.2 Interactions between the Redox Polymer and the Borosilicate Glass

Borosilicate glass (Figure 1) contains a boron modifier, typically B_2O_3, and silanol groups. Both contribute to the chemical and physical properties of the glass [2]. It is possible these properties of the borosilicate glass make it reactive with the redox polymer. Boron acts as a Lewis acid, and hence possesses a vacant orbital that can accept an electron pair. Silanol groups form hydrogen bonds when protonated, or may be attracted to cationic species when deprotonated. The redox polymer, illustrated in Figure 2, contains pyridine and pendent ethyl amine groups bound to pyridine (i.e., N-(2-aminoethyl) pyridinium).

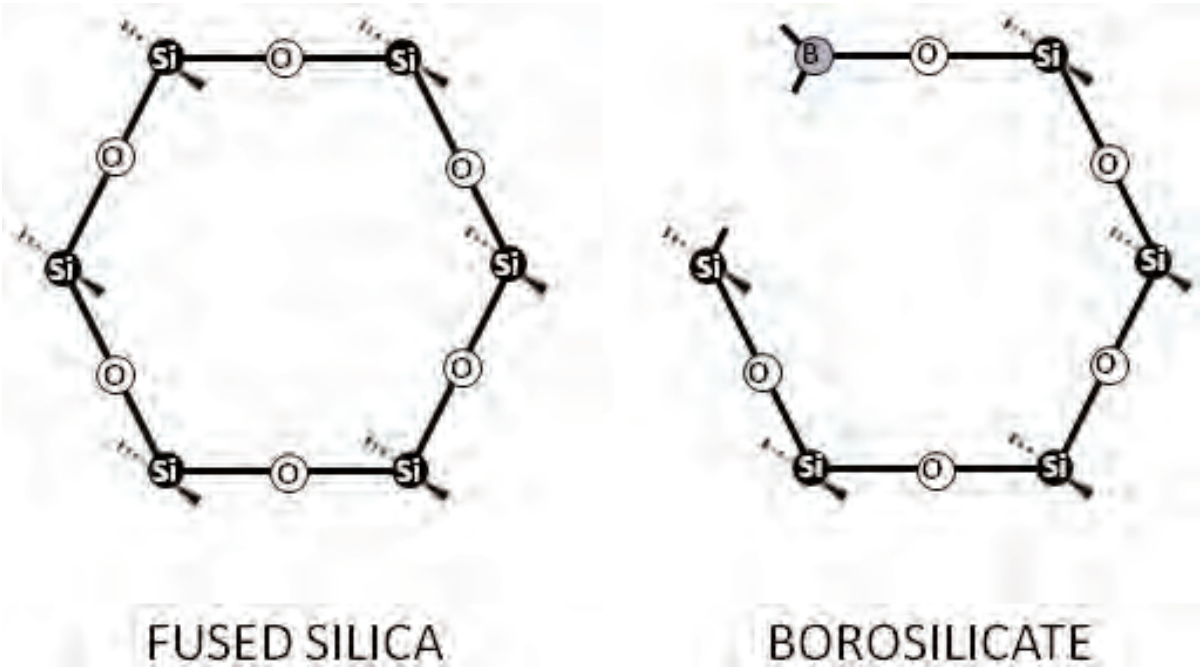

Figure 3-1. One-dimensional Fisher structure of fused silica and borosilicate[2]. The black circles indicate the position of silicon while the larger empty circles represent oxygen. Note the presence of boron in borosilicate.

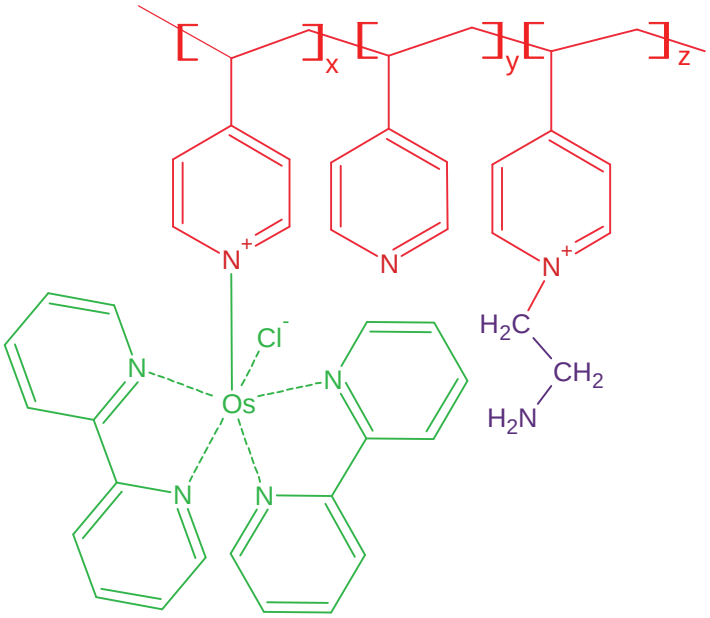

Figure 3-2. Structure of the redox hydrogel.

The pKa of the poly(4-vinyl-pyridinium) ion is about 3.3 [74]. The pKa of N-(2-aminoethyl) pyridinium is approximately 7.0 [75]. The pKa of silanol is in the acidic range [76]. Enzyme solutions are prepared with HEPES buffer (pH 8.0): after mixing the enzymes with the redox polymer and crosslinker, the entire casting mixture has a pH of 8.0. Thus, at pH 8.0, poly(4-vinyl-pyridinium) ion is completely deprotonated, N-(2-aminoethyl) pyridinium is partially protonated, and silanol groups on the glass surface are deprotonated. If interactions between the borosilicate and redox polymer at pH 8.0 are a factor that influence precipitate formation, they are likely the result electrostatic interactions between protonated N-(2-aminoethyl) pyridinium functionalities and deprotonated silanol groups. Electrostatic interactions between the cationic Os-redox complex, and deprotonated silanol groups may also play a role.

We first tested the hypothesis that precipitate formation originated from an interaction between the enzymes and the Os redox complex. The Os redox complex is cationic, and both enzymes are anionic at pH 8.0. (HRP contains at least seven isoenzymes with isoelectric points between 3.0 and 9.0[77], while AAOx has an isoelectric point of ca. [1]6.2.) Thus, an electrostatic interaction between the two seemed likely. We hypothesized that the conformation of the redox polymer changed when exposed to the borosilicate glass. Specifically, we rationalized that attractions between the protonated N-(2-aminoethyl) pyridinium functionalities and the deprotonated silanol groups caused the N-(2-aminoethyl) pyridinium functionalities to rotate towards the glass surface. We then rationalized that the Os redox mediator, with less steric protection than it once possessed, would be more accessible to the enzymes, and hence reactive. Although this is one possibility, the results of our experiments indicated it is certainly not the only one. That is, we found that a polymer similar to the redox polymer depicted in Figure 2, but lacking the Os redox couple (i.e., 0 Os), still precipitated when combined with the enzymes. Thus, the Os redox complex does not have to be present for precipitation to be observed when enzymes are added.

This latter piece of data, in conjunction with the knowledge that combination of the redox polymer with enzymes in polypropylene vessels does not lead to a precipitate, led us to believe that the precipitate most likely resulted because of electrostatic interactions between protonated N-(2-aminoethyl) pyridinium functionalities and the deprotonated silanol groups. In borosilicate glass, it appears that the energy required for the polymer to rearrange itself in the presence of the enzymes exceeds the amount of energy required to form a precipitate. Polypropylene is very

[1] L-ascorbate oxidase (EC. 1.10.3.3) from Cucurbita pepo var. melopepo (zucchini) (Swiss-Prot/TREMBLE accession number: P37064).

hydrophobic (Figure 3) and does not possess any charged surfaces that would favor interaction with the polymer.

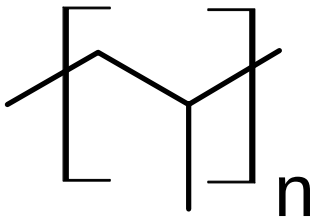

Figure 3-3. Structure of poly(propylene).

Thus, it is likely the polymer does not precipitate in polypropylene vessels because it can reorient itself, using a minimal amount of energy, when exposed to the enzymes. Hence, reorientation of the polymer in polypropylene vials is more energetically favorable than in borosilicate vials.

3.4.3 Exposure of Enzymes' Metal Centers by the $[Os(bpy)_2(py)Cl]^{+/2+}$ Redox Couple

We have recently found that preparation of casting mixtures with hydrogel that does not contain the Os redox couple (i.e., 0 Os), does not expose the enzymes' metal centers. This is evident because sensors prepared with these casting mixtures do not respond to hydroquinones, when operated amperometrically at -100 mV (Figure 4). In Figure 4, peroxide sensors were prepared with different Os loadings. Casting mixtures were prepared in borosilicate vials, and the sensors were prepared without a Nafion outerlayer. The sensors were placed in a well-stirred beaker of aCSF held at room temperature (top trace) or 37 ^{O}C (bottom trace), and operated amperometrically at -100 mV until a steady baseline current was achieved. At t=10 s, the

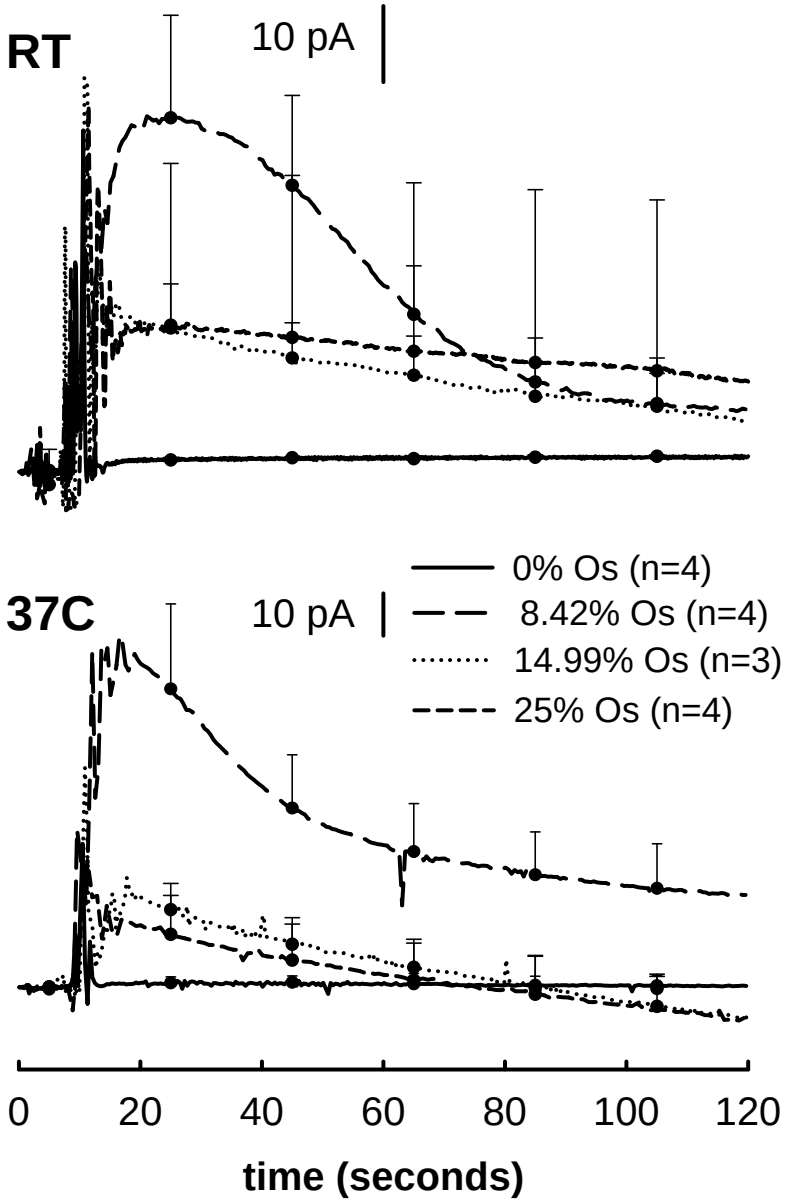

Figure 3-4. H_2O_2 sensors prepared with various loadings of the Os redox mediator were held amperometrically at -100 mV wrt. Ag/AgCl and exposed to 2.5 μM dopamine at t=10 s. Only sensors that were prepared with hydrogel containing the Os redox mediator responded to the addition of dopamine. Sensors did not contain a Nafion outerlayer, and experiments were carried out in a well-stirred beaker of 37 ^{O}C or room temperature aCSF. Error bars show the standard deviation.

sensors were exposed to 2.5 μM dopamine. Sensors prepared with hydrogel containing 8.5 Os, 15 Os, and 25 Os experienced a transient increase in reductive current, while those prepared with 0 Os did not. These findings were reproducible at room temperature and 37 ^{O}C. Although the polymer without the Os-redox component is still cationic in nature, it appears the Os-redox component is specifically responsible for exposing the metal centers of the enzymes.

In our previous work, we hypothesized that SDS functioned by countering the cationic nature of the redox polymer. Based on the evidence gathered in this study, SDS appears to have countered the charge on the Os redox couple to prevent the enzyme metal centers from becoming exposed, and countered the charge on the non-redox components of the hydrogel to prevent the precipitate. Polymers synthesized without the Os mediator produced a whitish precipitate when mixed with enzymes in borosilicate glass vials and a colloidal like suspension when combined with enzymes in polypropylene vials, but did not respond to 2.5 μM dopamine.

3.5 CONCLUSION

In this work, we have demonstrated that attractive interactions between the redox polymer and borosilicate are responsible for precipitate formation upon addition of enzymes. To prevent precipitation between the polymer and enzymes it appears necessary to mix the polymer and enzymes in a polypropylene vessel.

Interactions between the Os redox couple and the enzymes appear to be responsible for exposing the enzymes' metal centers. HEPES acid has a pKa of 7.5, and is thus suitable to prepare buffers in the pH range of 6.8 to 8.2. If electrostatic interactions between the Os redox mediator and the enzymes are responsible for exposing the enzymes' metal centers, perhaps

preparation of the enzymes in a more acidic buffer, closer to the enzymes' pI may be an alternative to using SDS. However, at the current time, inclusion of SDS into the casting mixture appears to be the only realistic solution to this problem.

4.0 CONTROLLING HYDROQUINONE INTERFERENCE AT AMPEROMETRIC ENZYME SENSORS THAT CONTAIN THE REDOX MEDIATOR $[Os(bpy)_2(py)Cl]^{+/2+}$ BY INCREASING $[Os(bpy)_2(py)Cl]^{+/2+}$ LOADING AND NAFION FILM THICKNESS

4.1 ABSTRACT

Amperometric enzyme sensors often rely on mediators of electron transfer to provide a means of electrochemical communication between enzymes and an electrode surface. Herein, we demonstrate that the ability of the $[Os(bpy)_2(py)Cl]^{+/2+}$ redox couple to mediate electron transfer between horseradish peroxidase and a carbon fiber electrode, in the presence of hydroquinones (e.g., dopamine and DOPAC), is significantly altered by two mechanisms: 1) generation/accumulation of an insulative hydroquinone oxidation product (presumably a melanin-like polymer) in the hydrogel that progressively decreases electron transfer between horseradish peroxidase and $[Os(bpy)_2(py)Cl]^{+/2+}$ sites, as well as between neighboring $[Os(bpy)_2(py)Cl]^{+/2+}$ sites, and 2) mediation of electron transfer between horseradish peroxidase and the electrode by the hydroquinone/ortho-quinone redox couple. Accumulation of hydroquinone oxidation product within the hydrogel irreversibly decreases sensor sensitivity, although the effect of fouling on electron hopping diffusion in the film is diminished at sensors prepared with greater $[Os(bpy)_2(py)Cl]^{+/2+}$ loads. Mediation of electron transfer by the hydroquinone/ortho-quinone redox couple cannot be accounted for by the current style of control

sensor. Thicker Nafion films minimize interference from physiological concentrations of DOPAC and dopamine, but at the expense of analyte sensitivity and slower response times.

4.2 INTRODUCTION

One method for preparing enzyme electrodes involves trapping the enzymes in a polymeric redox hydrogel [35, 36]. The polymer consists of a poly(vinylpyridine) backbone with pendent osmium-centered complexes ($[Os(bpy)_2(py)Cl]^{+/2+}$, where py is a pyridine unit of the backbone and bpy is bipyridine). Self-exchange between neighboring osmium complexes facilitates electron transfer between the enzyme and the electrode. We have developed hydrogen peroxide microsensors by entrapping horseradish peroxidase (HRP) on carbon fiber microelectrodes [43, 47, 73, 78]. We have also developed bienzyme sensors wherein the second enzyme is an oxidase, such as glucose-, choline-, or glutamate-oxidase [42-46, 78, 48, 49]. The bienzyme sensors detect the hydrogen peroxide generated within the hydrogel.

We focus on enzyme-based microelectrodes for chemical monitoring within living brain tissue. Brain tissue contains a number of substances with the potential to interfere with the sensors. Potential interference from electrochemical oxidation of brain tissue constituents on the electrode is prevented by the use of a low operating potential (usually -100 mV wrt. Ag/AgCl). However, ascorbate, which is present in brain tissue at concentrations between 200 and 400 μM, rapidly reduces the mediator (Reaction 6).

Reaction 6

$$AA + 2[Os(bpy)_2(py)Cl]^{2+} \rightarrow DHA + 2[Os(bpy)_2(py)Cl]^{+} + 2H^{+}$$

Where DHA is dehydroascorbate, this prevents transfer of electrons with the electrode and causes loss of the amperometric signal. Thick coatings of Nafion, a permselective film, and co-immobilization of ascorbate oxidase (which does not produce peroxide) prevent this form of ascorbate interference[79, 44].

However, thick Nafion films diminish the sensitivity and slow the response time of the sensors, especially in the case of the glutamate sensors. This is one factor that limits the use of these sensors for real-time monitoring of rapid chemical events in the brain, a topic of great current interest[80]. Thus, we became interested in the idea of increasing the sensitivity and response time of glutamate sensors by the use of thinner Nafion films. However, it became immediately apparent that sensors with thin Nafion films exhibit interference from brain hydroquinones, including dopamine and its principle metabolite, dihydroxyphenylacetic acid (DOPAC), at their respective brain concentrations, ca. 2 μM and 20 μM, respectively[7, 81].

The objective of the present work was to examine the hydroquinone interference when thin Nafion films are used. With an eye towards solving this problem, we have evaluated the mechanisms by which hydroquinones interfere with the operation of these sensors, which involves 1) reduction of the Os-centered mediator by hydroquinone, 2) reduction of quinones at the electrode surface, and 3) the formation of a hydroquinone/quinone polymer (melanin-like) within the hydrogel. Adjusting the recipe for preparing the sensors, especially the loading of the Os-centered redox complex, was only partially successful in overcoming these interferences. During the course of this work, we developed a rigorous calibration procedure that identifies hydroquinone interference. We used this procedure to confirm that hydroquinone interference is suppressed by thick Nafion films, which supports the value of our sensors for in vivo measurements aimed at evaluating time-averaged in vivo concentrations.

4.3 EXPERIMENTAL

4.3.1 Reagents

All reagents were used as received from their respective supplier. Horseradish peroxidase (EC 1.11.1.7, type II, HRP), ascorbate oxidase (EC 1.10.3.3; from *Cucurbita sp*., AAOx), L-glutamate oxidase (EC 1.4.3.11, from S*treptomyces sp.*), 3,4-dihydroxyphenethylamine (dopamine), 3,4-dihydroxyphenylacetic acid (DOPAC), sodium hydrosulfite, and 2-bromoethylamine were from Sigma (St. Louis, MO). Nafion (5 % wt. solution in a mixture of lower aliphatic alcohols and water, 1100 equiv. wt.), ammonium hexafluorophosphate, 4-(2-hydroxyethyl)-1-piperazineethanesulfonic (HEPES) acid, and HEPES sodium salt were from Aldrich (Milwaukee, WI). Poly(ethylene glycol 400 diglycidyl ether) (PEGDE) and poly(4-vinylpyridine) (PVP: MW 50K and 150-200K) were from Polysciences, Inc. (Warrington, PA). Potassium hexachloroosmate was from Alpha Aesar (Ward Hill, MA). 2,2´-bipyridine was from Acros (Morris Plains, NJ). Anion exchange beads (AG1-X4) were from Bio Rad (Hercules, CA).

4.3.2 Redox Polymer

Four batches of redox polymer hydrogel (POs-EA) were synthesized according to the procedure of Gregg and Heller [36] with two modifications. First, the amount of *cis*-bis(2,2´-bipyridine-N,N´)di-chloroosmium(II) [60] combined with 0.430 g PVP was 0, 25, 50, or 100% of the amount used by Gregg and Heller [36] (where 100% equals 0.494 g). For simplicity, we will refer to these as the 0 Os, 25 Os, 50 Os, or 100 Os polymers. Second, either 50K or 150-200K

MW PVP was used. The 0 Os polymer was prepared with 50K MW PVP, while the 25 Os, 50 Os, and 100 Os polymers were prepared with 150-200K MW PVP.

4.3.3 Carbon Fiber Microelectrodes

Microelectrodes were prepared by sealing individual carbon fibers, (10-μm diameter, Thornell P-55 fibers, Union Carbide, Greenville, SC), in pulled borosilicate glass capillary tubes (1.0 mm O.D, 0.58 mm I.D.) (Sutter Instrument Co., Novato, CA) with a low viscosity epoxy (Spurr low viscosity embedding kit, Polysciences, Inc., Warrington, PA). The epoxy was cured at 80 ^{O}C, after which the fibers were cut to a length of 400 μm with a scalpel blade.

4.3.4 Hydrogel Films

Redox polymer (1 mg·mL^{-1}, 2 mg·mL^{-1}, or 4 mg·mL^{-1}) and crosslinker (PEGDE, 3 mg·mL^{-1}) were dissolved in 18 Mohm-cm purified water (Nanopure, Barnstead), and prepared fresh daily. Enzymes were dissolved in HEPES buffer (pH 8.00, freshly prepared every 1 to 3 days in a borosilicate vial by the addition of the HEPES sodium salt to a 10 mM solution of the acid). Solutions of ascorbate oxidase and glutamate oxidase were prepared in the borosilicate vials in which the enzymes were received. Redox polymer solutions and horseradish peroxidase were prepared in polypropylene vials (Nalgene, Rochester, NY, USA). Crosslinker and enzyme solutions were prepared fresh daily. Reagents used for more than one day were stored at 2 to 8 ^{O}C.

Glutamate sensors were prepared by combining aliquots of the redox polymer (20 μL; 1, 2, or 4 mg·mL^{-1}), PEGDE (4 μL, 3 mg·mL^{-1}), HRP (10 μL, 660 U·mL^{-1}), AAOx (10-μL, 1400

$U \cdot mL^{-1}$), and GluOx (10 μL, 2 $mg \cdot mL^{-1}$) in 0.25 mL polypropylene microcentrifuge tubes (Fisher Scientific, Pittsburgh, PA) and sonicating for 15 s. All sensors were prepared with a 1 $mg \cdot mL^{-1}$ solution of redox polymer except the 200 Os and 400 Os hydrogels. The 200 Os and 400 Os hydrogels were prepared with a 2 $mg \cdot mL^{-1}$ and 4 $mg \cdot mL^{-1}$ solution of the 100 Os polymer, respectively. A 4–μL aliquot of the polymer/crosslinker/enzyme mixture was suspended on the end of a polypropylene pipette tip and painted onto two carbon fiber electrodes for 5 min. Polypropylene, PCR Clean epT.I.P.S. pipette tips (Eppendorf North America, USA) were used to transfer all reagents. The drop was passed over the carbon fiber tip about twice per second.

Hydrogen peroxide sensors were prepared in identical fashion as the glutamate sensors except HEPES buffer was substituted for GluOx. All sensors were dried at 37 ^{O}C for 1 hr, soaked in Nanopure water for 15 min, and dried in ambient air for 1 hour. Unless otherwise indicated, sensors were then coated with Nafion, and dried for 1.5 h at room temperature. Sensors were used immediately or stored for up to 2 days in a desiccator at 4-6 ^{O}C.

Note: Mixing the enzyme and the redox polymer solutions in borosilicate glass vials usually produces a thick precipitate that is not suitable for coating the carbon fibers[73]. However, mixing the reagents in polypropylene vials produced turbid mixtures, although individual particles were too small to see under 40x magnification. All the sensors in this paper were prepared from these turbid, colloidal-like mixtures.

4.3.5 Nafion Films

Thin Nafion films were prepared by dipping sensors in 0.5% Nafion seven times (1-5 min between dips). 0.5% wt. Nafion was prepared by diluting the as received 5% wt. Nafion with 2-

propanol. Thick Nafion films were created by dipping the sensors in a 0.5% Nafion solution six times (1-5 min between dips), and then in 5% Nafion seven times (5 min between dips). A longer dry time was needed for sensors dipped in 5% Nafion because it is less volatile than the 0.5% Nafion.

4.3.6 Electrochemical and Calibration Techniques

Amperometry was performed with the microsensors immersed in a 50-mL cell containing 40 mL of well stirred artificial cerebrospinal fluid (aCSF: 145 mM Na^{+}, 1.2 mM Ca^{2+}, 2.7 mM K^{+}, 1.0 mM Mg^{2+}, 152 mM Cl^{-}, 2.0 mM phosphate, pH adjusted to 7.4 with NaOH) or in a flow-injection analysis (FIA) system. Amperometry was carried out in 2-electrode mode, i.e. without an auxiliary electrode. The second electrode was a Ag/AgCl reference electrode. Cyclic voltammograms were collected at a sweep rate of υ= 0.10 $V \cdot s^{-1}$, and had a $E_{resting}$= -100 mV; $E_{anodic\ limit}$ = +700 mV; $E_{cathodic\ limit}$= -100 mV; initial sweep direction= (+). A variable speed, medium flow pump (Fisher Scientific, Pittsburgh, PA) was used to maintain constant flow (0.65 $mL \cdot min^{-1}$) through the FIA system. Experiments were performed in 37± 0.3 ^{O}C or room temperature (ca. 22 ^{O}C) aCSF, as noted. To maintain a constant 37± 0.3 ^{O}C environment for the duration of an experiment, beakers and submersible parts of the FIA system, including the injection loop (0.50 mL), all other fluid lines, and the flow cell were placed in a water bath (Precision Scientific, Chicago, IL, USA). Maintaining a constant temperature is important because the activities of the enzymes, and properties of the polymer are temperature dependent [45]. Submersible magnetic stirrers (Corning, Sigma-Aldrich) were used to stir the water bath, and contents of the beakers. Due to a large stainless steel platform (30.5cm x 25.5 cm x 0.2 mm, elevated 7cm from the bottom of the water bath), that the beakers sat on in the water-bath,

stirring the water bath was necessary to maintain the ±0.3 ^{O}C deviation in temperature. Placing the FIA system in a 37 ^{O}C oven as a means to maintain temperature control was not effective. Fluid traveling through the small diameter PTFE tubing used for the FIA system (i.e., 0.034 in., O.D., 0.0625 in. I.D.) fluctuated in temperature as the heating element of the oven turned on and off, enough such that aCSF traveling through the tubing caused an unstable baseline current. Standard solutions were prepared in aCSF, and were delivered manually to beakers with a pipette, or placed in-line, in the FIA system via a computer controlled, pneumatically-actuated valve.

4.3.7 Statistics

Data analysis was carried out with Origin Pro 7.5 software (OriginLab Corp., Northampton, MA, USA). Significance was determined using one-way ANOVAs. If an ANOVA indicated a significant difference existed, then a power analysis of the ANOVA and a Bonferroni post-hoc comparison of means were conducted. Unless otherwise indicated, only when a power analysis of the ANOVA yielded a value of P> 0.80 were data considered to be significantly different.

4.3.8 Animal and Surgical Procedures

In vivo experiments were carried out on male Sprague-Dawley rats (Hilltop Lab Animals Inc., Scottdale, PA, USA), with the approval of the Institutional Animal Care and Use Committee of the University of Pittsburgh. The rats weighed between 250 and 375 g, and were anesthetized with an initial dose of chloral hydrate (400 mg/kg i.p.) and given atropine (0.1

mg/kg i.p.). Subsequent chloral hydrate was delivered when gentle pressure to the hind paw resulted in any detectable motor response. The anesthetized rats were placed in a stereotaxic surgical frame with the incisor bar positioned 5 mm above the interaural line[61], and were wrapped in a homeothermic blanket that maintained body temperature at 37 ^{O}C. A midline incision made through the scalp allowed the scalp to be retracted and the skull exposed. Holes drilled in appropriate positions through the skull with a Dremel™ tool permitted the placement of the electrodes and microinfusion pipette. A glutamate sensor was positioned in the striatum, at a point 4.5 mm below dura, 2.5 mm anterior to bregma, and 2.5 mm lateral to the midline. A sentinel (i.e., peroxide) sensor was placed in the same coronal plane, approximately 150 μm away, at an 8^{O} angle to the peroxide sensor. A salt bridge, created by placing a Kimwipe® in the tapered end of a 1 mL disposable pipette tip filled with aCSF, functioned as the electrical contact between the brain and a Ag/AgCl reference electrode. This was typically placed in a small hole drilled in the anterior-most region of the exposed skull, away from the sensors.

Microinfusion pipettes were prepared from fused silica capillary tubing (25±1 μm I.D.; 360 μm O.D.) (Polymicro Technologies Inc., Phoenix, AZ, USA). The outlet end was etched to 35-40 μm O.D. with hydrofluoric acid, while the inlet end was attached to a 50-μL Gastight ™ syringe (Hamilton, Reno, Nevada, USA) mounted on a microprocessor-controlled driver (NA-1, Sutter Instruments, Novato, CA, USA).

4.4 RESULTS AND DISCUSSION

4.4.1 Mediation of Electron Transfer by $[Os(bpy)_2(py)Cl]^{+/2+}$

In the absence of other mediators (e.g., in aCSF), the $[Os(bpy)_2(py)Cl]^{+/2+}$ redox couple mediates electron transfer between HRP and the electrode following the HRP-catalyzed reduction of H_2O_2 (Scheme 3).

Scheme 3.

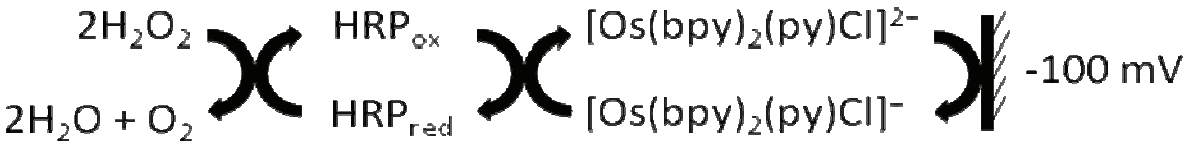

4.4.2 Mediation of Electron Transfer by Hydroquinones

The oxidation of hydroquinones, including dopamine and DOPAC, is reversible and leads to the formation of an ortho-quinone (hence forth simply called a quinone (Q)) which can be electrochemically reduced back to the parent hydroquinone at the operating potential of these electrodes (-100 mV wrt. Ag/AgCl). Other than accounts of hydroquinone oxidation by exposed metal centers [73], clear evidence of this reaction has not been previously noted in the context of these sensors. This is unusual however, as it is well known that HRP catalyzes the oxidation of hydroquinones by peroxide [82, 83], and the oxidized form of the Os-mediator reacts with hydroquinones [36, 70-72] (Reaction 7).

Reaction 7

$$H_2Q + 2[Os(bpy)_2(py)Cl]^{2+} \rightarrow Q + 2H^+ + 2[Os(bpy)_2(py)Cl]^+$$

We synthesized a PVP-based polymer lacking the Os-centered complexes (0 Os polymer, see the Experimental Section). Carbon fiber electrodes were coated with 0 Os hydrogels containing HRP: these sensors were not coated with Nafion. Cyclic voltammograms recorded in aCSF exhibited only capacitive background currents (Figure 1A).

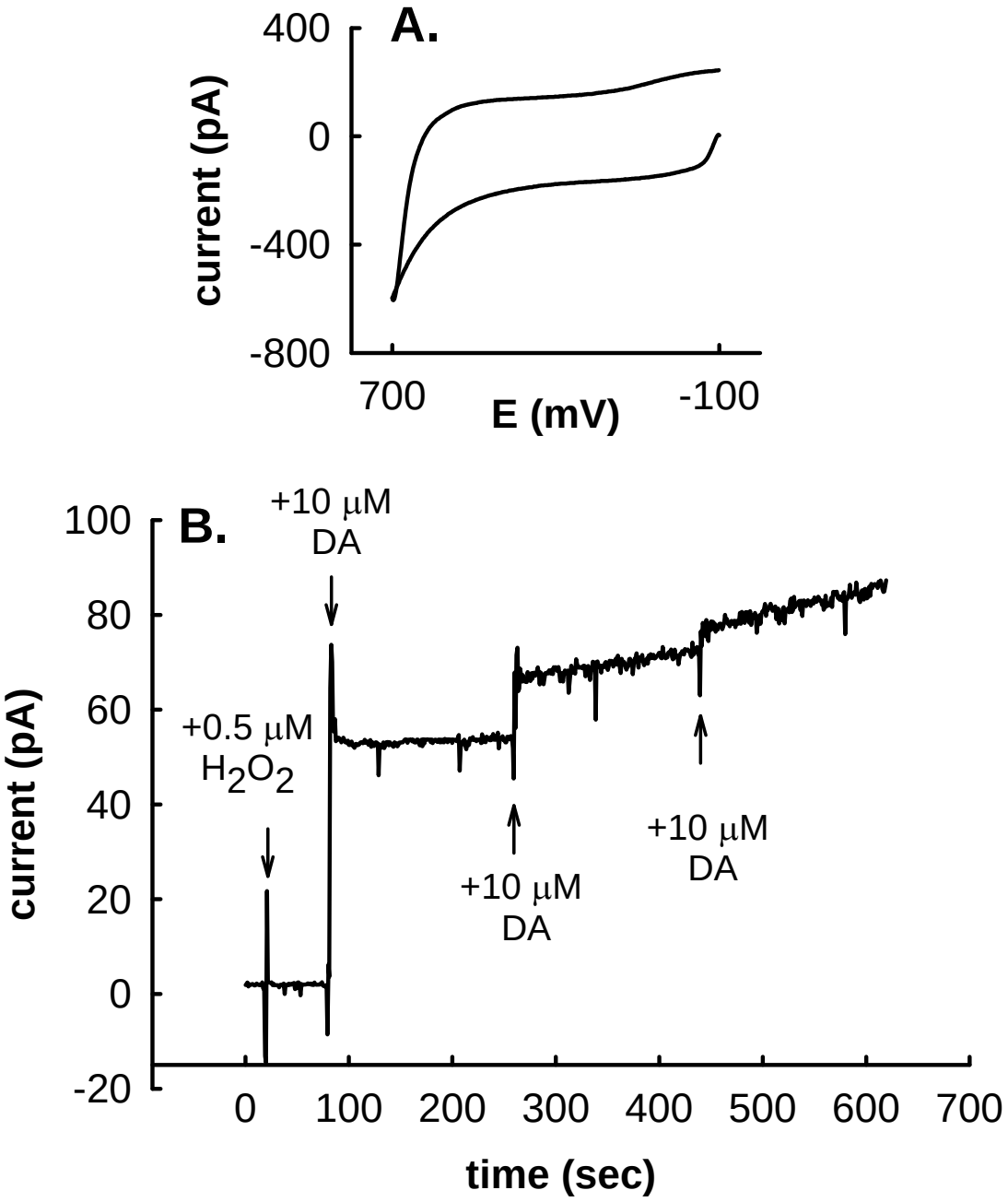

Figure 4-1. (A) Cyclic voltammogram (υ= 0.10 V·s^{-1}) of a peroxide sensor (n=1), not coated with Nafion, prepared with an $[Os(bpy)_2(py)Cl]^{+/2+}$ free version of the hydrogel (0 Os), in a stirred beaker of 37 ^{O}C aCSF. (Plot B) Response gathered from the same sensor held amperometrically at -100 mV when exposed to 0.5 μM H_2O_2, and the concentration of DA was increased to 10, 20, and 30 μM DA.

During amperometric experiments in well-stirred solutions, these sensors produced low picoamp background currents and did not respond when the solution was adjusted to 0.5 μM H_2O_2 (Figure 1B). The subsequent addition of 10 μM dopamine to the same solution caused the current to increase to a new steady state value just over 50 pA within 1 s. The positive current indicates an electrochemical reduction. The addition of dopamine alone, i.e., in the absence of H_2O_2, produced only a small transient (Chapter 3, Figure 3-4). Thus, the amperometric signal in Figure 1B is attributable to the reduction of quinone formed by the HRP-catalyzed oxidation of dopamine by peroxide. This confirms the ability of hydroquinones to mediate electron transfer between carbon fiber electrodes and hydrogel-entrapped HRP (Scheme 4).

Scheme 4.

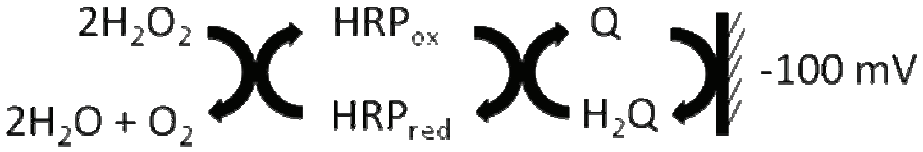

Subsequent 10-μM increments in the dopamine concentration produce smaller increases in current relative to that produced by the first aliquot of dopamine (Figure 1). This is consistent with saturable enzyme kinetics and suggests that the apparent K_M of the immobilized HRP for dopamine is below 10 μM. This confirms the involvement of the enzyme in the generation of the amperometric response in Figure 1B.

4.4.3 Calibration Considerations

To explore the role of hydroquinones as electron transfer mediators in the presence of the Os-centered mediator, peroxide sensors were calibrated under two sets of experimental conditions (Figure 2). These sensors were prepared with a thin Nafion layer (see Experimental Section, Nafion Films). The sensors were first calibrated in the FIA system and then in the well-stirred solution. Both calibrations were performed at 37 ^{O}C. In both cases, the sensors were calibrated in 5 μM H_2O_2 alone and in 5 μM H_2O_2 with 2.5 μM dopamine.

In the FIA system, the responses to H_2O_2 alone (solid line) and to H_2O_2 + DA (dashed line) were similar but not identical in both time course and amplitude (Figure 2A). The responses overlapped for the first 5-10 s and then diverged. The response observed in the presence of dopamine was 7% smaller at the end of the sample bolus (i.e., at t=55 s).

Overall, the sensors displayed a greater sensitivity in well-stirred solutions than in the FIA system (Figure 2B). Amperometric responses were ca. 5-fold greater in well-stirred solution; note that the current scale bars show 20 pA in Figure 2A and 100 pA in Figure 2B. Hence, the amperometric signals are sensitive to convection in the bulk solution. Furthermore, in the well-stirred solution, different amperometric responses were obtained upon the addition of H_2O_2 alone and upon the addition of H_2O_2 + DA. The response to H_2O_2 alone (Figure 2B, solid line) increased about 100 pA within 10 s and then gradually at a rate of 3.0 pA·sec^{-1} from t=25 to t=120 s. The response to H_2O_2 + DA (Figure 2B, dashed line) increased about 185 pA within 10 s, and then slowly at a rate of 1.1 pA·sec^{-1} from t=25 to t=120 s. The current traces cross near t=60 s.

The difference between the signals observed in the well-stirred solution upon the addition

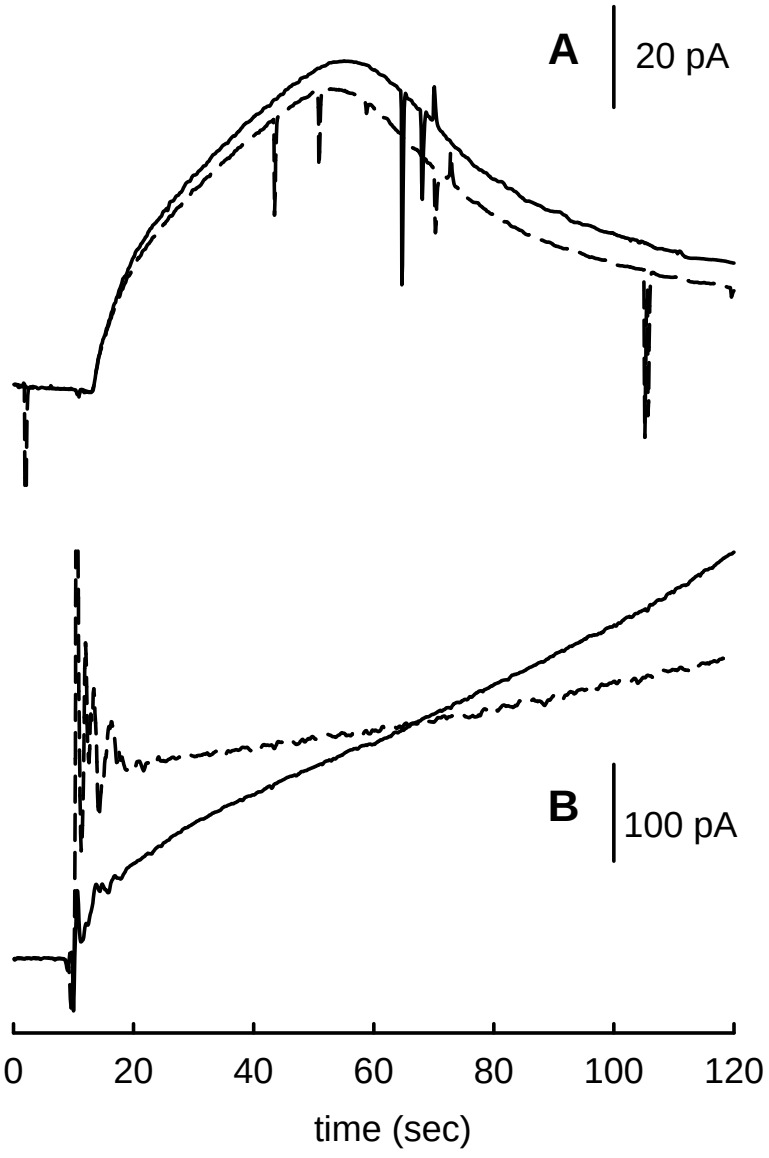

Figure 4-2. Sensors prepared with hydrogels containing 100 Os, coated with a thin Nafion film, operated amperometrically at -100 mV wrt. Ag/AgCl, were exposed to 5 μM H_2O_2 (solid line) or 5 μM H_2O_2 + 2.5 μM DA (dashed lined) at t=10 s. Experiments were conducted in 37 ^{O}C aCSF, in a FIA system (A) and a stirred beaker (B) over a 2-minute period. Traces in plot A are the average of n=6 responses at n=2 sensors, and were gathered using flow rate of ca. 0.65 mL·min^{-1}. Traces in plot B are the average of n=2 responses at n=2 sensors.

of H_2O_2 alone and H_2O_2 + DA suggests that different rate determining steps control the two responses. The response to H_2O_2 alone involves the mediation of electron transfer by the Os-centered complexes, since no other mediator is available. However, in the presence of H_2O_2, the possibility exists (Figure 1) that dopamine may also serve as the mediator. Since the presence of DA changes both the time course and amplitude of the amperometric response (Figure 2B), we conclude that DA and its quinone participate in the mediation. This result identifies the possibility that hydroquinones can mediate electron transfer between HRP and carbon electrodes even in the presence of the Os-centered mediator.

The current responses to H_2O_2 alone and H_2O_2 + DA are different only when the sensors are operated under high-convection conditions (e.g., in well-stirred solutions) such that mass transfer of small molecules from the bulk solution into the hydrogel layer is not the rate determining step in signal transduction. Thus, calibration in well-stirred solutions provides a means to investigate the interaction of hydroquinones with the sensors. Furthermore, observation of hydroquinone redox chemistry in this work requires hydrogen peroxide to drive hydroquinone oxidation in the hydrogel.

4.4.4 Three Factors other than Convection Influential on Hydroquinone Redox Chemistry: H_2O_2 Concentration, Hydroquinone Concentration, and Sensor Sensitivity

Although convection plays a significant role in the hydroquinone redox chemistry observed at sensors prepared with hydrogels containing the Os-centered mediator (section 4.4.3), there appears to be a few other factors which also contribute. From the responses in Figure 2B, when t>60 s, it appears that transport of the redox equivalents to the electrode is less efficient in

the presence of the hydroquinone/quinone mediator. This however, is not always the case. In Figure 3, we exposed peroxide sensors containing a thin film of Nafion (n=6, 25 Os hydrogel), equilibrated in the presence of 0, 2.5, 7.5, and 10 μM dopamine concentrations, to 0.5, 1.0, 2.5, 5.0, and 10 μM H_2O_2 at t=10 s. These experiments were performed in a well-stirred beaker of 37 ^{O}C aCSF. All calibrations were performed in a given dopamine concentration before being repeated in another dopamine concentration, and in the following order: 0, 2.5, 7.5, 10, 0 μM DA. At t=60 s, the experiment was ended and the change in current noted over the 50 s duration that H_2O_2 was in contact with the sensor was recorded. As Figure 3 illustrates, when convection in the bulk solution remains constant, the efficiency of the transport of redox equivalents is also dependant on: 1) the concentration of H_2O_2, 2) the concentration of dopamine, and 3) the sensitivity of the sensor.

The current-time traces for one of the sensors used to construct Figure 3 are depicted in Figure 4: note the more rapid response times when calibrations are carried out in the presence of dopamine. Compared to the sensitivity of these sensors prior to dopamine exposure: When the $[H_2O_2] \leq 1$ μM, 2.5 to 10 μM dopamine increase the efficiency by which redox equivalents reach the surface. When $[H_2O_2] = 2.5$ μM, 2.5 μM dopamine decreases, while 7.5 to 10 μM dopamine increase the efficiency by which redox equivalents reach the surface. When $[H_2O_2] \geq 5$ μM, 2.5 to 10 μM dopamine increase the efficiency by which redox equivalents reach the surface. Calibration of these sensors in aCSF alone, after prior calibrations in the presence of dopamine, illustrates that the sensors have lost sensitivity. The loss of sensitivity is attributable to dopamine, and will be discussed later. Compared to the sensitivity of these sensors (i.e., in aCSF alone) after dopamine exposure, 2.5 to 10 μM dopamine increases the efficiency by which redox equivalents reach the surface, independent of the H_2O_2 concentration.

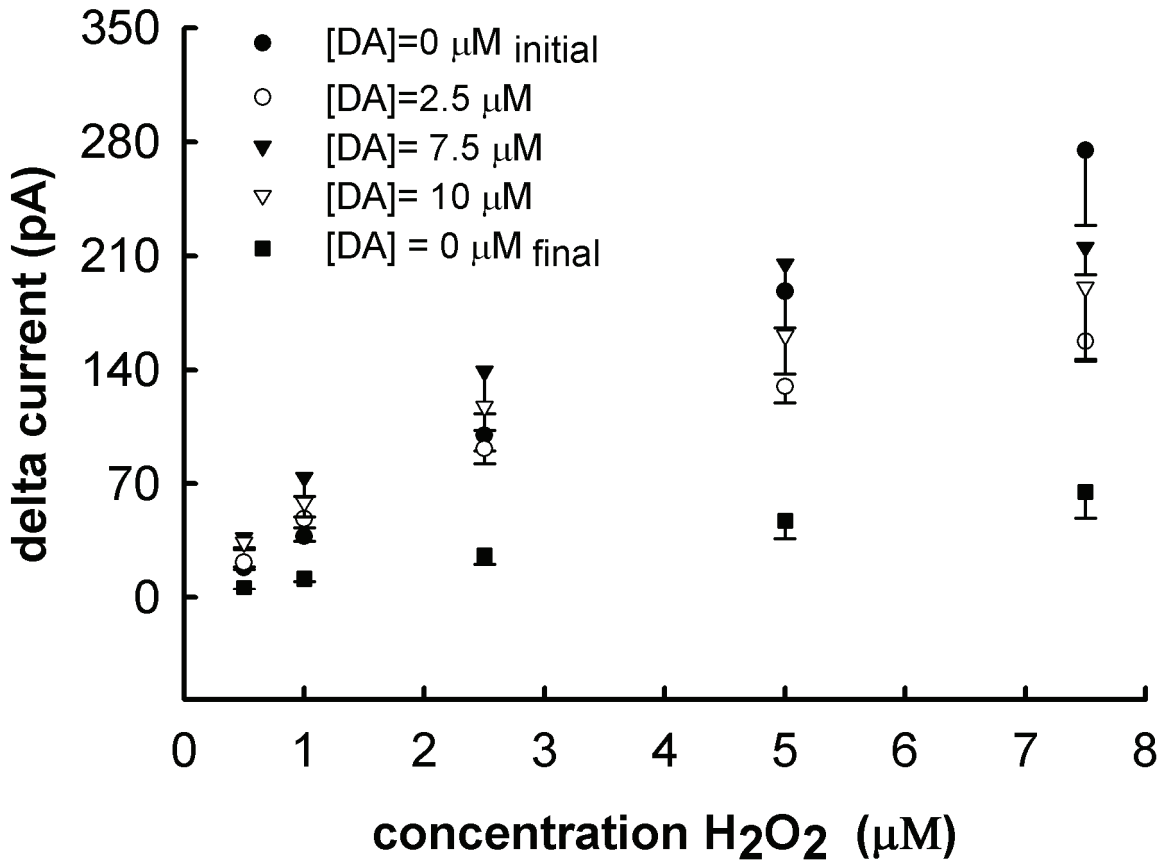

Figure 4-3. Peroxide sensors (n=6) were prepared with a hydrogel containing 25 Os, coated with a thin Nafion film, held at -100 mV wrt. Ag/AgCl, and calibrated in the presence of 0, 2.5, 7.5, and 10 μM dopamine. Experiments were performed in a well stirred beaker of 37 ^{O}C aCSF. Sensors were equilibrated in the given dopamine solution until a stable baseline was achieved, then exposed to H2O2 at t=10 s. Experiments were ended 50 s following exposure to H_2O_2 regardless of whether responses had reached a steady state.

Thus, the data Figure 3 and Figure 4 clearly demonstrate two important points. One, an increase in hydroquinone concentration in a sensor in which H_2O_2 is present or being generated may result in an increase or decrease in current even when the substrate which the sensor is selective for remains at a constant concentration. Whether an increase or decrease in current is realized upon increasing the hydroquinone concentration depends on the sensitivity of the sensor

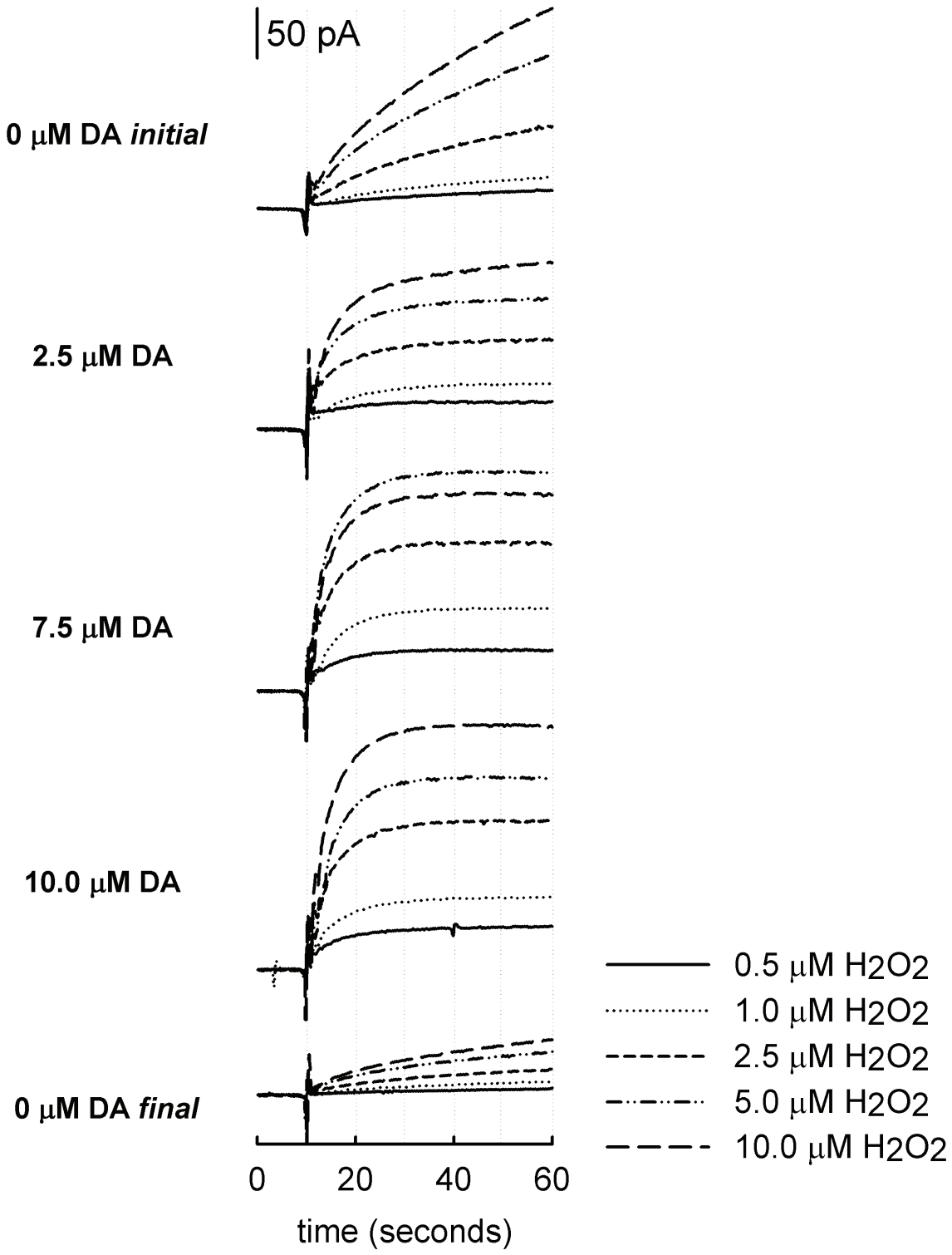

Figure 4-4. Current-time traces for a single peroxide sensor used to gather data for Figure 3-3. The sensor was operated at -100 mV, and calibrated in the presence of 0, 2.5, 7.5, and 10 μM DA.

at that given moment (i.e., if it were to be calibrated in the absence of hydroquinone). Second, under all conditions, calibrations in the presence of dopamine decreased response time. For example, in the presence of 7.5 μM dopamine, steady state responses were obtained at peroxide sensors within 10 s of the addition of H_2O_2 (Figure 4).

4.4.5 Anion Interference at Sensors with Thick Nafion Films

To confirm the effectiveness of Nafion as a tool for preventing potential interference by anionic substances, we examined glutamate and peroxide sensors coated with thick Nafion films. Calibrations were performed in well-stirred solutions and currents were recorded at steady state or non-steady state conditions. Non-steady state currents are reported for the glutamate sensors with thick Nafion films because of their very slow response time (greater than 45 min in some cases). Non-steady state currents were recorded at 50 s after adding glutamate to the solution. The sensor (n=4) response was linear over the range of glutamate concentration we examined (25-100 μM, r^2= 0.988) but was low in sensitivity, 13 fA·μM^{-1} (Figure 5).

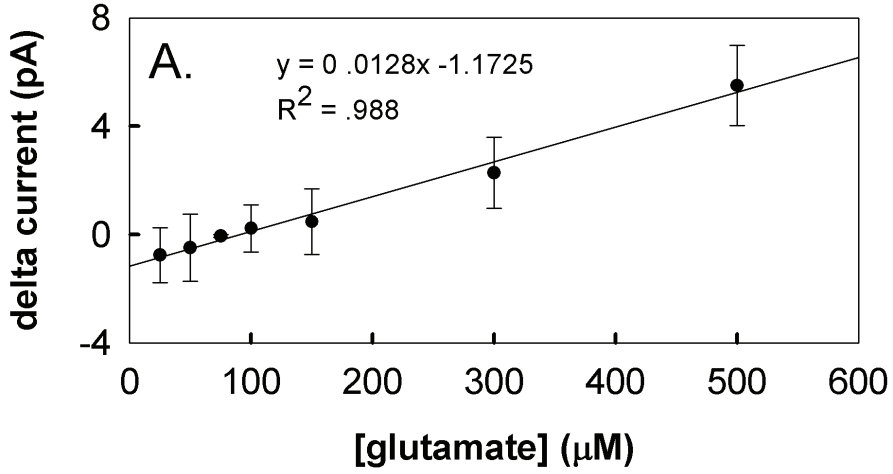

Figure 4-5. Calibration plot of glutamate sensors (n=4) prepared with hydrogel containing 100 Os, coated with a thick Nafion outerlayer under non-steady state conditions. Calibrations were carried out at sensors held at -100 mV (wrt. Ag/AgCl), in a stirred beaker containing 37 ^{O}C aCSF. Error bars show standard deviation.

Sensors with thick Nafion films are far less sensitive than those with thin Nafion films (Figure 6A). The sensor with a thick Nafion film, however, was highly sensitive to peroxide (Figure 6B), producing 160 pA 50 s after addition of 5 μM H_2O_2 and eventually reaching a steady-state current over 1 μA. This confirms that the low glutamate sensitivity (Figure 6A) is not a result of ineffective mediation of electron transfer in the hydrogel nor a loss of HRP activity. The large H_2O_2 current is a consequence of the ability of peroxide, a small, neutral molecule, to penetrate Nafion films and the hydrogel. Furthermore, the steady-state current was unaffected by two subsequent additions of 200 μM ascorbate (Figure 6B), confirming that thick Nafion films, in conjunction with ascorbate oxidase, prevent ascorbate interference. The thick Nafion film also prevents interference by 20 μM DOPAC (Figure 6C). These results confirm that thick Nafion films prevent potential inferences by ascorbate and DOPAC, both anions, even in the presence of substantial concentrations of peroxide. However, thick Nafion films cause low sensitivity for glutamate.

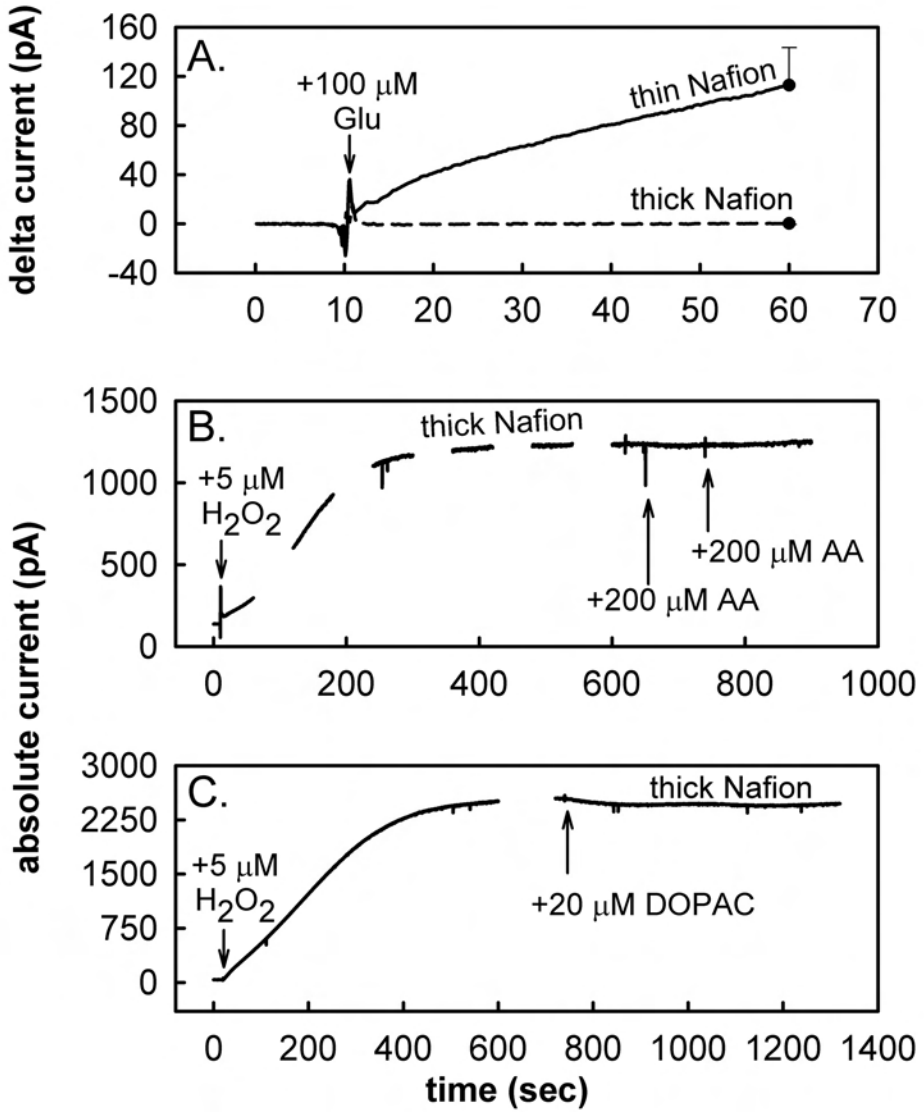

Figure 4-6. A) Average current-time responses of glutamate sensors (n=4) prepared with hydrogels containing 100 Os, with *thick* and *thin* Nafion outerlayers, when exposed to 100 μM glutamate for a period of 50 s. B) One of the glutamate sensors from plot A with a thick Nafion film exposed to 5 μM H_2O_2 and two subsequent additions 200 μM ascorbic acid. C) Response at peroxide sensors (n=4) with thick Nafion films when exposed to 5 μM H_2O_2 at t=20 s and 20 μM DOPAC at t=740 s. Experiments depicted in all plots were carried out at sensors operated amperometrically at -100 mV (wrt. Ag/AgCl), in a stirred beaker containing 37 ^{O}C aCSF. Error bars show the standard deviation.

4.4.6 Anion Interference at Sensors with Thin Nafion Films

We also examined glutamate sensors coated with thin Nafion films (n=4, 100 Os hydrogel). Compared to sensors with thick Nafion films, sensors with thin Nafion films produced a higher glutamate sensitivity (ca. 1.2 $pA \cdot \mu M^{-1}$), and responded linearly over the range 25-100 μM glutamate (r^2=0.995) when calibrated under the non-steady state conditions described above (Figure 7A, top trace). Sensors with thin Nafion films exhibited faster response times (although not apparent from the non-steady state i-t responses Figure 7B), but substantial interference by 200 μM AA (Figure 7B), and thus, are not suitable for in vivo measurements.

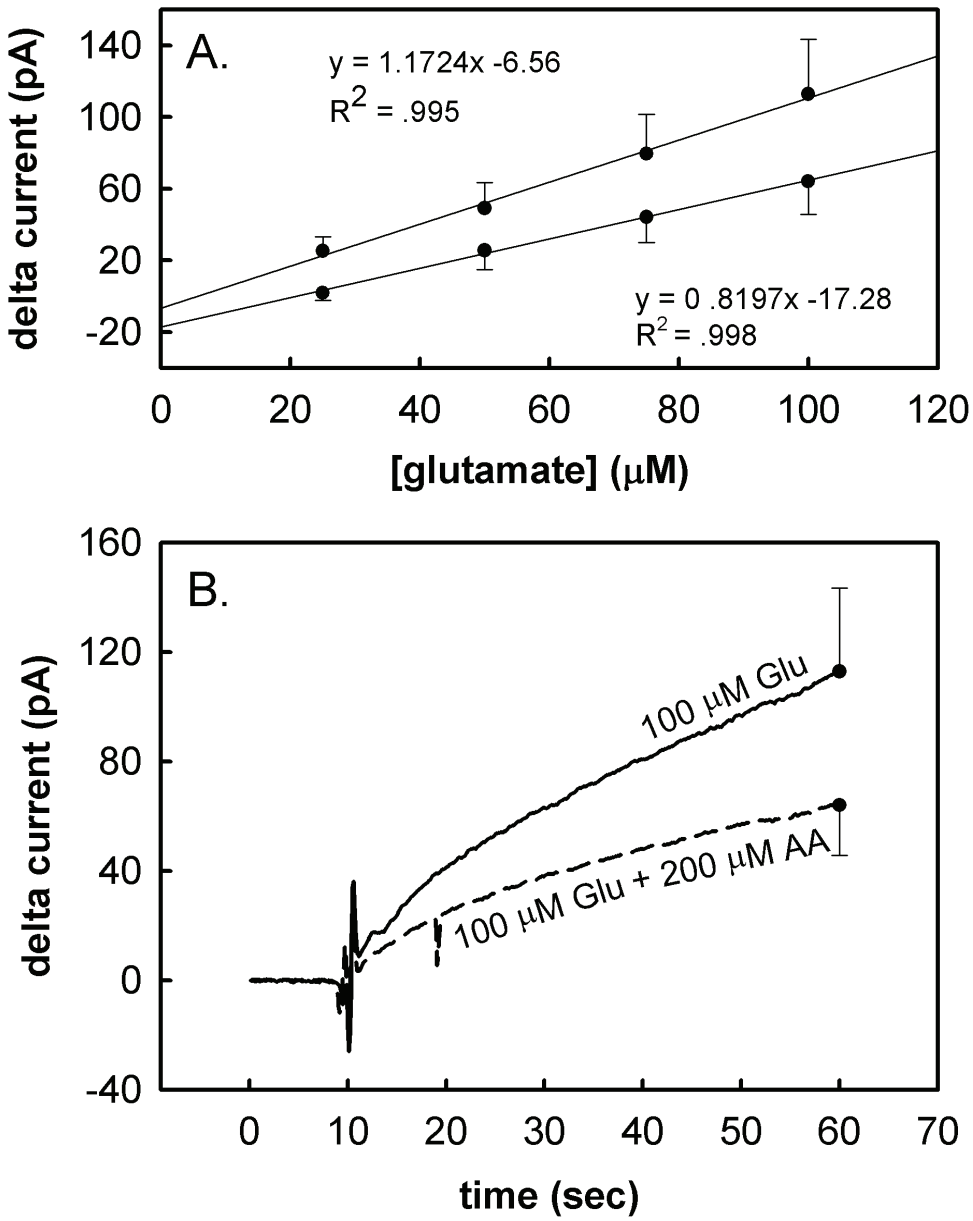

Figure 4-7. A) Calibration of glutamate sensors (n=4) prepared with hydrogel containing 100 Os, coated with a thin Nafion outerlayer, in the presence (lower trace) and absence (upper trace) of 200 μM ascorbate, under non-steady state conditions. B) Current vs time traces following exposure to 100 μM glutamate (t=10 s) gathered in the presence and absence of 200 μM ascorbate. Experiments depicted in both plots were carried out at sensors held at -100 mV (wrt. Ag/AgCl), in a stirred beaker containing 37 ^{O}C aCSF. Error bars show standard deviation.

4.4.7 The Effect of Osmium Loading

We examined whether adjusting the loading of the Os-centered redox complex in the hydrogel would be a means to control interferences when thin Nafion films are used. We reasoned that a competition exists between the Os complex and hydroquinone for the oxidized form of HRP (see again Figure 1). Thus, a higher Os loading might suppress hydroquinone oxidation. So, we prepared peroxide sensors using 25, 50, 100, 200, and 400 Os loading (see the Experimental Section for the explanation of these Os loading numbers). Sensors of each type were cycled through a 5-step experiment in well-stirred 37 ^{O}C solution. Step 1: a cyclic voltammogram was recorded in aCSF alone before any exposure of the sensor to H_2O_2 (see "1" in Figure 8A: the Steps in this experiment correspond to the numbers in Figure 8A: the rest of Figure 8 follows the same numbering sequence). Step 2: an amperometric response was recorded upon the addition of 5 μM H_2O_2. Step 3: the amperometric response was recorded upon the addition of 20 μM DOPAC (still in the presence of 5 μM H_2O_2). Step 4: the sensor was returned to a beaker of aCSF alone, and allowed to return to a steady state background signal before a second amperometric response was recorded in 5 μM H_2O_2. Step 5: a final cyclic voltammogram was recorded in aCSF alone. A detailed analysis of the plots in Figure 3-8 are reported in Tables 1 and 2. Sensors prepared with 1 mg·mL^{-1} stock solutions of the redox polymer were statistically evaluated separate from sensors prepared with 2 or 4 mg·mL^{-1} stock solutions of the redox polymer. Hence, the reason for two separate tables.

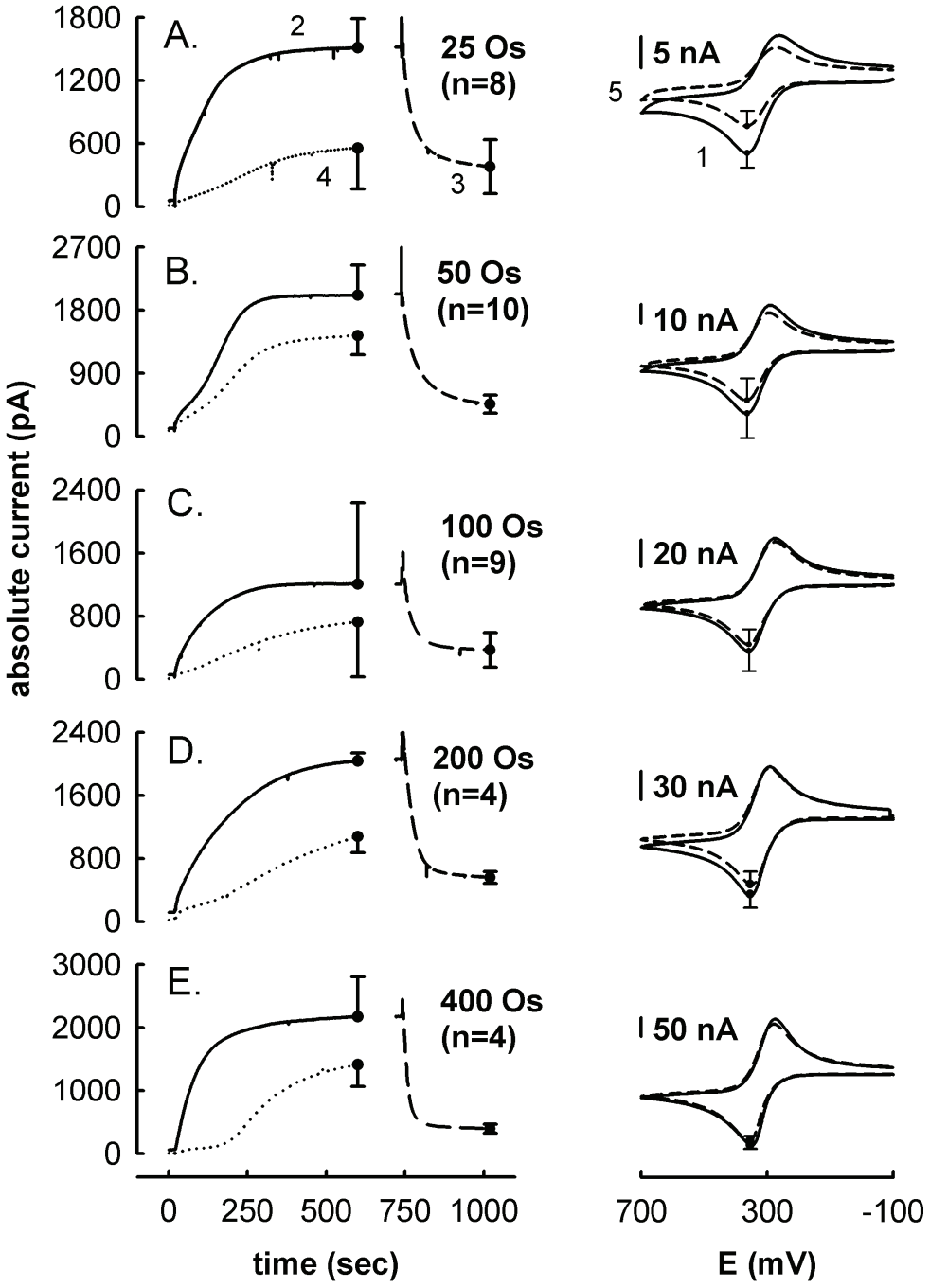

Figure 4-8. (Left): Responses of hydrogen peroxide sensors prepared with hydrogel containing 25, 50, 100, 200, and 400 Os, coated with thin Nafion films, held amperometrically at -100 mV wrt. Ag/AgCl, and exposed to 5 μM H_2O_2 at t=20 s (solid line), and 20 μM DOPAC at t= 720 s (dashed line). Responses to 5 μM H_2O_2 in pure aCSF following exposure to DOPAC for 5 minutes are depicted by the dotted line. (Right): Voltammograms (υ=0.10 $V \cdot s^{-1}$) taken in pure aCSF, before (solid) and after (dashed) exposure to DOPAC. Error bars show the standard deviation.

Table 4-1. Statistical Analysis of H_2O_2 sensors in Figure 4-8 prepared with 25, 50, and 100 Os

	Concentration of hydrogel ($mg \cdot mL^{-1}$) and loading of $[Os(bpy)_2(py)Cl]^{+/2+}$ in the hydrogel		
	"25 Os" 1 $mg \cdot mL^{-1}$ of 25 Os	**"50 Os" 1 $mg \cdot mL^{-1}$ of 50 Os**	**"100 Os" 1 $mg \cdot mL^{-1}$ of 100 Os**
number of sensors tested	8	10	9
absolute amperometric current (nA) 5 min after exposure to DOPAC	379± 256	460± 127	371± 221
change in amperometric current 5 min after exposure to DOPAC, relative to the increase induced by H_2O_2	-75.5± 12.9%	-75.4± 7.0%	-55.9 ± 20.7%
absolute change in the peak height (nA) of the oxidative sweep after exposure to DOPAC for 5 min	-4.1± 1.6	-6.9± 5.6	-5.4± 3.4
change in the peak height of the oxidative sweep after exposure to DOPAC for 5 min, relative to before DOPAC	-38.9± 15.7%	-37.0± 38.9%†	-10.2± 4.5%
		**	
sensitivity (pA) to 5 μM H_2O_2 in aCSF alone, before exposure to DOPAC	1452± 260	1898± 439	1151± 1000
	***	*	***	*	*
sensitivity (pA) to 5 μM H_2O_2 in aCSF alone, after exposure to DOPAC	544± 372	1356± 282	715±692
change in sensitivity to 5 μM H_2O_2 in aCSF alone after exposure to DOPAC, relative to before DOPAC		*	
	-63.3± 24.8%	-28.0± 5.4%	-37.7± 13.1%
		*	
response time (sec, t_{90}) for 5 μM H_2O_2 in aCSF alone, before exposure to DOPAC	205± 114	232± 61	229± 83
	*	**	**	**	***
response time (sec, t_{90}) for 5 μM H_2O_2 after exposure to DOPAC:	437± 72	312± 58	432± 5

*p< 0.05, **p<0.01, ***p<0.001: Bonferroni post-hoc comparison of means
†excluded from ANOVA due to large SD

Table 4-2. Statistical Analysis of H_2O_2 sensors in Figure 4-8 prepared with 200 and 400 Os

	Concentration of hydrogel ($mg \cdot mL^{-1}$) and loading of $[Os(bpy)_2(py)Cl]^{+/2+}$ in the hydrogel	
	"200 Os" 2 $mg \cdot mL^{-1}$ of 100 Os	**"400 Os" 4 $mg \cdot mL^{-1}$ of 100 Os**
number of sensors tested	4	4
absolute amperometric current (nA) 5 min after exposure to DOPAC	560± 75	390± 67
change in amperometric current 5 min after exposure to DOPAC, relative to the increase induced by H_2O_2	-71.3± 2.8%	-81.1± 2.8%
absolute change in the peak height (nA) of the oxidative sweep after exposure to DOPAC for 5 min	-10.7± 1.7	-10.2± 4.4
change in the peak height of the oxidative sweep after exposure to DOPAC for 5 min, relative to before DOPAC	*, a -13.6± 3.9%	-5.4± 2.2%
sensitivity (pA) to 5 μM H_2O_2 in aCSF alone, before exposure to DOPAC	1919± 138	2114± 628
	***	*
sensitivity (pA) to 5 μM H_2O_2 in aCSF alone, after exposure to DOPAC	1056± 211	1403± 340
change in sensitivity to 5 μM H_2O_2 in aCSF alone after exposure to DOPAC, relative to before DOPAC	* -45.3± 7.2%	-32.9± 3.3%
response time (sec, t_{90}) for 5 μM H_2O_2 in aCSF alone, before exposure to DOPAC	247± 123	200± 63
	**	**
response time (sec, t_{90}) for 5 μM H_2O_2 after exposure to DOPAC:	408± 107	457± 13

* $p<0.05$, ** $p<0.01$, *** $p<0.001$: Bonferroni post-hoc comparison of means
[a] power analysis of ANOVA indicated P= 0.75

The amplitude of the initial cyclic voltammograms (Step 1, Figure 8) increased with the Os loading in a predictable manner. The steady state amperometric current upon the initial exposure to H_2O_2 did not vary in any consistent manner with the Os loading, likely because these sensors contained a similar quantity of HRP, i.e., the rate of peroxide reduction is controlled by the HRP activity. The amperometric current decreased upon the addition of 20 μM DOPAC, for the reasons explained above. However, after the addition of DOPAC, the signals all dropped to a very similar current level, i.e., the Os loading did not solve the DOPAC interference problem.

Exposure of the sensors to DOPAC in the presence of H_2O_2 causes irreversible damage to the sensor response (Step 4, Figure 8). The amperometric response observed upon the second exposure of the sensors to a fresh sample of H_2O_2 was consistently and substantially smaller than the first response (compare Step 2 and Step 4 in Figure 8). We suspect that this is due to fouling of the hydrogel layer by the well-known formation oligomeric products following the oxidation of hydroquinones[84, 85]. From Figure 1, and several other experiments described in Appendix B, we have determined that hydroquinones in the hydrogel film can be oxidized by four separate mechanisms: 1) enzymatically, by HRP in the presence of H_2O_2, 2) by exposed metal centers in ascorbate oxidase, 3) by exposed metal centers in HRP, and 4) by the oxidized form of the Os redox couple. This fouling seems to "turn off" the oxidation of the Os mediator by HRP, enabling the hydroquinone to "take over" the mediation process. Although there is no correlation between the Os loading and the relative decrease in the response to H_2O_2 alone, which occurs after exposure to DOPAC (i.e., Step 4 compared to Step 2, Figure 8; r^2= 0.140), DOPAC interference was greatest at the 25 Os sensors. Increasing the Os loading to 50 Os decreased this, but did not eliminate DOPAC interference. However, further increases in Os

loading did not further diminish DOPAC interference. Thus, increasing the Os loading only partially decreased DOPAC interference.

We noticed, however, that the amplitude of the final cyclic voltammogram (Step 5 in Figure 8) was a function of the osmium loading, with the amplitude of the CV peaks showing greater stability at higher Os loadings. At the highest osmium loading (400 Os, Figure 8E), the initial and final CV peaks were essentially the same. Thus, the increased osmium loading diminished the effect of fouling on electron hopping diffusion in the film, even though it offered little protection against DOPAC interference.

In Appendix C, the results of an experiment similar to that described in Figure 8 are depicted. The results are consistent with the findings reported in Figure 8, but show the loss of sensitivity of peroxide sensors following exposure to DOPAC (in the presence of 5 μM H_2O_2) after 60 minutes.

4.4.8 Dopamine Interference at Sensors with Thick Nafion Films

In previous work on the calibration of these sensors, we have routinely employed the flow-injection analysis (FIA) system. However, here we have demonstrated that operating the sensors in a well-stirred solution offers a more rigorous test for interferences (Figure 2). This test is even more rigorous when carried out in high concentrations of peroxide to drive the hydroquinone oxidation reactions. Thus, we applied the more rigorous test to question whether interference by dopamine occurs (Figure 9). Dopamine is a cationic hydroquinone present in the striatal region of the brain, where it serves as a neurotransmitter. Therefore, it is especially important not to confuse glutamate with dopamine in this brain region. Although we have previously reported that dopamine does not interfere with these sensors, this is somewhat of a

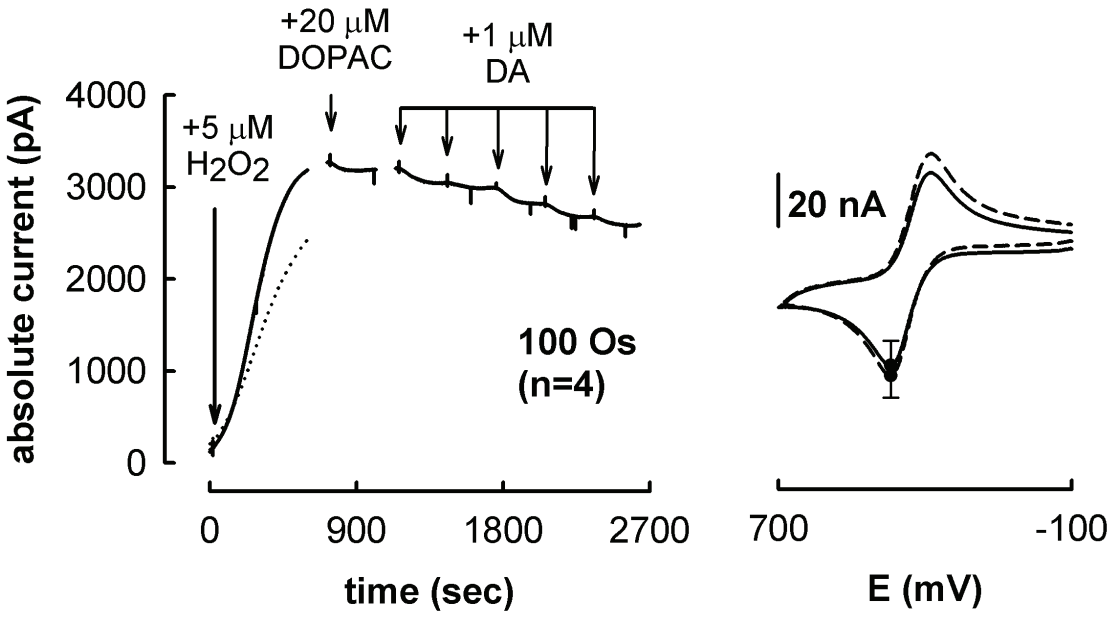

Figure 4-9. (Left): Responses of hydrogen peroxide sensors (n=4) prepared with hydrogels containing 100 Os, coated with thick Nafion films, held amperometrically at -100 mV wrt. Ag/AgCl, upon addition of 5 μM H_2O_2 at t=20 s, 20 μM DOPAC at t=720 s, 1 μM DA at t=1160, 2 μM DA at t=1460, 3 μM DA at t=1760 s, 4 μM DA at t=2060 s, and 5 μM DA at t=2360 s, cumulatively (solid lines). Responses to 5 μM H_2O_2 in pure aCSF following co-exposure to DOPAC and dopamine are depicted by the dotted line. (Right): Voltammograms (υ= 0.10 $V \cdot s^{-1}$) taken in pure aCSF, before (solid) and after (dashed) co-exposure to DOPAC and dopamine. Error bars show the standard deviation.

surprise as dopamine is cationic and thus Nafion is not expected to be permselective against dopamine. Indeed, many workers coat their dopamine electrodes with Nafion[86, 87].

Peroxide sensors were prepared with thick Nafion films and were subjected to the same 5-step experiment described above, with one modification. After the initial addition of 20 μM DOPAC to the solution, 5 subsequent additions of 1-μM dopamine were performed (Figure 9); the final dopamine concentration, 5 μM, exceeds the highest estimates of the resting extracellular dopamine concentration in the rat striatum. The addition of 20 μM DOPAC to the solution caused a 2.3% decrease in the steady-state peroxide current, a far smaller interference than in any example in Figure 8. The subsequent dopamine additions caused cumulative decreases in the current by 6.7%, 8.4%, 13.8%, 18.1%, and 20.7% from the original peroxide current (Figure 9). The thick Nafion films also prevented changes in the Os cyclic voltammograms and partially prevented fouling of the response to the second exposure to fresh peroxide solution. Overall, these data confirm that dopamine has the capacity to interfere with these sensors, although it is apparently necessary to employ these rigorous test conditions to observe this effect. We conclude that even though Nafion is not permselective against dopamine, the film limits the flux of dopamine into the hydrogel layer by electrostatic attractions. It is well know that cations diffuse slowly in cast Nafion films, due to this mechanism[88]. The relatively minor degree of interference by dopamine at sensors coated with thick Nafion films, in the presence of a high stirring velocity, and a large concentration of peroxide to drive dopamine oxidation, validates our prior reports that dopamine does not interfere with these sensors under less rigorous calibration conditions.

4.4.9 In Vivo Experiments

Several glutamate and sentinel sensors prepared with hydrogel containing 25 and 100 Os and thin Nafion films were evaluated in the extracellular space brain of anesthetized rats. The sensors were placed in the striatum, and a glutamate solution (10 mM) was infused adjacent to the sensors via a micropipette. Responses obtained at sensors prepared with hydrogel containing 25 Os were very different than responses obtained at sensors prepared with 100 Os.

Glutamate sensors prepared with hydrogel containing 25 Os (n=2) responded selectively following the infusion of glutamate (Figure 10). In Figures 10A and 10B, the horizontal lines indicate the time over which glutamate (10 mM, 200 nL) was infused. The increase in reductive current was only 5-10 pA in either experiment, which is small compared to the 30-40 pA increase observed in previous accounts of these sensors[48]. However, based on the postcalibration sensitivities of these sensors, the concentration of glutamate detected is similar to that observed in previous accounts[48]. Postcalibration of the glutamate sensors in Figures 10A and 10B indicated the sensors had sensitivities of 55.8 $fA \cdot \mu M^{-1}$ and 37.1 $fA \cdot \mu M^{-1}$. This correlates to a 90% and 93% decrease in sensitivity, respectively, over the time course of the experiment (ca. 60 min).

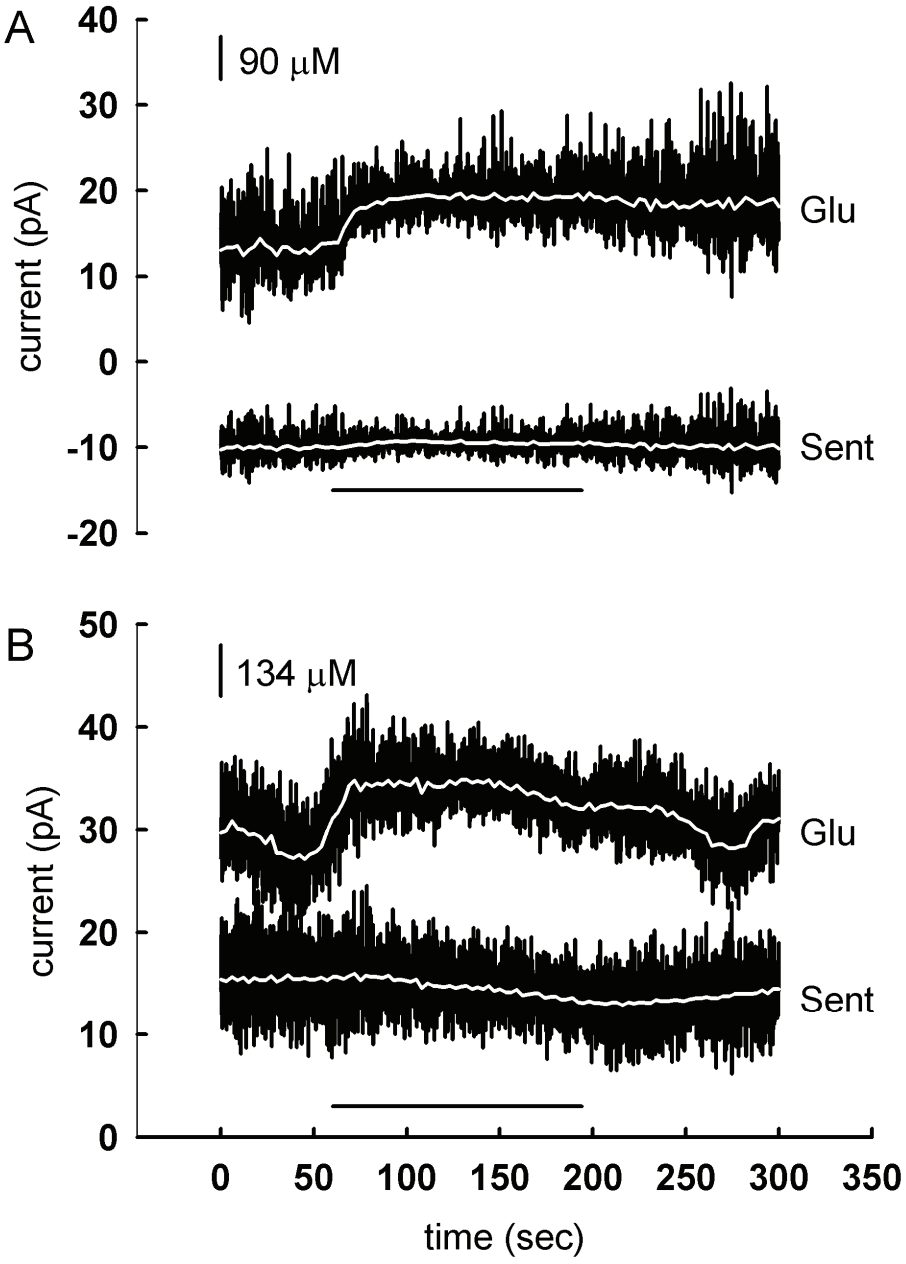

Figure 4-10. Responses of glutamate and sentinel (i.e., H_2O_2) sensors prepared with 25 Os, in the striatum of anesthetized rats, following a local infusion of 200 nL of 10 mM glutamate (horizontal line). Sensors were coated with a thin film of Nafion, and operated amperometrically at -100 mV wrt. Ag/AgCl. Concentration scale bars were prepared using the postcalibration sensitivities of the sensors.

In Figures 11A and 11B, the responses of a single glutamate sensor prepared with 100 Os were evaluated following two separate additions of glutamate (10 mM, 1200 nL). The first infusion of glutamate is shown in Figure 11A. Approximately 30 minutes later, the infusion was repeated (Figure 11B). Sentinel sensors were not used in this experiment because our focus was on preparing a glutamate sensor that produced a large increase in reductive current following the infusion of glutamate. The first infusion of glutamate produced a response that increased gradually, ca. 30 pA over a 400 second period (Figure 11A). After the response reached its maximum, the signal remained constant. The second response was qualitatively and quantitatively different than the first response. During the second infusion, the response increased, but not smoothly as in Figure 11A. Instead, the current rapidly increased and leveled off three separate times. The total increase in current observed during the second infusion was roughly four times that observed of the first. Postcalibration of the glutamate sensor in Figure 11B indicates the sensors had a sensitivity of 3.72 $pA \cdot \mu M^{-1}$. This corresponds to an 83% decrease over the time course of the in vivo experiment, ca. 60 min.

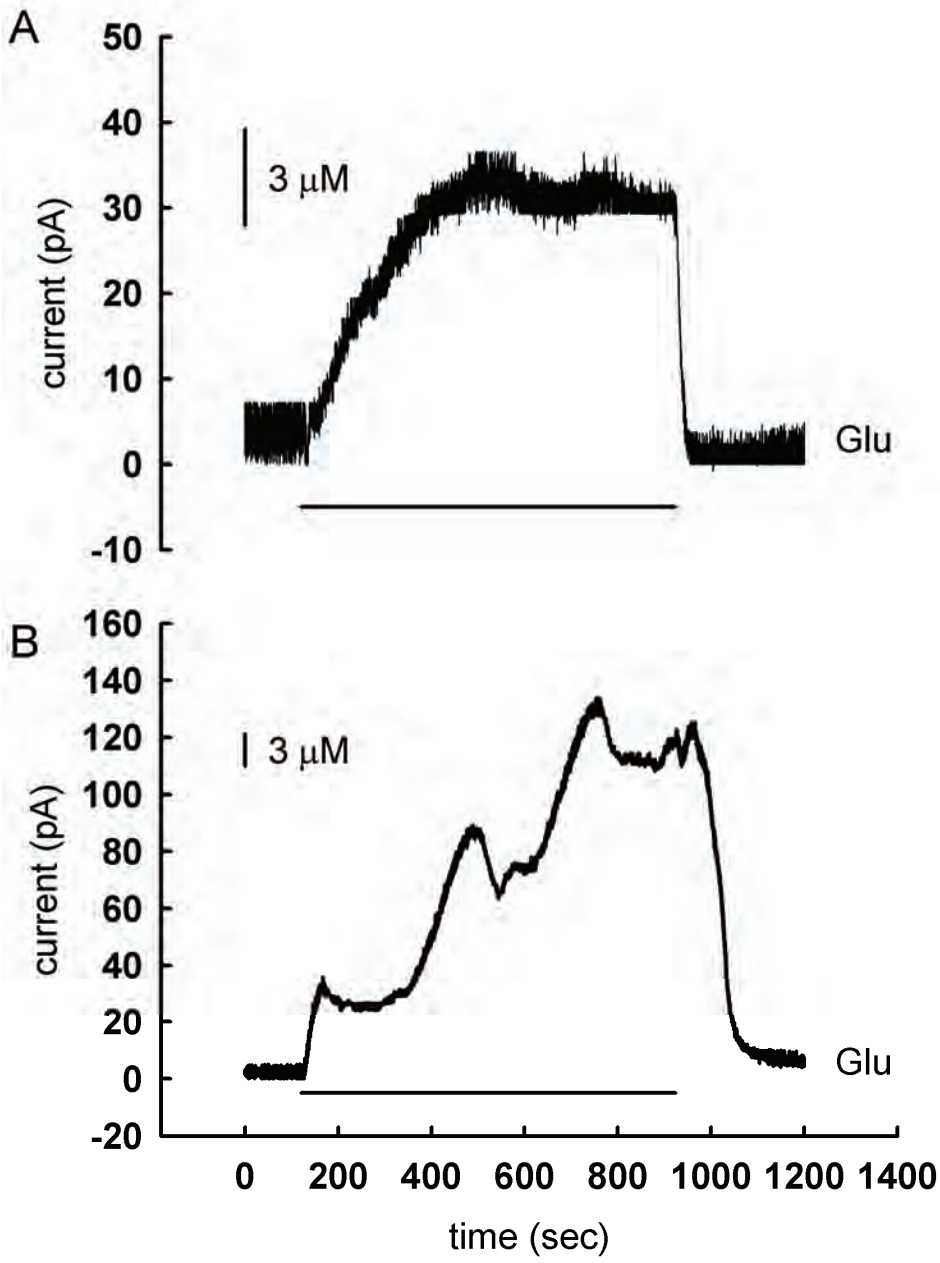

Figure 4-11. Responses of a single glutamate sensor prepared with 100 Os, in the striatum of an anesthetized rat, following the local infusion of 1200 nL of 10 mM glutamate (horizontal line). Note the difference between the first (A) and second (B) infusion of glutamate. Sensors were coated with a thin film of Nafion, and operated amperometrically at -100 mV wrt. Ag/AgCl. Calibration bars were prepared using the postcalibration sensitivities of the sensors.

Although the in vivo experiments depicted in Figure 11 need to be carried out several more times, they appear to be consistent with the data gathered in beakers, in the sense that sensors prepared with 25 Os appear to be more prone to fouling by hydroquinones than sensors prepared with 100 Os. It is also interesting to note the different responses obtained at the same glutamate sensor (Figure 11) when glutamate is infused a second time. Although this may be an artifact of the diffusion, it may also be due to the excitotoxicity of glutamate in the local tissue.

4.5 CONCLUSIONS

Overall, the results presented in this report confirm that electrochemical sensors based on the entrapment of enzymes in the redox-polymer hydrogel are useful for in vivo monitoring in the case that thick Nafion films are used. Although the thick Nafion film prevents interferences, even from the cationic substance dopamine, these films also limit the sensitivity and response time of the sensors. Increasing the Os loading of the hydrogel layer preserved the stability of the Os CV peaks but was only partially effective, at least in our hands, at eliminating fouling of the sensor response due to the accumulation of oligomeric products following hydroquinone oxidation. In a previous report we mentioned that sensors without Nafion films "were quickly passivated [i.e., lost all sensitivity] during in vivo experiments"[48]. In light of the new results presented above, especially Fig 4, we now realize that the rapid in vivo failure of sensors without Nafion is likely due to the formation of these oligomeric substances.

In previous in vivo work with these sensors, we have typically employed so-called sentinel electrodes. For example, during in vivo measurements of glutamate we compared amperometric currents from sensors prepared with and without glutamate oxidase. We now

realize, however, that this approach to sentinel detection must be used with care, for a sentinel electrode will not detect signals arising from hydroquinones in the presence of peroxide, at the primary (non-sentinel) sensor. Thus, the glutamate sensor, which contains a peroxide-generating enzyme, might respond to a hydroquinone when the sentinel does not, because the sentinel does not contain a peroxide forming enzyme. In theory, the perfect control sensor would be one in which H_2O_2 generation within the hydrogel film is identical to that in the primary sensor, but is produced from an enzyme other than to which the primary sensor is selective toward the substrate of. Preparing such a control sensor would be extremely complicated, if not impossible.

A better sentinel design involves a sensor with a different oxidase enzyme: in a previous study, we described the use of glucose oxidase for this purpose[42]. In previous work aimed at monitoring in vivo levels of glutamate, we additionally monitored ascorbate levels to confirm that changes in ascorbate levels were not affecting the sensors[47]. Since the present work raises the possibility that hydroquinones, such as dopamine, also have the potential to interfere with the sensors it may also be worthwhile to monitor hydroquinones under the same experimental conditions. Fortunately, various forms of in vivo voltammetry have been widely applied to the in vivo monitoring of hydroquinones by several research groups.

4.6 ACKNOWLEDGMENTS

This work was supported by NSF grant DBI-0553306.

APPENDIX A

POLYMER/SDS MIXTURE

A.1 TEM IMAGES OF POLYMER/SDS MIXTURE

Several TEM images of the polymer/SDS mixture upon drying were obtained. Drying the sample is a necessary step needed to obtain these images with the TEM. These pictures do not characterize the colloidal like suspension in solution, but provide some insight what the polymer/SDS mixture looks like upon drying.

A.1.1 Polymer/SDS mixture (684x zoom)

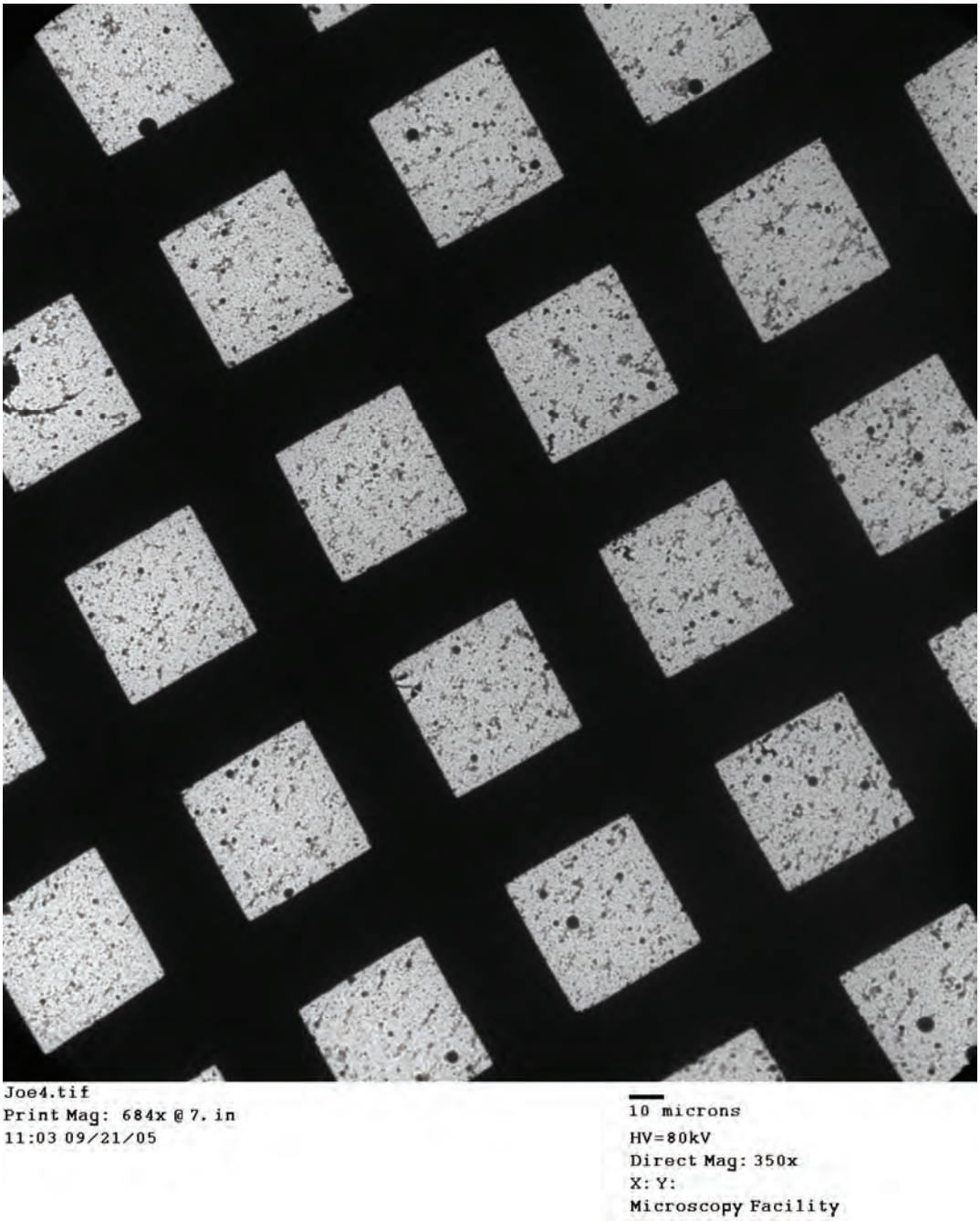

Figure A-1. Image of polymer/SDS mixture dried on a TEM grid.

A.1.2 Polymer/SDS mixture (10100x zoom)

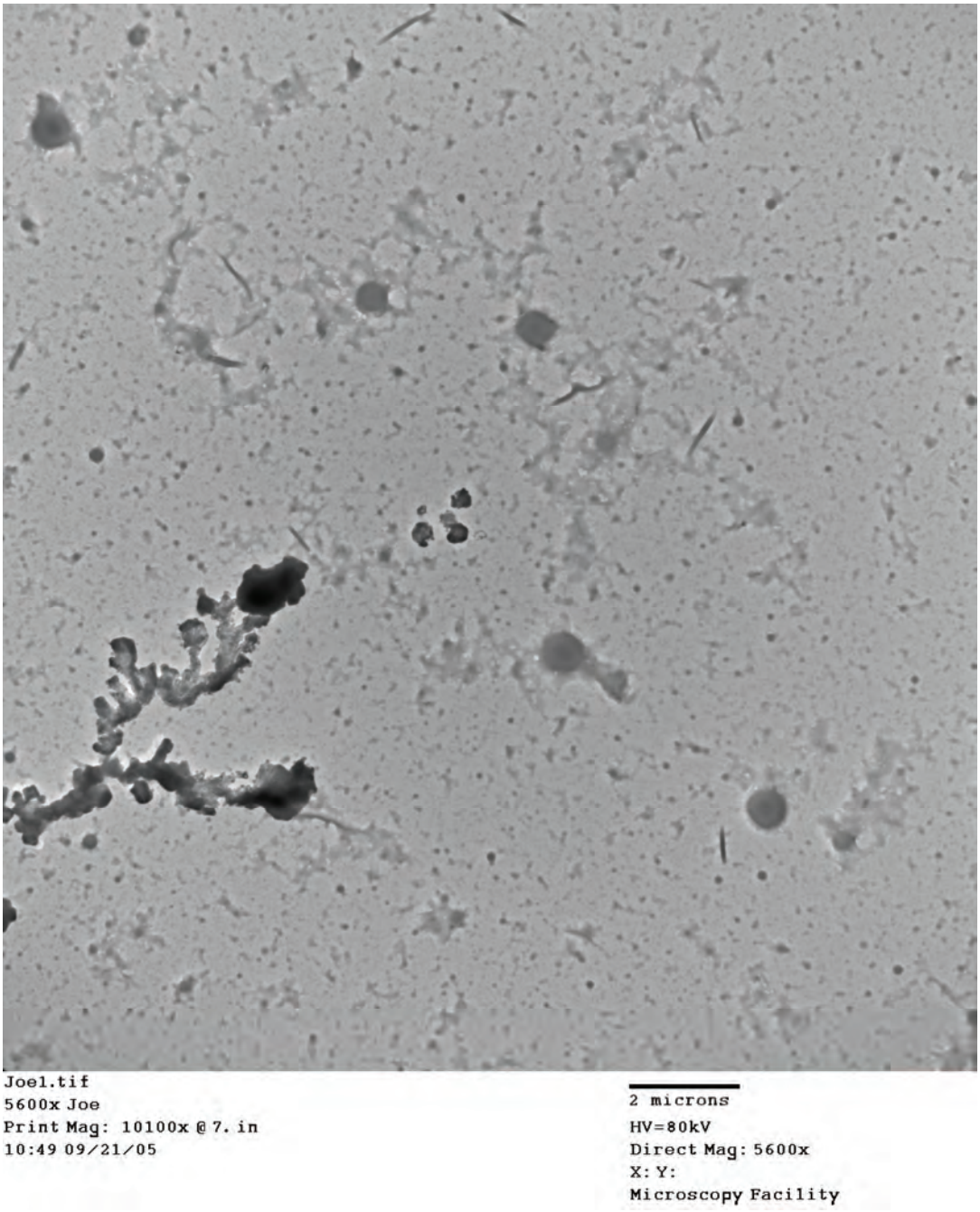

Figure A-2. TEM image of a dried mixture of polymer/SDS. Note the array of shapes found: large spheres, small spheres, lines, and a larger complex on the left side.

A.1.3 Polymer/SDS mixture (21500x zoom)

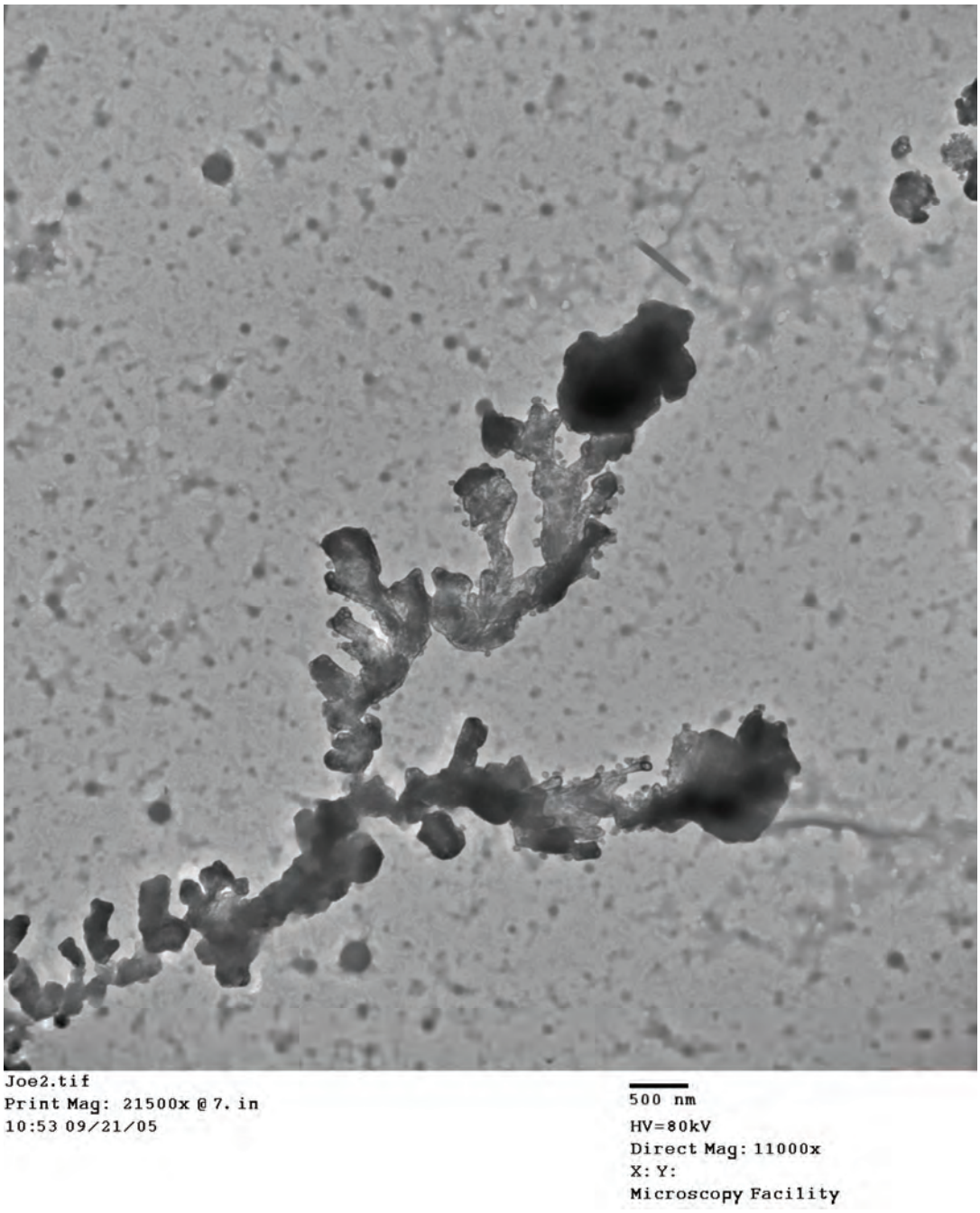

Figure A-3. TEM image of a dried mixture of polymer/SDS. A closer look at the complex noted in Figure A-2.

A.1.4 Polymer/SDS mixture (139000x zoom)

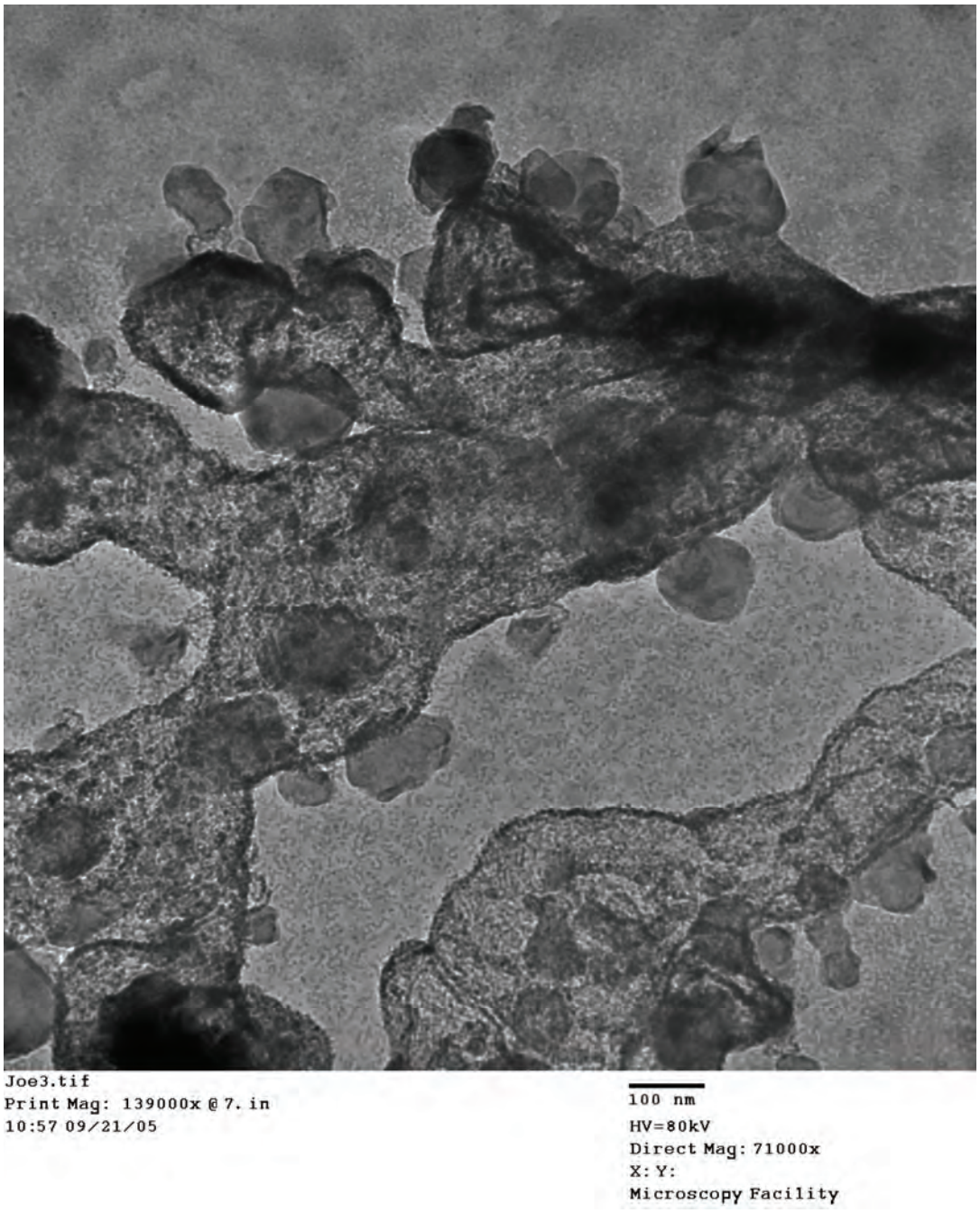

Figure A-4. TEM image of a dried mixture of polymer/SDS. An even closer look at the complex depicted in Figures A-2 and A-3.

A.1.5 Polymer/SDS mixture (55000x zoom)

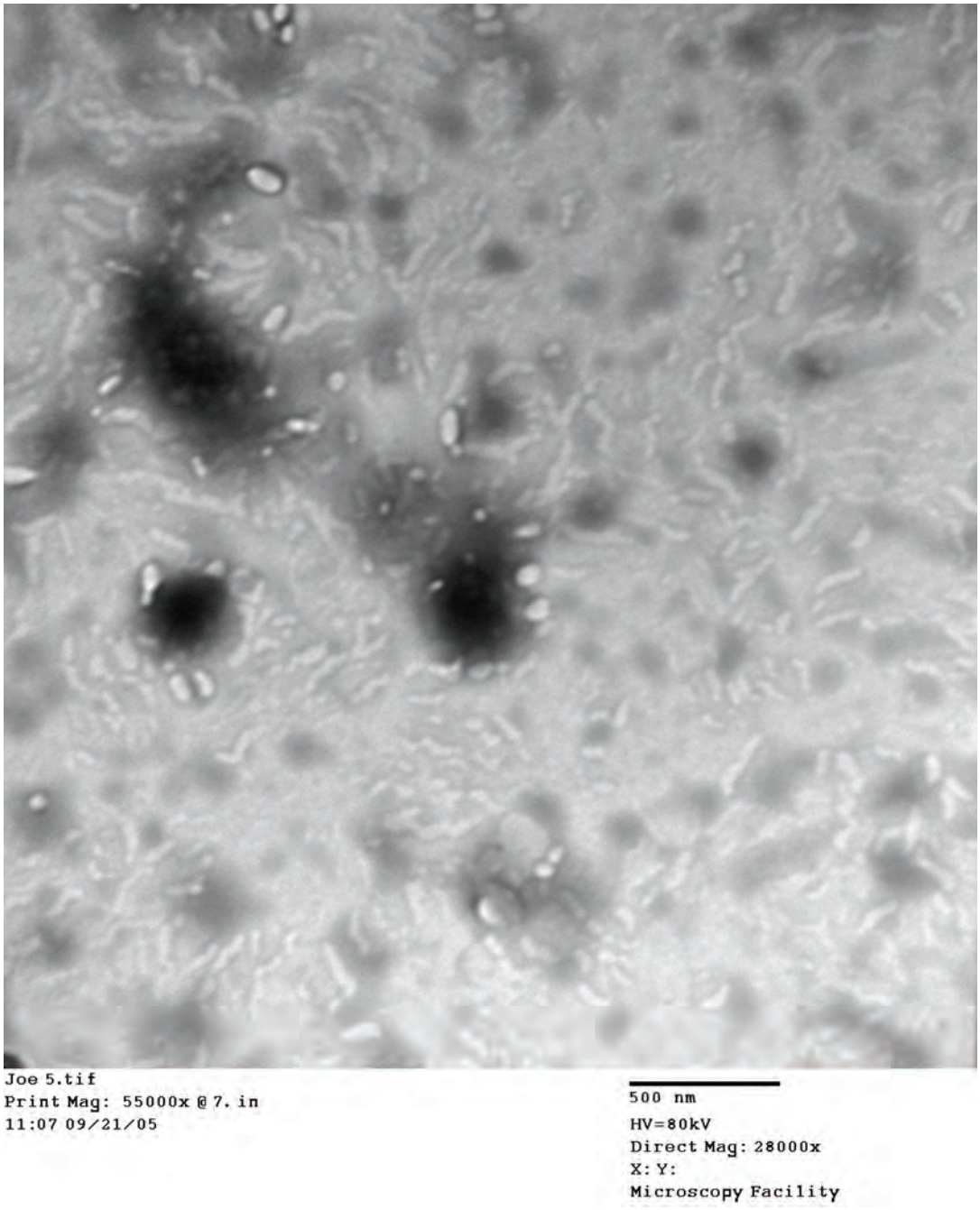

Figure A-5. TEM image of a dried mixture of polymer/SDS. A closer look at the smaller black sphere illustrated in Figures A-2 and A-3.

APPENDIX B

EVIDENCE OF HYDROQUINONE OXIDATION IN FILMS CONTAINING ENZYMES IMMOBILIZED IN A REDOX HYDROGEL

B.1 CYCLIC VOLTAMMOGRAMS TAKEN AT SENSORS PREPARED WITH HYDROGEL CONTAINING THE OS REDOX MEDIATOR

In Chapter 4, we mentioned there were four separate mechanisms by which hydroquinones may become oxidized in the hydrogel film. The first mechanism we mentioned by which hydroquinone oxidation may occur was enzymatically, by HRP in the presence of H_2O_2 (Figure 4-1). The other three mechanisms are depicted in this section, and include oxidation by exposed metal centers from ascorbate oxidase (Figure B-1, case 5), oxidation by exposed metal centers from HRP (Figure B-1, case 7), and oxidation by the oxidized form of the Os mediator, $[Os(bpy)_2(py)Cl]^{+/2+}$ (Figure B-1, case 11). Figure B-1 is a plot of CVs taken at several different sensors prepared with hydrogel containing 25 Os before (solid lines) and after (dotted lines) exposure to 12 different conditions (see the Experimental section of Chapter 4 for an explanation of 25 Os) The identity of the sensors, and conditions under which the sensors were evaluated are described in Table B-1.

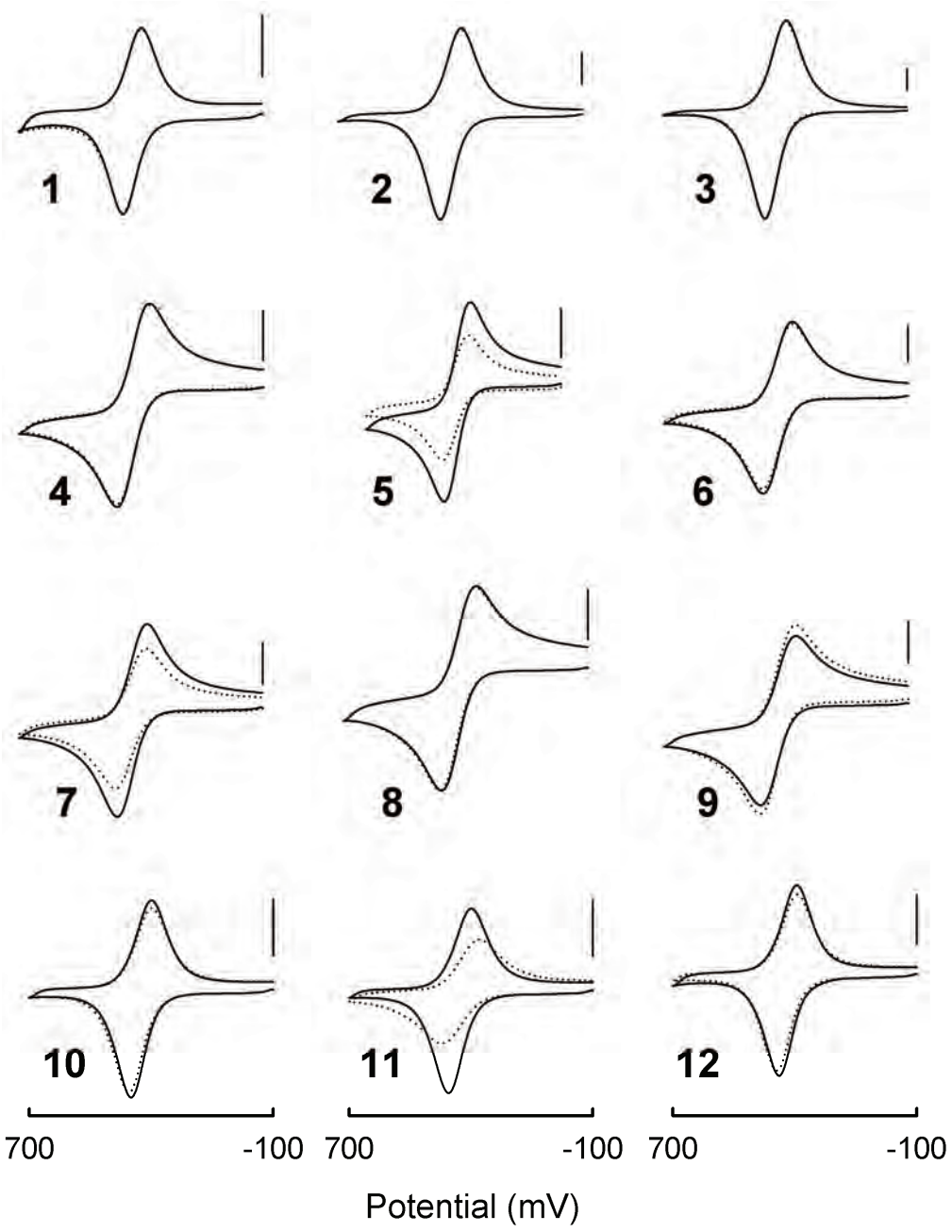

Table B-1. Cyclic voltammograms (υ=0.10 V·s^{-1}) of several styles of sensors taken in pure aCSF or 1.8% NaCl solution, before and after applying a -100 or +700 mV amperometric current (wrt. Ag/AgCl) in the presence of aCSF, 20 μM DOPAC, 5 μM H_2O_2, or 1.8% NaCl. The numbers identifying each plot correspond to the case number in Table B-1, and identify the components of the hydrogel. Each plot is accompanied by a vertical scale bar that indicates 5 nA of current. Sensors were prepared with hydrogel containing 25 Os.

Table B-1. Stability of the $[Os(bpy)_2(py)Cl]^{+/2+}$ mediator in the presence and absence of enzymes, at +700 or -100 mV, in various solutions.

case	components of hydrogel	$E_{applied}$ (mV) wrt. Ag/AgCl	sample	duration (min)	(*n*) sensors evaluated	relative change in amplitude of oxidative peak following exposure to sample
1	polymer, PEGDE	-100	ACSF	20	2	±5%
2	polymer, PEGDE	-100	DOPAC	20	4	±5%
3	polymer, PEGDE	-100	H_2O_2	20	2	±5%
4	polymer, PEGDE, AAOx	-100	ACSF	20	2	±5%
5	polymer, PEGDE, AAOx	-100	DOPAC	20	2	(-)35-40%
6	polymer, PEGDE, HRP	-100	ACSF	20	2	±5%
7	polymer, PEGDE, HRP	-100	DOPAC	20	2	(-)25-30%
8	polymer, PEGDE, AAOx, HRP	-100	ACSF	20	2	±5%
9	polymer, PEGDE, AAOx, HRP	-100	H_2O_2	20	4	(+)10-15%
10	polymer, PEGDE	+700	ACSF	20	2	(-)5-10%
11	polymer, PEGDE	+700	DOPAC	20	2	(-)50-55%
12	polymer, PEGDE	+700	1.8% NaCl	20	2	±5%

APPENDIX C

LOSS OF SENSITIVITY AT PEROXIDE SENSORS EXPOSED TO H_2O_2 AND DOPAC FOR 60 MINUTES

Similar to the findings depicted in Figure 4-8 (Chapter 4), a series of experiments carried out at peroxide sensors prepared with hydrogel containing 25 and 100 Os, coated with a thin layer of Nafion, produced similar responses when exposed to DOPAC (in the presence of H_2O_2) (Figure C-1). The experiments were performed according to the 5-step procedure described in *The Effect of Os Loading* (Chapter 4). However, unlike the sensors depicted in Figure 4-8 which were exposed to DOPAC for 5 min, the sensors described here were exposed to DOPAC for 60 min. (Note: The amperometric current is only shown for 30 minutes following exposure to DOPAC). The fouling experienced by peroxide sensors after exposure to DOPAC for 60 minutes at sensors is greater than when similarly prepared sensors were exposed to DOPAC for 5 min. A detailed analysis of the plots in Figure C-1 are reported in Table C-1.

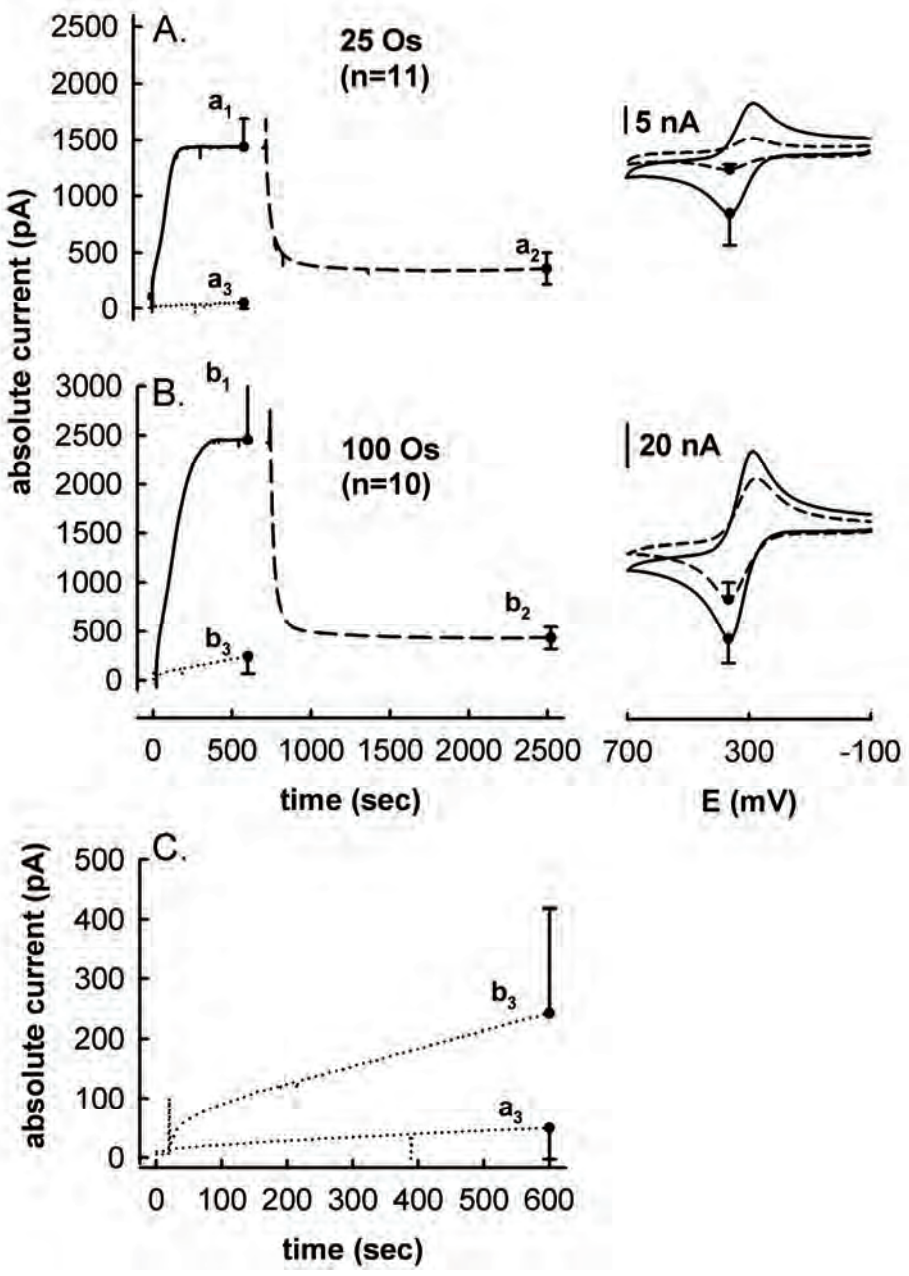

Figure C-1. Responses of hydrogen peroxide sensors prepared with hydrogel containing 25 Os (A) and 100 Os (B), coated with thin Nafion films, held amperometrically at -100 mV wrt. Ag/AgCl, and exposed to 5 μM H_2O_2 at t=20 s (solid line), and 20 μM DOPAC at t=720 s (dashed line). Responses to 5 μM H_2O_2 in pure aCSF following exposure to DOPAC for 60 minutes are depicted by the dotted line, and compared (C).Voltammograms (υ=0.10 $V \cdot s^{-1}$) taken in pure aCSF, before (solid) and after (dashed) exposure to DOPAC. Error bars show the standard deviation.

Table C-1. Statistical Analysis of H_2O_2 sensors in Figure C-1 prepared with 25 and 100 Os

	Concentration of hydrogel ($mg \cdot mL^{-1}$) and loading of $[Os(bpy)_2(py)Cl]^{+/2+}$ in the hydrogel	
	"25 Os" 1 $mg \cdot mL^{-1}$ of 25 Os	**"100 Os" 1 $mg \cdot mL^{-1}$ of 100 Os**
number of sensors tested	11	10
absolute amperometric current (nA) 30 min after exposure to DOPAC	357± 140	432± 113
change in amperometric current 30 min after exposure to DOPAC, relative to the increase induced by H_2O_2	*, a	
	-72.3± 9.1%	-81.0± 6.2%
absolute change in the peak height (nA) of the oxidative sweep after exposure to DOPAC for 60 min	**	
	-9.2± 6.0	-19.1± 4.5
change in the peak height of the oxidative sweep after exposure to DOPAC for 60 min, relative to before DOPAC	***	
	-76.9± 6.4%	-38.7± 3.6%
sensitivity (pA) to 5 μM H_2O_2 in aCSF alone, before exposure to DOPAC	***	
	1307± 256	2383± 532
sensitivity (pA) to 5 μM H_2O_2 in aCSF alone, after exposure to DOPAC	*** * ***	
	45± 51	231± 171
change in sensitivity to 5 μM H_2O_2 in aCSF alone after exposure to DOPAC for 60 min, relative to before DOPAC	*	
	-96.9± 3.9%	-90.7± 5.2%
response time (sec, t_{90}) for 5 μM H_2O_2 in aCSF alone, before exposure to DOPAC	*	
	132± 22	214± 69
response time (sec, t_{90}) for 5 μM H_2O_2 after exposure to DOPAC:	*, c *, b ***	
	310± 232	503± 20

*p<0.05, **p<0.01, ***p<0.001: Bonferroni post-hoc comparison of means
[a] power analysis of ANOVA indicated P= 0.67
[b] power analysis of ANOVA indicated P= 0.69
[c] power analysis of ANOVA indicated P= 0.62

APPENDIX D

PRE- AND POST-CALIBRATION EVALUATION OF SENSORS USED IN VIVO

Table D-1. Pre-and postcalibration data for sensors evaluated in Figures 13 and 17 (Chapter 2)

Figure ID	date of experiment	pre-in vivo sensitivity ($pA \cdot \mu M^{-1}$)	post- in vivo sensitivity ($pA \cdot \mu M^{-1}$)	pre- in vivo r^2	post- in vivo r^2
13A	061604	24	0.23	0.970	0.710
13B	080604	78	0	0.998	--
13C	081104	61	0	0.998	--
13D	083104	432	173	0.998	0.999
17A	120104B	175	175	0.999	0.999
17B	120804	112	88	0.996	0.998
17C	113004	106	126	0.997	0.998

BIBLIOGRAPHY

(1) Senior, S. Z.; Mans, L. L.; VanGuilder, H. D.; Kelly, K. A.; Hendrich, M. P.; Elgren, T. E. Catecholase Activity Associated with Copper-S100B, *Biochem.* **2003**, *42*, 4392-4397.

(2) Jennings, W. G. *Comparisons of Fused Silica and Other Glass Columns in Gas Chromatography*; Dr. Alfred Huthig Lerlag: New York, 1981.

(3) Rice, M. E.; Avshalumov, M. V.; Patel, J. C. In *Electrochemical Methods for Neuroscience*; Michael, A. C., Borland, L. M., Eds.; CRC Press: Boca Raton, 2007, pp 205-232.

(4) Daws, L. C.; Toney, G. M. In *Electrochemical Methods for Neuroscience*; Michael, A. C., Borland, L. M., Eds.: Boca Raton, 2007, pp 63-81.

(5) Daws, L. C.; Irvine, R. J.; Callaghan, P. D.; Toop, N. P.; White, J. M.; Bochner, F. Differential behavioral and neurochemical effects of para-methoxyamphetamine and 3,4-methylenedioxymethamphetamine in the rat, *Prog. Neuro-Psychopharm.and Biol. Psych.* **2000**, *24*, 955-977.

(6) Blaha, C. D.; Phillips, C.; Phillips, A. G. Does monoamine oxidase inhibition by pargyline increase extracellular dopmaine concentrations in the striatum?, *Neurosci.* **1996**, *75*, 543-550.

(7) Borland, L.; Michael, A. Voltammetric Study of the Control of Striatal Dopamine Release by Glutamate, *J. Neurochem.* **2004**, *91*, 220-229.

(8) Pennington, J. M.; Millar, J.; Jones, C. P. L.; Owesson, C. A.; McLaughlin, D. P.; Stamford, J. A. Simultaneous real-time amperometric measurement of catecholamines and serotonin at carbon fibre 'dident' microelectrodes, *J. Neurosci. Meth.* **2004**, *140*, 5-13.

(9) Lippincott-Schwartz, J.; Snapp, E.; Kenworthy, A. Studying protein dynamics in living cells, *Nat. Rev. Mol. Cell Biol.* **2001**, *2*, 444-456.

(10) Heim, R.; Prasher, D. C.; Tsien, R. Y. Wavelength mutations and posttranslational autooxidation of green fluorescent protein, *Proc. Natl. Acad. Sci. USA* **1994**, *91*, 12501-12504.

(11) Jung, J. C.; Mehta, A. D.; Aksay, E.; Stepnoski, R.; Schnitzer, M. J. In vivo mammalian brain imaging using one- and two-photon fluorescence microendoscopy, *J. Neurophysiol.* **2004**, *92*, 3121-3133.

(12) Levene, M. J.; Dombeck, D. A.; Kasischke, K. A.; Molloy, R. P.; Webb, W. W. In vivo multiphoton microscopy of deep brain tissue, *J. Neurophysiol.* **2004**, *91*, 1908-1912.

(13) Lippincott-Schwartz, J.; Patterson, G. H. Development and use of fluorescent protein markers in living cells, *Sci.* **2003**, *300*, 87-91.

(14) Potter, S. M. Vital Imaging: Two photons are better than one, *Current Biology* **1996**, *6*, 1595-1598.

(15) Guerrero, G.; Siegel, M. S.; Roska, B.; Loots, E.; Isacoff, E. Y. Tunneling FlaSh: redesign of the dynamics, voltage range, and color of the genetically encoded optical sensor of membrane potential., *Biophys. J.* **2002**, *83*, 3607-3618.

(16) Kuner, T.; Augustine, G. J. A genetically encoded ratiometric indicator for chloride: capturing chloride transients in cultured hippocampal neurons, *Neuron* **2000**, *27*, 447-459.

(17) Truong, K.; Sawano, A.; Mizuno, H.; Hama, H.; Tong, K. I.; Mal, T. K.; Miyawaki, A.; Ikura, M. FRET-based in vivo Ca^{2+} imaging by a new calmodulin-GFP fusion molecule, *Nat. Struct. Biol.* **2001**, *8*, 1069-1073.

(18) Bozza, T.; McGann, J. P.; Mombaerts, P.; Wachowiak, M. In Vivo Imaging of neuronal activity by targeted expression of a genetically encoded probe in the mouse, *Neuron* **2004**, *42*, 9-21.

(19) Ng, M.; Roorda, R. D.; Lima, S. Q.; Zemelman, B. V.; Morcillo, P.; Miesenbock, G. Transmission of olefactory information between three populations of neurons in the antennal lobe of the fly, *Neuron* **2002**, *36*.

(20) Michalet, X.; Pinaud, F. F.; Bentolila, L. A.; Tsay, J. M.; Doose, S.; Li, J. J.; Sundaresan, G.; Wu, A. M.; Gambhir, S. S.; Weiss, S. Quantum dots for live cells, in vivo imaging, and diagnostics, *Sci.* **2005**, *307*, 538-544.

(21) Larson, D. R.; Zipfel, W. R.; Williams, R. M.; Clark, S. W.; Bruchez, M. P.; Wise, F. W.; Webb, W. W. Water soluble quantum dots for multiphoton fluorescence imaging in vivo, *Sci.* **2003**, *300*, 1434-1436.

(22) So, M.-K.; Xu, C.; Loening, A. M.; Gambhir, S. S.; Rao, J. Self-illuminating quantum dot conjugates for in vivo imagining, *Nat. Biotech.* **2006**, *24*, 339-343.

(23) Troy, T.; Jekic-McMullen, D.; Sambucetti, L.; Rice, B. Quantitative comparison of the sensitivity of detection of fluorescent and bioluminescent reporters in animal models, *Mol. Imaging* **2004**, *3*, 9-23.

(24) Tuchin, V. *Tissue Optics*; SPIE Press: Bellingham, 2000.

(25) Bourne, J. A. Intracerebral microdialysis: 30 years as a tool for the neuroscientist, *Clin. Exp. Pharmacol. and Physiol.* **2003**, *30*, 16-24.

(26) Adell, A.; Artigas, F. In *In Vivo Neuromethods*; Boulton, A. B., Baker, A. A., Bateson, A. N., Eds.; Humana Press: Totowa, 1998; Vol. 32.

(27) Chen, Z.; Wu, J.; Baker, G. B.; Parent, M.; Dovichi, N. J. Application of capillary electrophoresis with laser-induced fluoroescence detection to the determination of biogenic amines and amino acids in brain microdialysate and homogenate samples, *J. Chrom. A* **2001**, *914*, 293-298.

(28) Powell, P. R.; Ewing, A. G. Recent advances in the application of capillary electrophoresis to neuroscience, *Anal. Bioanal. Chem.* **2005**, *382*, 581-591.

(29) Dale, N.; Hatz, S.; Tian, F.; Llaudet, E. Listening to the brain: microelectrode biosensors for neurochemicals, *Trends in Biotech.* **2005**, *23*, 420-428.

(30) Clark, L. C.; Lyons, C. Electrode systems for continuous monitoring in cardiovascular surgery, *Ann. NY Acad. Sci.* **1962**, *102*, 29.

(31) Updike, S. J.; Hicks, G. P. The enzyme electrode, *Nature* **1967**, *214*, 986.

(32) Guilbault, G. G.; Lubrano, G. J. An enzyme electrode for the amperometric determination of glucose, *Analytica Chimica Acta* **1972**, *64*, 439-455.

(33) Feldman, B.; McGarraugh, G.; Heller, A.; Bohannon, N.; Skyler, J.; DeLeeuw, E.; Clarke, D. Freestyle(TM): A smal-volume electrochemical glucose sensor for home blood glucose testing, *Diabetes Technology and Therapeutics* **2000**, *2*, 221-229.

(34) Husain, M.; Husain, Q. Applications of Redox Mediators in the Treatment of Organic Pollutants by Using Oxidoreductive Enzymes: A Review, *Critical Reviews in Environmental Science and Technology* **2008**, *38*, 1-42.

(35) Gregg, B. A.; Heller, A. Cross-Linked Redox Gels Containing Glucose Oxidase for Amperometric Biosensor Applications, *Anal. Chem.* **1990**, *62*, 258-263.

(36) Gregg, B. A.; Heller, A. Redox Polymer Films Containing Enzymes. 1. A Redox-Conducting Epoxy Cement: Synthesis, Characterization, and Electrocatalytic Oxidation of Hydroquinone, *J. Phys. Chem.* **1991**, *95*, 5970-5975.

(37) Robinson, J., Cooper, J. M. Method of Determining Oxygen Concentrations in Biological Media Suitable for Calibration of the Oxygen Electrode, *Anal. Biochem.* **1970**, *33*, 390-399.

(38) Villarta, R. H.; Cunningham, D. D.; Guilbault, G. G. Amperometric Enzyme Electrodes for the Determination of L-glutamate, *Talanta* **1991**, *38*, 49-55.

(39) Galiatsatos, C.; Ikariyama, Y.; Mark, J. E.; Heineman, W. R. Immobilization of Glucose Oxidase In a Poly [Vinyl Alcohol] Matrix on Platinized Graphite Electrodes by Gamma-Irradiation, *Biosens. Bioelectron.* **1990**, *5*, 47-61.

(40) Wang, J.; Myung, N. V.; Yun, M.; Monbouquette, H. G. Glucose Oxidase Entrapped in Polypyrrole on High-Surface-Area Pt Electrodes: A Model Platform for Sensitive Electroenzymatic Biosensors, *J. Electroanal. Chem.* **2005**, *575*, 139-146.

(41) Heller, A. Electrical Connection of Enzyme Redox Centers to Electrodes, *J. Phys. Chem.* **1992**, *96*, 3579-3587.

(42) Cui, J.; Kulagina, N. V.; Michael, A. C. Pharmacological Evidence for the Selectivity of In Vivo Signals Obtained With Enzyme-Based Electrochemical Sensors, *J. Neurosci. Meth.* **2001**, *104*, 183-189.

(43) Garguilo, M. G.; Huynh, N.; Proctor, A.; Michael, A. C. Amperometric Sensors for Peroxide, Choline, and Acetylcholine Based on Electron Transfer between Horseradish Peroxidase and a Redox Polymer, *Anal. Chem.* **1993**, *65*, 523-528.

(44) Garguilo, M. G.; Michael, A. Optimization of Amperometric Microsensors for Monitoring Choline in the Extracellular Fluid of Brain Tissue, *Anal. Chim. Acta* **1995**, *307*, 291-299.

(45) Garguilo, M. G.; Michael, A. Quantitation of Choline in the Extracellular Fluid of Brain Tissue with Amperometric Microsensors, *Anal. Chem.* **1994**, *66*, 2621-2629.

(46) Garguilo, M. G.; Michael, A. C. Amperometric Microsensors for Monitoring Choline in the Extracellular Fluid of Brain, *J. Neurosci. Meth.* **1996**, *70*, 73-82.

(47) Kulagina, N. V.; Michael, A. C. Monitoring Hydrogen Peroxide in the Extracellular Space of the Brain with Amperometric Microsensors, *Anal. Chem.* **2003**, *75*, 4875-4881.

(48) Kulagina, N. V.; Shankar, L.; Michael, A. C. Monitoring Glutamate and Ascorbate in the Extracellualr Space of Brain Tissue with Electrochemical Microsensors, *Anal. Chem.* **1999**, *71*, 5093-5100.

(49) Shankar, L.; Garguilo, M. G.; Michael, A. In *Methods in Biotechnology*; Mulchandani, A., Rogers, K. R., Eds.; Humana Press: Totowa, NJ, 1998; Vol. 6, pp 121-132.

(50) Vreeke, M.; Maidan, R.; Heller, A. Hydrogen Peroxide and Beta-Nicotinamide Adenine Dinucleotide Sensing Amperometric Electrodes Based on Electrical Based on Electrical Connection of Horseradish Peroxidase Redox Centers to Electrodes through a Three-Dimensional Electron Relaying Polymer Network, *Anal. Chem.* **1992**, *64*, 3084-3090.

(51) Messerschmidt, A., *Adv. Inorg. Chem.* **1993**, *40*, 121-185.

(52) Wilson, G.; Gifford, R. Biosensors for Real-Time In Vivo Measurements, *Biosens. Bioelectron.* **2005**, *20*, 2388-2403.

(53) Wilson, G.; Hu, Y. Enzyme Based Biosensors for In Vivo Measurements, *Chem. Rev.* **2000**, *100*, 2693-2704.

(54) Hu, Y.; Wilson, G. Rapid changes in local extracellular rat brain glucose observed with an in vivo glucose sensor, *J. Neurochem.* **1997**, *68*, 1745-1752.

(55) Hu, Y.; Mitchell, K.; Albahadily, F.; Michaelis, E.; Wilson, G. DIRECT MEASUREMENT OF GLUTAMATE RELEASE IN THE BRAIN USING A DUAL ENZYME-BASED ELECTROCHEMICAL SENSOR, *Brain Res.* **1994**, *659*, 117-125.

(56) Burmeister, J.; Gerhardt, G. Self referencing ceramic based multisite microelectrodes for the detection and elimination of interferences from the measurement of L-glutamate and other analytes, *Anal. Chem.* **2001**, *73*, 1037-1042.

(57) Parikh, V.; Pomerleau, F.; Huettl, P.; Gerhardt, G.; Sarter, M.; Bruno, J. Rapid assessment of in vivo cholinergic transmission by amperometric detection of changes in extracellular choline levels, *Eur. J. Neurosci.* **2004**, *20*, 1545-1554.

(58) Pomerleau, F.; Day, B.; Huettl, P.; Burmeister, J.; Gerhardt, G. Real time in vivo measures of L-glutamate in the rat central nervous system using ceramic-based multisite microelectrode arrays, *Glutamate and Disorders of Cognition and Motivation: Ann. N.Y. Acad. Sci.* **2003**, *1003*, 454-457.

(59) Mitchell, K. Acetylcholine and Choline Amperometric Enzyme Sensors Characterized In Vitro and In Vivo, *Anal. Chem.* **2004**, *76*, 1098-1106.

(60) Lay, P. A.; Sargeson, A. M.; Taube, H. In *Inorganic Syntheses*; Shreeve, H. J. M., Ed.; Wiley: New York, 1986; Vol. 24, pp 291-299.

(61) Pellegrino, L. J.; Pellegrino, A. S.; Cushman, A. J. *A Stereotaxic Atlas of the Rat Brain*, 2nd ed.; Plenum Press: New York, 1979.

(62) Grinstead, R. R. Metal-catalyzed Oxidation of 3,5-di-t-Butyl Pyrocatechol, and Its Significance in the Mechanism of Pyrocatechase Activity, *Biochem.* **1964**, *3*, 1308-1314.

(63) Jarabak, R.; Harvey, R. G.; Jarabak, J. Redox Cycling of Polycyclic Aromatic Hydrocarbon o-Quinones: Metal Ion-Catalyzed Oxidation of Catechols Bypasses Inhibition by Superoxide Dismutase, *Chem. Biol. Interact.* **1998**, *115*, 201-213.

(64) Li, Y.; Trush, M. A. Oxidation of Hydroquinone by Copper: Chemical Mechanism and Biological Effects, *Arch. Biochem. Biophys.* **1993**, *300*, 346-355.

(65) Mentasti, E.; Pelizzetti, E.; Baiocchi, C. Interactions of Fe(III) with Adrenaline, L-DOPA, and Other Catechol Derivatives: Electron-Exchange Kinetics and Mechanism in Acidic Perchlorate Media, *J. Inorg. Nucl. Chem.* **1976**, *38*, 2017-2021.

(66) Miller, D. M.; Buettner, G. R.; Aust, S. D. Transition Metals as Catalysts of "Autoxidation" Reactions, *Free Radical Biol. Med.* **1990**, *8*, 95-108.

(67) Walaas, E.; Walaas, O.; Haavaldsen, S. Spectrophotometric and Electron-Spin Resonance Studies of Complexes of Catecholamines with Cu(II) Ions and the Interaction of Ceruloplasmin with Catecholamines, *Arch. Biochem. Biophys.* **1963**, *100*, 97-109.

(68) Tse, D. C. S.; McCreery, R. L.; Adams, R. N. Potential Oxidative Pathways of Brain Catecholamines, *Journal of Medicinal Chemistry* **1975**, *19*, 37-40.

(69) Lotti, V. J.; Porter, C. C. Potentiation and Inhibition of Some Central Actions of L(-)-DOPA by Decarboxylase Inhibitors, *J. Pharmacol. Exp. Ther*. **1970**, *172*, 406-415.

(70) Ju, H.; Ni, J.; Gong, Y.; Chen, H.; Leech, D. Electrocatalytical Oxidation and Determination of Dopamine at Redox Polymer/Nafion Modified Electrodes, *Analytical Letters* **1999**, *32*, 2951-2964.

(71) Ni, J.-A.; Ju, H.-X.; Chen, H.-Y.; Leech, D. Amperometric Determination of Epinephrine with an Osmium Complex and Nafion Double-Layer Membrane Modified Electrode, *Analytica Chimica Acta* **1999**, *378*, 151-157.

(72) Ni, J.-A.; Ju, H.-X.; Chen, H.-Y.; Leech, D. $[Os(bpy)_2(PVP)_{10}Cl]Cl$ Polymer and Nafion Dual-Film Modified Graphite Electrode for the Amperometric Detection of Trace Amounts of Norepinephrine, *Analyst* **1998**, *123*, 2895-2898.

(73) Mitala Jr., J. J.; Michael, A. Improving the Performance of Electrochemical Microsensors Based on Enzymes Entrapped in a Redox Hydrogel, *Analytica Chimica Acta* **2006**, *556*, 326-322.

(74) Ferruti, P.; Barbucci, R., *Adv. Poly. Sci.* **1984**, *58*, 55.

(75) Van Poucke, L. C.; De Brabander, H. F.; Eeckhaut, Z. Ag(I) Complexes of Some w'-aminoalkylpyridinium Compounds, *Bull. Soc. Chim. Belges* **1969**, *78*, 131-134.

(76) Hau, W. L. W.; Trau, D. W.; Sucher, N. J.; Wong, M.; Zohar, Y. Surface-chemistry technology for microfluidics, *J. Micromech. Microeng.* **2003**, *13*, 272-278.

(77) Sigma-Aldrich; P8250 Peroxidase from Horseradish, Type II, Essentially Salt-Free, Lyophilized Powder, 150-250 Units/mg Solid (using Pyrogallol): Product Information Sheet, 2008.

(78) Garguilo, M. G.; Michael, A. C. Enzyme-Modified Electrodes for Peroxide, Choline, and Acetylcholine, *Trends in Anal. Chem.* **1995**, *14*, 164-169.

(79) Oldenziel, W. H.; de Jong, L. A. A.; Dijkstra, G.; Cremers, T. I. F. H.; Westerink, B. H. C. Improving the Performance of Glutamate Microsensors by Purification of Ascorbate Oxidase, *Anal. Chem.* **2006**, *78*, 2456-2460.

(80) Venton, B. J.; Wightman, R. M. Pharmacologically Induced, Subsecond Dopamine Transients in the Caudate-Putamen of the Anesthetized Rat *Synapse* **2007**, *61*, 37-39.

(81) Crespi, F.; Keane, P. E.; Morro, M. In Vivo Evaluation by Differential Pulse Voltammetry of the Effect of Thyrotropin-Releasing Hormone (TRH) on Dopaminergic and Serotoninergic Synaptic Activity in the Striatum and Nucleus Accumbens of the Rat, *Exp. Brain Res.* **1986**, *62*, 329-334.

(82) Ferrari, R. P.; Laurenti, E. Oxidation of Catechols and Catecholamines by Horseradish Peroxidase and Lactoperoxidase: ESR Spin Stabilization Approach Combined with Optical Methods, *Spectrochimica Acta* **1993**, *49A*, 1261-1267.

(83) O'Connor, M.; Kim, S. N.; Killard, A. J.; Forster, R. J.; Smyth, M. R.; Papadimitrakopoulos, F.; Rusling, J. F. Mediated Amperometric Immunosensing Using Single Walled Carbon Nanotube Forests, *Analyst* **2004**, *129*, 1176-1180.

(84) Buszman, E.; Betlej, B.; Wrzesniok, D.; Radwanska-Wala, B. Effect of Metal Ions on Melanin: Local Anaesthetic Drug Complexes, *Bioinorg. Chem. and App.* **2003**, *1*, 113-122.

(85) Kobayashi, S.; Higashimura, H. Oxidative Polymerization of Phenols Revisited, *Prog. Polym. Sci.* **2003**, *28*, 1015-1048.

(86) Crespi, F.; Mobius, C. In Vivo Selective Monitoring of Basal Levels of Cerebral Dopamine using Voltammetry with Nafion Modified (NA-CRO) Carbon Fibre Micro-Electrodes, *J. Neurosci. Meth.* **1992**, *42*, 149-161.

(87) Jones, S. R.; Garris, P. A.; Wightman, M. R. Different Effects of Cocaine and Nomifensine on Dopamine Uptake in the Caudate-Putamen and Nucleus Accumbens, *J. Pharmacol. Exp. Ther.* **1995**, *274*, 396-403.

(88) White, H. S.; Leddy, J.; Bard, A. J. Polymer Films on Electrodes. 8. Investigation of Charge-Transport Mechanisms in Nafion Polymer Modified Electrodes, *J. Am. Chem. Soc.* **1982**, *104*, 4811-4817.